GEORGIA INSTITUTE OF TECHNOLOGY
Engineering Experiment Station

N0516 93

PROJECT INITIATION

Date: July 25, 1973

Project Title: Harbour Traffic Control Study

Project No.: A-1548

Project Director: Mr. M. T. Tuley

Sponsor: Naval Coastal Systems Laboratory; Panama City, Florida 32401

Effective . . . . June 7, 1973. . . . . Estimated to run until: October 15, 1973 . . . . . .

Type Agreement: Contract No. N61331-73-C-0087 (Fixed-Price) . . Amount: $ 9,951.00 . . . . . .

REPORTS REQUIRED: Summary Letter

Sponsor Contact Persons:

Technical Matters
(Individual Not Named)

Contractual Matters
(thru GTRI)
Mr. O. R. Holley, Code 412
Contracting Officer
Naval Coastal Systems Laboratory
Panama City, Florida 32401
Phone: (904)234-4413

Defense Priority Rating: DO-C9 under DMS Reg. 1.

Assigned to . . Sensor Systems . . . . . Division

COPIES TO:

Project Director	Photographic Laboratory
Director	Security, Property, Reports Coordinator
Assistant Director	EES Accounting
GTRI	EES Supply Services
Division Chief(s)	Library
Service Groups	Rich Electronic Computer Center
Patent Coordinator	Project File
	Other _____

RA-62

GEORGIA INSTITUTE OF TECHNOLOGY
Engineering Experiment Station

Post B
Eng

PROJECT TERMINATION

Date November 9, 1973

PROJECT TITLE: Harbour Traffic Control Study

PROJECT NO: A-1548

PROJECT DIRECTOR: Mr. M. T. Tuley

SPONSOR: Naval Coastal Systems Laboratory; Panama City, Florida

TERMINATION EFFECTIVE: 10-15-73 (Contract Expiration)

CHARGES SHOULD CLEAR ACCOUNTING BY: N/A -- Fixed-price contract

CONTRACT CLOSEOUT ITEMS REMAINING: Bill Sponsor ASAP
Final Patent Report
Classified Material Cert.

no property

SENSOR SYSTEMS DIVISION

COPIES TO:

Project Director
Director
Associate Director
Assistant Directors
Division Chief
Branch Head
Accounting
Engineering Design Services
General Office Services
Photographic Laboratory
Purchasing
Report Section
Library
✓Security
Rich Electronic Computer Center

FINAL REPORT

PROJECT NO. A-1548

HARBOR TRAFFIC CONTROL STUDY

By
M. T. Tuley and F. B. Dyer

Contract No. N61331-73-C-0087
Department of the Navy
Naval Coastal Systems Laboratory
Panama City, Florida 32401

6 October 1973

1973

ENGINEERING EXPERIMENT STATION
Georgia Institute of Technology
Atlanta, Georgia

ENGINEERING EXPERIMENT STATION
Georgia Institute of Technology
Atlanta, Georgia 30332

FINAL REPORT

EES/GIT Project A-1548

HARBOR TRAFFIC CONTROL STUDY

by

M. T. Tuley and F. B. Dyer

Prepared for

DEPARTMENT OF THE NAVY
NAVAL COASTAL SYSTEMS LABORATORY
PANAMA CITY, FLORIDA 32401

Under

Contract N61331-73-C-0087

6 October 1973

DISCLAIMER

The discussion of particular commercial systems in this report is not to be construed as endorsement or approval of these systems by either the Georgia Institute of Technology or the United States Navy.

Contract N61331-73-C-0087
Department of the Navy
Naval Coastal Systems Laboratory
Panama City, Florida 32401

A-1548 Final Report
Engineering Experiment Station
Georgia Institute of Technology
Atlanta, Georgia 30332

HARBOR TRAFFIC CONTROL STUDY

by

M. T. Tuley and F. B. Dyer

ABSTRACT

A significant problem during operation in harbor and coastal areas is that of detecting and identifying marine traffic. In this report a study using computer modeling techniques is performed to specify what parameters should be chosen for a van portable radar system which is capable of performing the harbor surveillance function. The composite model used contains: (1) an algorithm for characterizing sea and target return as functions of target elements, geometry, and weather and sea conditions; (2) a semi-empirical model for computing single-scan probability-of-detection; and (3) a computer program which combines (1) and (2) into a functional framework.

In addition, several readily available radars are chosen and their performances versus the optimum radar and each other are compared. Also investigated is the potential for use of automated displays and radar beacon or transponder systems to aid in identifying targets, and to provide additional information on their movements. Results of a field operation evaluating one such automated display are presented.

TABLE OF CONTENTS

TABLE OF CONTENTS (Cont.)

LIST OF FIGURES

LIST OF FIGURES (Cont.)

LIST OF FIGURES (Cont.)

LIST OF FIGURES (Cont.)

LIST OF TABLES

I. Introduction

A. Goals of the Study

A significant problem during operations in harbor and coastal areas is that of detecting and identifying marine traffic. Surveillance is a necessary measure for detecting potentially hostile craft and for aiding smooth operation in regions where friendly military and civilian craft operate simultaneously. The system performing these functions must be portable, must operate in daylight or darkness, must perform in fog and rain, and must provide sufficient acquisition range to detect hostile craft before they may do harm. The requirements just stated point to radar as the potential sensor for a system to perform the functions described. The purpose of this study is to analyze the parameters which might provide the optimum radar system to be used in the coastal detection and surveillance environment. In addition, several available systems are presented, and their performance relative to the optimum system and to each other is discussed. Secondly, the problem of identification of individual targets in high-density traffic is considered. In this regard, signal processing,automated display and radar beacon/IFF coding are indicated as potential solutions, and their implementation is briefly analyzed.

B. Operational Requirements

The operational requirements which must be met by a satisfactory system place a number of constraints on the parameters to be considered. Portability limits available power, size, antenna height, and possibly antenna scan rate. Detection is required on targets ranging from small open boats with radar cross-sections of about one square meter to large ships with radar cross-sections in the thousands of square meters. Operation is required in all weather, a factor influencing power and frequency selection.

Because of the constraints imposed, the following limitations are inherent in the analysis:

(1) Antenna heights are those practical with a portable tower; a maximum height of 100 feet is considered.

(2) Antenna size is limited to that compatible with a portable tower, a cut parabolic dish 8 feet long is considered the maximum practical size.

(3) Radars considered must be van portable.

(4) Operation in rain or fog must be a design consideration.

(5) Pulse repetition frequencies and scan rates are limited to those allowing at least a 30 nmi theoretical range capability.

C. The Radar Model

The radar detection model used in the present analysis was developed during earlier Navy programs and is reported more fully in References 1 and 2. It is composed of several elements, including the properties of the radar and its operator, the target, and the environment as it affects both the electromagnetic field incident on the target and the background clutter in which the target is to be detected. Figure 1 presents a simplified flow chart for the model; each element is discussed briefly below in terms of that chart.

The form of the description of target and clutter cross-section is dictated in part by the requirements of the radar processor model assumed. As no exhaustive studies have been performed to model the human operator, an empirical approach derived from extensive at-sea testing is used [3, 4]. Detection probabilities are computed using signal-to-background ratio and false-alarm rate as parameters. The signal-to-background ratio is formed by comparing the predicted value of the modeled cross-section for a given target and the greater of the equivalent cross-sections of the two possible backgrounds, specified as average noise and "peak" sea clutter. Peak clutter is defined as the value of clutter cross-section exceeded only one percent of the time. Peak clutter, along with a constant false-alarm rate, are used, since operators tend to adjust display and receiver controls to maintain a constant false-alarm rate which is typically such that 10 to 100 false alarms appear on the display on any one scan. The model chosen was selected so as to represent the median cross-section (versus aspect); it is anticipated that the predicted signal-to-background ratios are typical of those that might be observed. In this approach to the specification of signals, probability distribution concepts are not abandoned

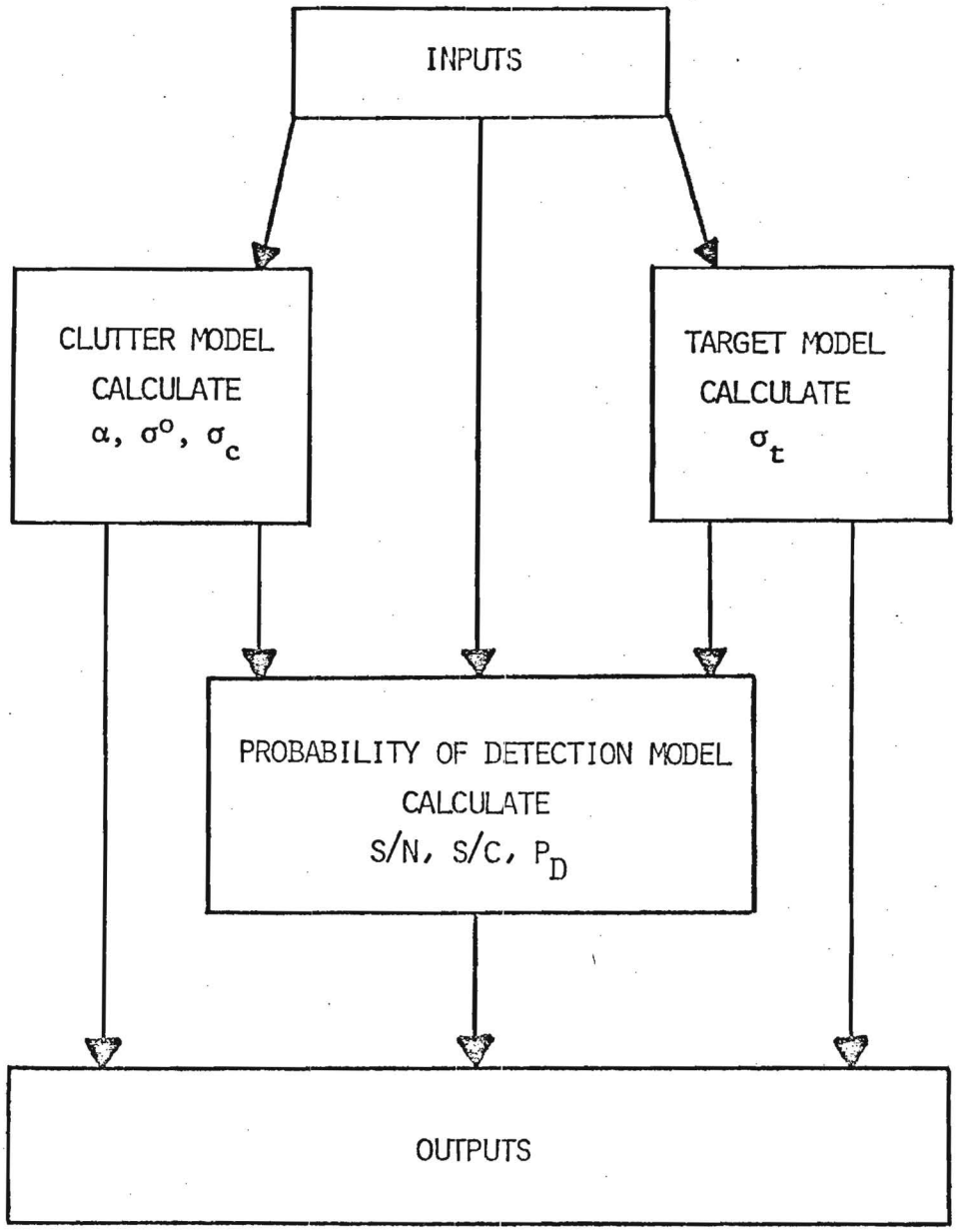

Figure 1. Flow Chart of the Model.

but rather are used to choose the appropriate peak value for calculating target-to-background ratios. Thus, the model implemented treats each component part as a deterministic factor for purposes of computation, each component having a parameter adjustment to account for its statistical nature; however, the final probability-of-detection calculations are made with a statistical model.

Table I gives a complete list of the variables used in the model, and the following tables list the equations for the models. No attempt is made to indicate which set of units is used in each equation. However, the units are consistent, even though the variables for any given equation may be entered in different, non-consistent sets of units.

1. Sea-Clutter Model

The sea-clutter model is described more completely in Reference 1 where the source data, from which the equations and parameter values were derived, are presented. Table II lists the regions over which the model is valid. Caution is suggested in using the model outside the range of Table II, especially for very high or very low frequencies, vertical polarization, very low wind speeds, and very low incidence angles.

The input variables to the model are listed in Table III. The model predicts σ^o, the average radar cross-section per unit area of sea surface, and σ^o, the average radar clutter cross-section. The input variables are entered in units common to their usage, rather than in the units which are consistent with those used in the modeling equations. For example, the wave length is entered in meters and the antenna height is entered in feet.

The clutter model equations are listed in Table IV. Notice that the incidence angle is corrected for earth curvature, and that the wind speed and wave height are coupled by an equation representing the relationships characteristic of a fully arisen sea condition. This is consistent with the goal of the model, which is to predict clutter for fully developed sea conditions, as contrasted to "spiky" conditions.

TABLE I

Variable List

Math Symbol	Units	Definition
σ_x	dB	Standard deviation of received signal
B	MHz	Receiver bandwidth
f_r	Hz	Pulse repetition frequency
T_s	sec	Scan-time interval
k_a	$dBm \cdot m^2$	Radar power constant $k_a = \frac{P_t G^2 \lambda^2}{(4\pi)^3}$
K_o	--	Radar display constant (set = 0.4 in program)
τ	sec	Radar pulse length
θ_a	rad	Aximuth beamwidth (one-way, 3-dB)
λ	m	Radar wavelength
φ	deg	Angle between upwind and boresight
h_D	ft	Duct height constant
NF	--	Receiver noise figure (NG, dB; NF, ratio)
A_e	m	Effective earth radius
r_i	ft	Radius of cylinder i
ℓ_i	ft	Length of cylinder i
h_i	ft	Distance from sea surface to top of cylinder i
R_D	nmi	Displayed range (PPI radius)
h_a	ft	Antenna height
λ	ft	Radar wavelength
h_{av}	ft	Sea-wave height (average)
R	nmi	Range
α	rad	Local incidence angle at target
q_λ	--	Exponent
A_a	--	Upwind/downwind factor
σ_φ	rad	Standard deviation of interference phase
A_i	--	Interference factor

TABLE I (Cont.)

Math Symbol	Units	Definition
K_p	--	Reflection coefficient scale factor
V_w	kt	Wind speed
A_w	--	Wind-speed factor
σ°	dB	Clutter cross-section per unit area (average)
A_c	dBsm	Radar cell area
σ_c	dBsm	Clutter cross-section (average)
σ_t	m^2	Target cross-section
ρ	--	Reflection coefficient of water
θ_{Bi}	rad	Intermediate factors in target cross-section calculation
θ_{ci}	rad	
σ_i	m^2	
θ_G	rad	
S_1	--	
S_2	--	
σ_{ti}	m^2	
Y_n	dB	S/N for $P_D = 0.5$
W_t	dBm	Received target power
W_c	dBm	Received clutter power
W_n	dBm	Receiver noise power
X_n	dB	Excess signal-to-noise power
X_c	dB	Excess signal-to-clutter power
S	dB	Excess signal-to-background power
ERF	prob	Error function
P_D	prob	Probability of detection
K	J/deg K	Boltzmann's constant
T	deg K	Absolute temperature
Ma	--	Threshold setting
S/N	dB	Signal-to-noise ratio
S/C	dB	Signal-to-clutter ratio

TABLE II

Range of Variables in Clutter Model

Frequency	400 MHz to 18 GHz
Polarization	Horizontal
Wind speed	7 to 30 kts
Wave height (average)	0.5 to 12 ft
Incidence angle	0.1 to 10 degrees

TABLE III

Principal Variables of the Clutter Model

Math Symbol	Unit	Definition
R	nmi	Range from radar to target
h_a	ft	Antenna height
A_e	m	Effective earth radius
λ	m^2	Radar wavelength
α	rad	Incidence angle
h_D	ft	Duct height constant
ϕ	deg	Angle between boresight and upwind
h_{av}	ft	Average sea-wave height
V_w	kts	Wind speed
τ	sec	Radar pulse length
θ_a	rad	Azimuth beamwidth
σ°	dB	Average cross-section per unit area
σ_c	dBsm	Average clutter cross-section

TABLE IV

Sea Clutter Model Equations

1. $$\alpha' = \frac{h_a}{R} - \frac{R}{2A_e}$$

$$\alpha = \left[\alpha'^2 + \left(\frac{\lambda}{4\, h_D} \right)^2 \right]^{1/2}$$

$$q_\lambda = \lambda^{-0.44}$$

$$A_a = \exp \left\{ 0.828\, q_\lambda \quad (1 - 1.4\, \alpha) \quad (0.5 - \frac{\varphi}{180}) \right\}$$

2. $$\sigma_\varphi = \frac{5\, \alpha\, h_{av}}{\lambda}$$

$$A_i = 1 - \frac{4}{3} \exp \left[\frac{4.92\, \sigma_\varphi^2}{4} \right] + \frac{1}{3} \exp \left\{ 4.92\, \sigma_\varphi^2 \right\}$$

3. $$q_w = 1.59\, \lambda^{-0.35}$$

$$V_w = 10.47\, h_{av}^{0.4}$$

$$A_w = (V_w)^{q_w}$$

4. $$\sigma^\circ = 10 \log \left\{ 9 \times 10^{-7}\, \lambda\, \alpha^{0.4}\, A_a\, A_i\, A_w \right\}$$

$$A_c = 10 \log \left[\frac{c\tau}{2} \quad \frac{R\, \theta_a}{\sqrt{2}} \right]$$

$$\sigma_c = \sigma^\circ + A_c$$

2. Target Model

The target model used is intended to represent the radar cross-section of targets which lie on or close to the sea surface. The targets are modeled as segments of cylinders whose radii and lengths are parameters. The model is a highly modified form of one originally conceived by Dr. R. Hess of Airtronics, Inc. [2]. The radii used in the modeling are based on "effective" radar dimensions of the target, guided by experimental data rather than actual physical dimensions.

The model has the capability of approximating any target by as many as ten cylinders. In the cases treated here, however, a maximum of three cylinders are used. It is felt that this number sufficiently describes the hull, superstructure, and mast structure of the type of ship targets considered. The output of the model is peak cross-section in dBsm, with no tilt or azimuth angular dependence assumed. Lack of circular symmetry of the targets is accounted for through use of an "effective" radius characterizing the bow-on rather than the broadside cross-section, which is the "worse-case" for detection. The input variables are listed in Table V and the model equations are given in Table VI.

In the calculations, the peak coherent cross-section of each cylindrical section is computed and summed incoherently (a summation of power) with that of the other sections. Correction for nonuniform weighting of the incident field is made by taking account of the interference between direct and surface-reflected waves. The coherent reflection coefficient of the surface is reduced as the sea-surface roughness and incidence angle increase. In addition, a correction is made to the height of the target to account for shadowing of the lower part of the target due to the spherical earth and for the effect of the rough surface in raising the effective reflecting plane above mean sea-surface level.

3. Probability-of-Detection Model

This section describes the model used to predict the probability of detecting the presence of a target with a single scan of the radar. The model computes received signal power, received clutter power, noise power, signal-to-background ratios, and the probability-of-detection for the predicted signal-to-background ratio. The various signal powers are

TABLE V

Input Variables to the Target Model

Math Symbol	Units	Definition
r_i	ft	Radius of cylinder i
ℓ_i	ft	Length of cylinder i
h_{av}	ft	Average sea-wave height
λ	m	Radar wavelength
α	rad	Incidence angle
h_i	ft	Distance from sea surface to top of cylinder i
K_p	--	Reflection coefficient scale factor

TABLE VI

Target Model Equations

1. $\rho = K_p \exp\left[-4\pi\left(\frac{h_{av}\alpha}{\lambda}\right)^2\right]$

2. Do for cylinder 1

$$\sigma_1 = \frac{2\pi r_1 h_1^2}{\lambda}$$

$$\theta_G = \frac{4\pi\alpha h_1}{\lambda}$$

$$S_1 = \left[(1+\rho^2)\ \frac{\text{Sin}\ \theta_G}{\theta_G} - 2\rho\right]^2$$

$$S_2 = \left[(1-\rho^2)\ \frac{1-\cos\theta_G}{\theta_G}\right]^2$$

$$\sigma_{t_1} = \sigma_1\ (S_1 + S_2)$$

3. Do for Cylinders 2 through n

$$\sigma_i = \frac{2\pi r_i \ell_i 2}{\lambda}$$

$$\theta_{Bi} = \frac{2\pi\alpha \ell_i}{\lambda}$$

$$\theta_{ci} = \frac{2\pi\alpha\ (2h_i - \ell_i)}{\lambda}$$

$$S_1 = \left[(1+\rho^2)\ \frac{\sin\theta_{Bi}}{\theta_{Bi}}\ \cos\theta_{ci} - 2\rho\right]^2$$

3. Continued

$$S_2 = \left[(1-\rho^2) \frac{\sin \theta_{Bi}}{\theta_{Bi}} \sin \theta_{ci} \right]^2$$

$$\sigma_{ti} = \sigma_i (S_1 + S_2)$$

4. Total target cross-section

$$\sigma_t = \sum_{i=1}^{n} \sigma_{ti}$$

computed as intermediate steps so that they are available to be compared with measured data.

The probability-of-detection is represented as the error function of the normalized ratio (in dB) of signal-to-noise ratio. This representation is suggested by the observed tendency of the logarithm of target signal-strength data to be distributed as a Gaussian random variable when ensembled from many observations presumably taken under the same nominal conditions. The representation is justified in part by the accuracy of modeling noise and clutter signals by log-normal functions over the limited regions of signal dynamic range effective in typical display presentations [5].

Table VII gives a list of the input variables and Table VIII lists the equations for the single-look probability-of-detection model.

D. Propagation in Surface Evaporation Ducts

An additional phenomenon exists which can tend to aid the radar operating close to the ocean's surface. This phenomenon is the formation of a surface duct which provides enhanced microwave propagation conditions. As this effect is not always present, it should not be used when projecting ranges at which a target may be detected; however, when it is present, maximum detection ranges of low-sited radars can be competitive with the optimum-sited systems as described in Chapter III. The following brief summary is abstracted from material in Reference 6. Detailed discussions of all aspects of radio wave propagation may be found in Reference 7. Additional discussions are to be found in References 1, 2, and 3. Reference 2 also includes an extensive bibliography of material on refraction and microwave propagation.

The surface ducts important to this study are formed by a negative gradient of atmospheric refractive index with altitude that is produced either by decreasing water vapor or by increasing temperature with altitude. The condition of negative gradient will trap microwave energy, provided the gradient is strong enough and its height extent is great enough. Lower frequencies require greater height extents (or much greater gradients) than do higher frequencies for a given amount of duct leakage. When strong trapping exists, energy is bound in the vertical plane to a

TABLE VII

Input Variables for the Probability Model

Math Symbol	Units	Definition
T_s	sec	Scan time interval
R_D	nmi	Displayed range (PPI radius)
σ_t	m^2	Target cross-section
k_a	$dBm \cdot m^2$	Radar power constant
R	m	Range from radar to target
σ_c	dBsm	Clutter cross-section
B	MHZ	Receiver bandwidth
NF	---	Receiver noise figure (NF, ratio)
σ_x	dB	Standard deviation of received signal
T	deg K	Absolute temperature
K	J/deg K	Boltzmann's constant

TABLE VIII

Equations for the Single-Scan Probability-of-Detection Model

1. $K_o = 0.4$

$$S = \frac{60}{T_s}$$

$$Y_n = \{10 \log_{10} K_D \, S^{0.26} \, R_D^{0.44}\}$$

$$Y_c = Y_n$$

2. $W_t = k_a + 10 \log (\sigma_t) - 40 \log (R)$

$W_c = k_a + \sigma_c - 40 \log (R)$

$W_n = 10 \log \{K \cdot T \cdot B \cdot NF\}$

3. $X_n = W_t - W_n - Y_n$

$X_c = W_t - W_c - Y_c$

$X = \text{Min} \{X_n, X_c\}$

$$Y = \frac{M_a - 10 \log_{10} (1 + \exp (.23X))}{\sigma_x}$$

$P_D = [1/2 + \text{ERF} (Y)]$

layer of constant altitude, and spreading occurs only in the horizontal plane. For the typical surface evaporation duct, field strengths tend to be a maximum about 10 feet above the surface at I-Band and 20 feet for F-Band. The exact height is variable and depends on the shape of the refractive gradient curve and antenna altitude and range. Coupling to a duct is strongest when antennas and targets are located at the heights of the maximum field strengths.

When surface trapping exists, signal strengths at a few tens of miles are typically equal to free space or stronger by as much as 10 dB. When the duct conditions are weakened so that energy is not trapped, signal strengths are described by the curved earth diffraction theory, perhaps with a modified earth radius to account for the refraction that does exist. Ducts tend to exist or not; that is, the time spent in either the trapped condition or the diffraction state is long compared to the duration of transition between the two states.

Some rules for the formation of surface ducts can be stated [8,9]. Trapping occurs for conditions in which warm dry air passes over cooler water as from over land, or for the condition of a sea breeze or low wind sustaining layered flow and minimum vertical mixing. When very dry air from land blows over warm water, high wind speeds can still allow negative refraction gradients [10]. Air cooler than water is allowed if of short duration and preceded by trapping conditions, as overnight. Standard diffraction conditions exist whenever vertical homogeneity of the atmosphere is achieved, as by turbulence. Such a condition of vertical mixing is produced by high or gusty winds, strong surface heating, or a frontal zone. Negligible gradients can also exist for conditions when the air has traveled over the water for a considerable distance at speeds of about 15 kts or greater, achieving saturation and mixing in the process, or when the air temperature is substantially lower than that of the water and has been so for several hours. Substandard conditions of positive gradient with altitude can be created by fog or by warm moist air flowing over cool water, as from tropical maritime regions.

It is important to note in the above rules the influence of the history of the air mass over the water, the conditions which affect ver-

tical mixing and transfer of water vapor from the surface, and the role of land in determining the boundary conditions for the maritime air mass. Because the conditions for trapping are directly related to the meteorological conditions, the durations of trapping or diffraction or substandard periods tend to be from hours to days.

The percentage of time one expects to experience each of the propagation modes is important but difficult to predict at present. It is known that the probability of surface trapping is different for different frequencies (more likely at higher frequencies), and at different times of the year (more likely in summer than in winter) and of the day (more likely in the afternoon and evening than in the morning). Reference 8 presented an analysis of experience at F-Band in the Massachusetts Bay area. For observations in that band in the months of August through October, the percentages of 6-hour periods in which each of the three conditions was observed were as shown in Table IX. The total is more than 100% because in many 6-hour periods more than one propagation condition was observed. These data were from F-Band observations and relate to higher band use only by implying that the frequency of observation of trapping should be increased over the entries of Table IX.

Although a large body of direct experimental evidence is available for analysis, most of the observations in I-Band have been made with antenna heights substantially greater than 10 feet, thus reducing the pertinence of the data for description of the evaporation-duct trapping phenomenon. One recent experiment series with appropriately low antenna heights [10,11,12,13] indicated that, out of 11 days of operation in three locations on the U.S. east coast, on 8 days ($\sim$75%) strong trapping was experienced at I-Band or lower frequencies, with signal strengths and range dependence of the order of free-space propagation.

TABLE IX

Distribution of Propagation Conditions
(from Reference 8, for F-Band)

	Percentage of 6-Hour Periods Experiencing:		
Month	Trapping	Diffraction	Substandard
August	50%	85%	5 - 10%
September	35%	90%	none
October	30%	85%	10 - 15%

II. SPECIFICATION OF AN OPTIMUM RADAR

The goal of this chapter is to specify some set of radar parameters which define an "optimum" system for the performance of harbor surveillance, within the constraints noted previously. As the intent of this study is to aid in the selection of components for a demonstration system which must be ready within a relatively short time frame, only those choices which seem readily realizable are considered. Thus, the "optimum" radar specified here is optimum in the sense that it offers the best performance for a radar which might be easily constructed from readily available components, or by modification of some existing radar system. Only the basic parameters of the radar are considered. Possible methods of clutter reduction and the effects of rain or fog are discussed. However, signal processing for use with an automated display is considered separately.

A. Antenna Design Constraints

Due to the required portability of the system postulated, one of the first problems which must be considered is that of antenna specifications. The maximum size antenna which is allowed in this study is an 8-foot-long, cut parabolic antenna. For a search application such as this, it is desirable that the antenna vertical beamwidth be such that it covers from the minimum desired range to the horizon. For a tower height of 100 feet and a minimum range of 1/2 mile, a 6^{o} beamwidth is required. To take care of misalignment and tilt, a 10^{o} vertical beamwidth is assumed at each frequency investigated.

For a typical antenna with a parabolic shape, Skolnik [14] quotes a formula for approximate 3 dB beamwidths of

$$\Theta^{o} = \frac{65\lambda}{\ell} ,$$

where ℓ is the dimension of the antenna in the plane of the angle Θ, λ is the wavelength, and λ and ℓ are measured in the same units. Applying this formula to the postulated parabolic antenna results in the azimuth beamwidths listed in Table X at the frequencies noted. Using the previously assumed 10^{o}

TABLE X

Calculated Antenna Beamwidth and Gain for Several Frequencies

Frequency (GHz)	Azimuth Beamwidth (degrees)	Antenna Gain* (dB)
3.0	2.7	30.0
5.6	1.5	33.0
9.4	0.9	35.0
16.5	0.5	37.5

*Vertical Beamwidth = 10^{o}

vertical beamwidth and the azimuthal beamwidth just calculated, another rule-of-thumb [15] is

$$G \simeq \frac{30,000}{\theta_1 \theta_2},$$

where G is maximum antenna gain and θ_1 and θ_2 are the 3 dB beamwidths in the two orthogonal principal planes. This relation may be used to arrive at the corresponding antenna gains also listed in Table X.

Since radar cell size and radar resolution are both dependent on beamwidth, it is advantageous to use as small a beamwidth as practical. Mitigating against an extremely narrow beamwidth is the desire for a hit/scan ratio on a target of about 10. This factor is considered further in the discussion on pulse repetition frequency and antenna scan rate. In the remaining analysis of Chapter II, the numbers calculated here are used in specification of the radar parameters entered into the computer model.

B. Antenna Height

One of the primary limitations on the system considered is that of antenna height. As it must be portable, the antenna mounting hypothesized is an erectable tower. For the antenna size used, the maximum height which might be obtained is on the order of 100 feet. Figure 2 shows the distance to the optical horizon versus observer height. It can be seen that even for an antenna height of 100 feet, the horizon is only 12 nmi. Thus, at ranges past 12 nmi, at least a portion of the target will be obscured. Previous data collected [1] have shown that for low-sited radars and targets close to the ocean surface, an effective earth's radius, due to refraction effects, should be substituted for the actual radius. In this report an effective earth's radius of 10,000 nmi, a number empirically supported in the data mentioned, is used. For this reason the target does not disappear as fast as might be expected. However, antenna height remains the most severe limitation on the maximum detection range for large targets. In Chapter III the effect of antenna heights of 30, 60, and 100 feet are demonstrated for several targets and radars. For the optimum radar an antenna height of 100 feet is assumed.

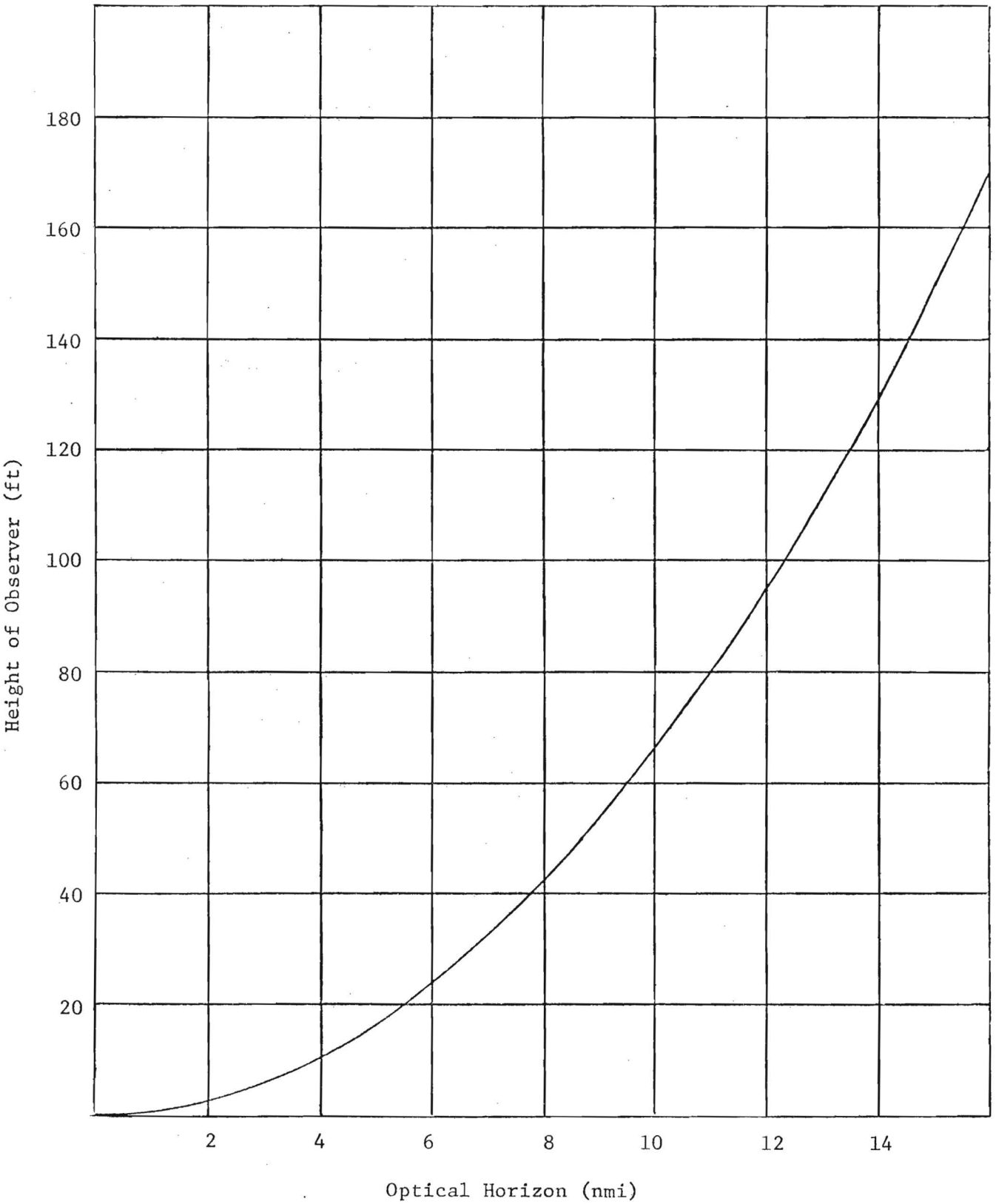

Figure 2. Range to Optical Horizon vs. Height of Observer Above the Surface.

C. Antenna Scan Rate and Pulse Repetition Frequency

The selection of an antenna scan rate and a radar pulse repetition frequency are closely tied to the maximum range desired. In a conventional pulse radar, the range data have ambiguities at time delay intervals equal to the repetition period. Thus

$$R_{unamb} = C/2f_r$$

where C is the velocity of light and f_r the pulse repetition frequency. For R_{unamb} equal to 30 nmi, the maximum f_r is 2700 per sec, thus setting the upper limit on PRF.

For maximum information from a target, Barton [16] shows that a minimum of 6 to 10 hits/scan of the radar should be obtained. The number of hits in a scan depends on beamwidth, PRF, and scan speed. For simplicity, assuming a 2.5 kHz PRF and a 1^o beamwidth, it would require 4.4×10^{-3} sec for 10 pulses to reach a target at 30 nmi and return. For minimum scanning loss the antenna should traverse less than the beamwidth in this time, leading to a maximum scan speed of 38 rpm.

The data rate available to be processed is maximized for the larger PRF and scan speed. Thus, in the final system, the highest usable PRF and scan speed which result in an acceptable hit/scan ratio should be used. Using these data from Sections A, B, and C radars are postulated whose characteristics are given in Table XI. A parametric study is performed on pulse width, power, and frequency to determine optimum selections.

D. Pulse Width

The pulse width chosen affects the range resolution, energy in each pulse, cell size, and thereby target and clutter return. The maximum pulse width is nominally determined by the duty factor of the output magnetron. Typically for high-power magnetrons, duty factors range from 0.0005 to 0.0025 with 0.001 considered a reasonable value. For PRF of 2.5 kHz and a duty cycle of 0.001, the maximum allowable pulse width is 0.4 μsec.

TABLE XI

Characteristics of Radars Postulated for Parametric Studies

Parameter	F-Band	G-Band	I-Band	J-Band
Frequency (GHz)	3.2	5.6	9.4	16.5
PRF (Hz)	2000	2000	2000	2000
Scan rate (sec)	2	2	2	2
Pulse width* (μsec)	0.5 0.25 0.1	0.5 0.25 0.1	0.5 0.25 0.1	0.5 0.25 0.1
Azimuth beamwidth (radians)	0.052	0.026	0.0157	0.0087
Noise figure (dB)	5.0	5.0	6.0	9.0
Peak power* (kW)	5,50,500	5,50,500	5,50,500	5,50,500

*Parametric studies performed on values indicated.

A parametric study is presented in Figures 3 and 4 of the effect of altering pulse width on signal-to-noise ratio, when the target is a 100 foot class boat as described in Chapter III, Section B. A 2 kHz PRF is assumed so that a 0.5 μsec pulse may be considered along with pulse widths of 0.25 and 0.1 μsec. Figures 5 and 6 present the same results for a 30-foot class boat. The radar shown is the G-Band radar from Table XI; however, the same general results hold for the other frequencies. As can be seen, at short ranges, the signal-to-noise ratio is degraded for the wider pulse due to its larger clutter cell. However, at longer ranges the increased energy in the return of the wider pulse results in a better signal-to-noise ratio. These results are most dramatically illustrated in Figure 6, a clutter-limited case, where the short pulse provides much better signal-to-noise ratios inside 8 nmi, which is effectively the maximum detection range.

Although it provides better performance at long range, the 0.5 μsec pulse does possess clutter limitations and has a range resolution of 82 yards compared to 40 yards for the 0.25 μsec pulse and 8 yards for the 0.1 μsec pulse. For these reasons it is felt that the 0.25 μsec pulse is the best compromise choice. In the further parametric studies this value of pulse width is assumed.

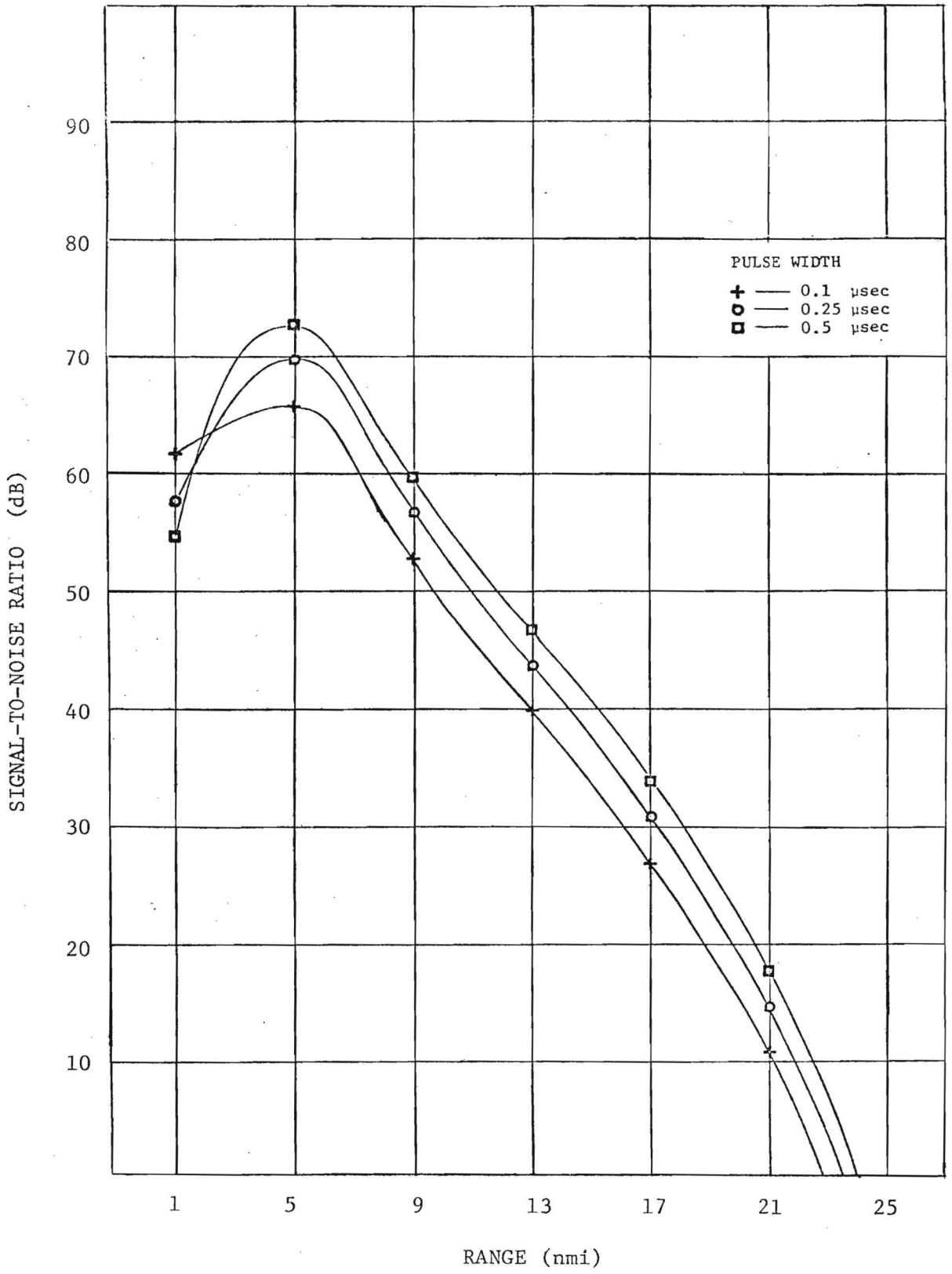

Figure 3. Comparison of Signal-to-Noise Ratios with Pulse Width as a Parameter for a G-Band Radar with an Antenna Height of 100 Feet, Sea State 1, Target II (Approximately 100 Foot Length - See Chapter III, Section B).

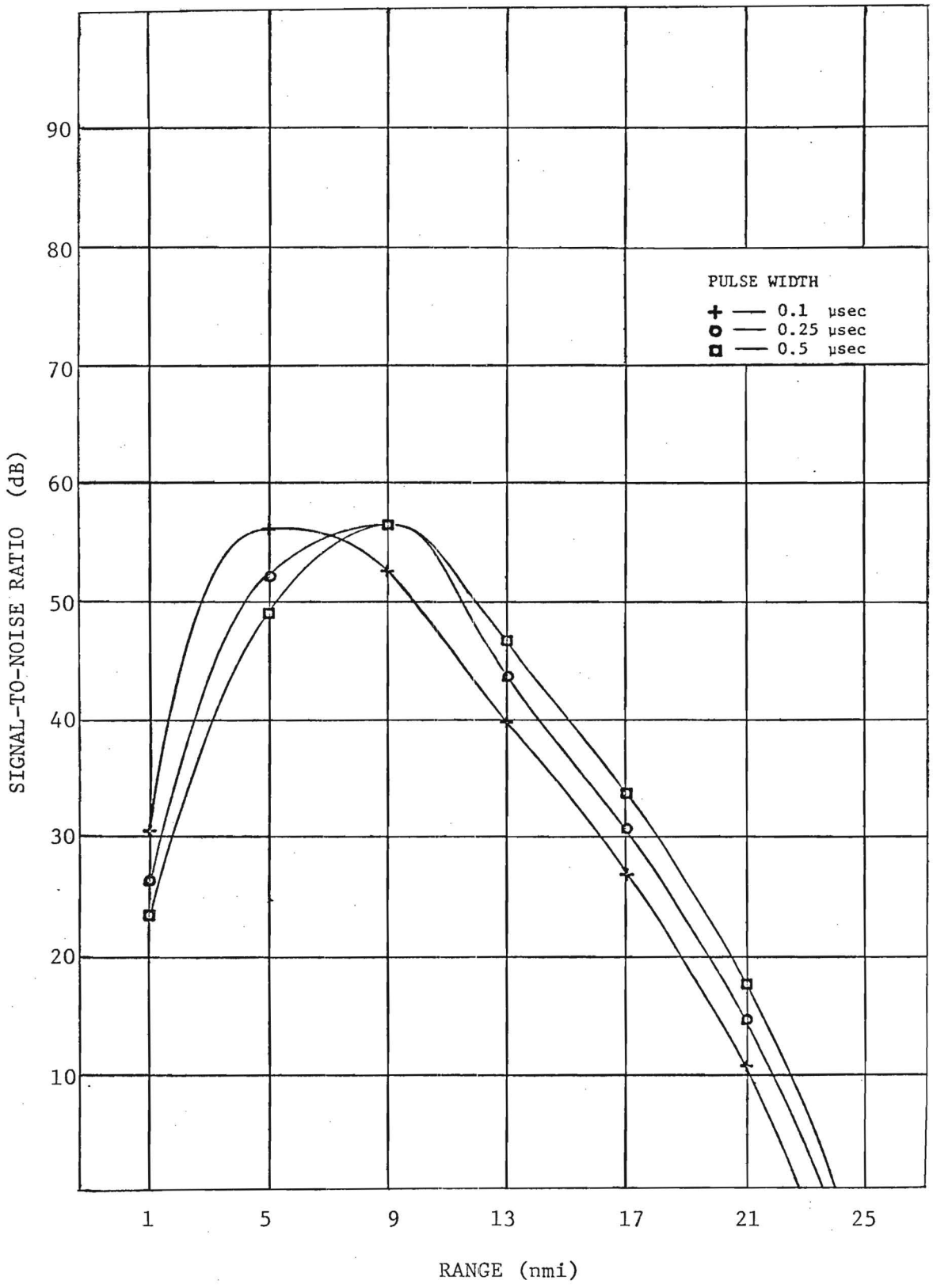

Figure 4. Comparison of Signal-to-Noise Ratios with Pulse Width as a Parameter for a G-Band Radar with an Antenna Height of 100 Feet, Sea State 3, Target II (Approximately 100 Foot Length - See Chapter III, Section B).

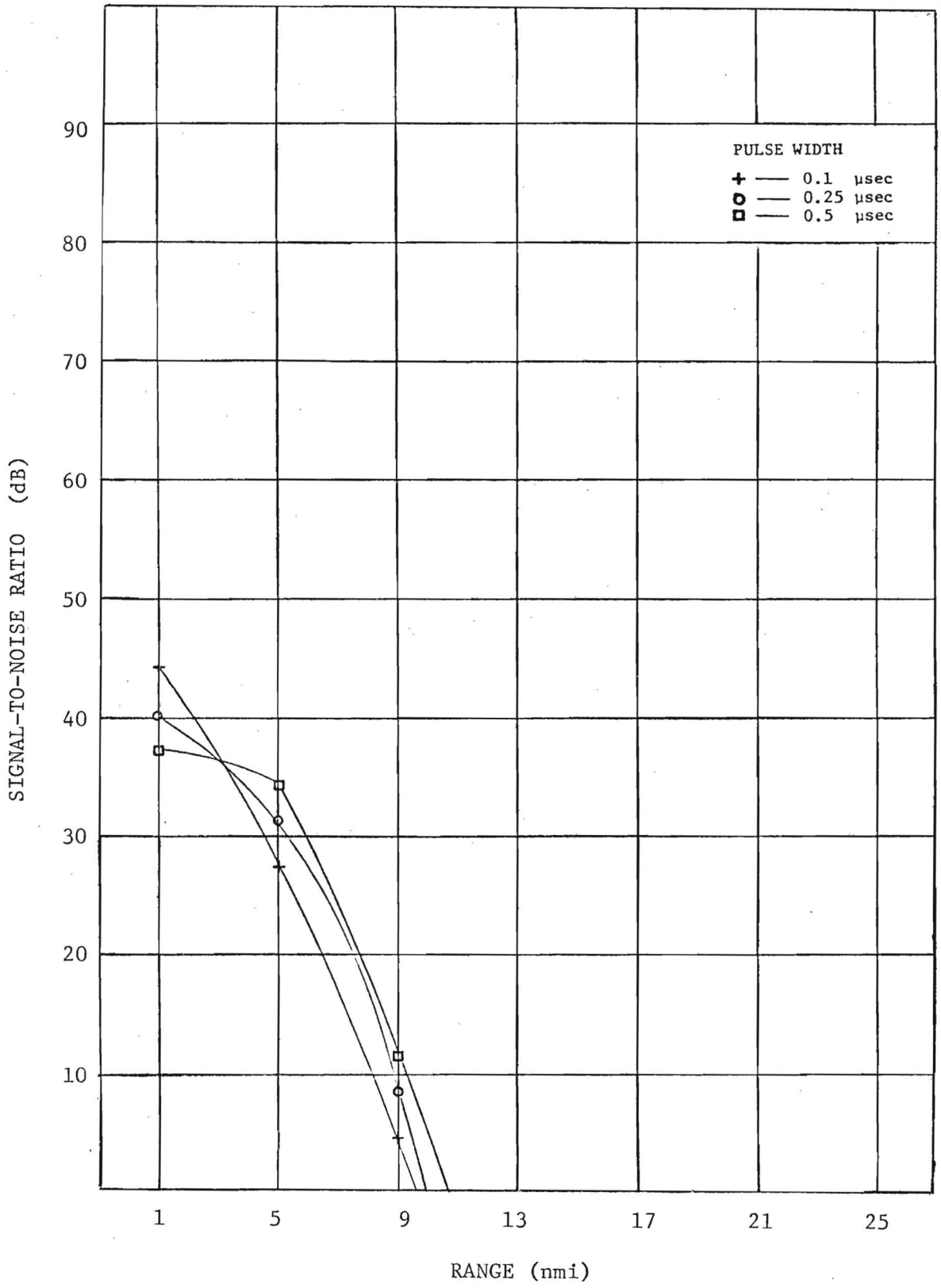

Figure 5. Comparison of Signal-to-Noise Ratios with Pulse Width as a Parameter for a G-Band Radar with an Antenna Height of 100 Feet, Sea State 1, Target III (Approximately 30 Foot Length - Sea Chapter III, Section B).

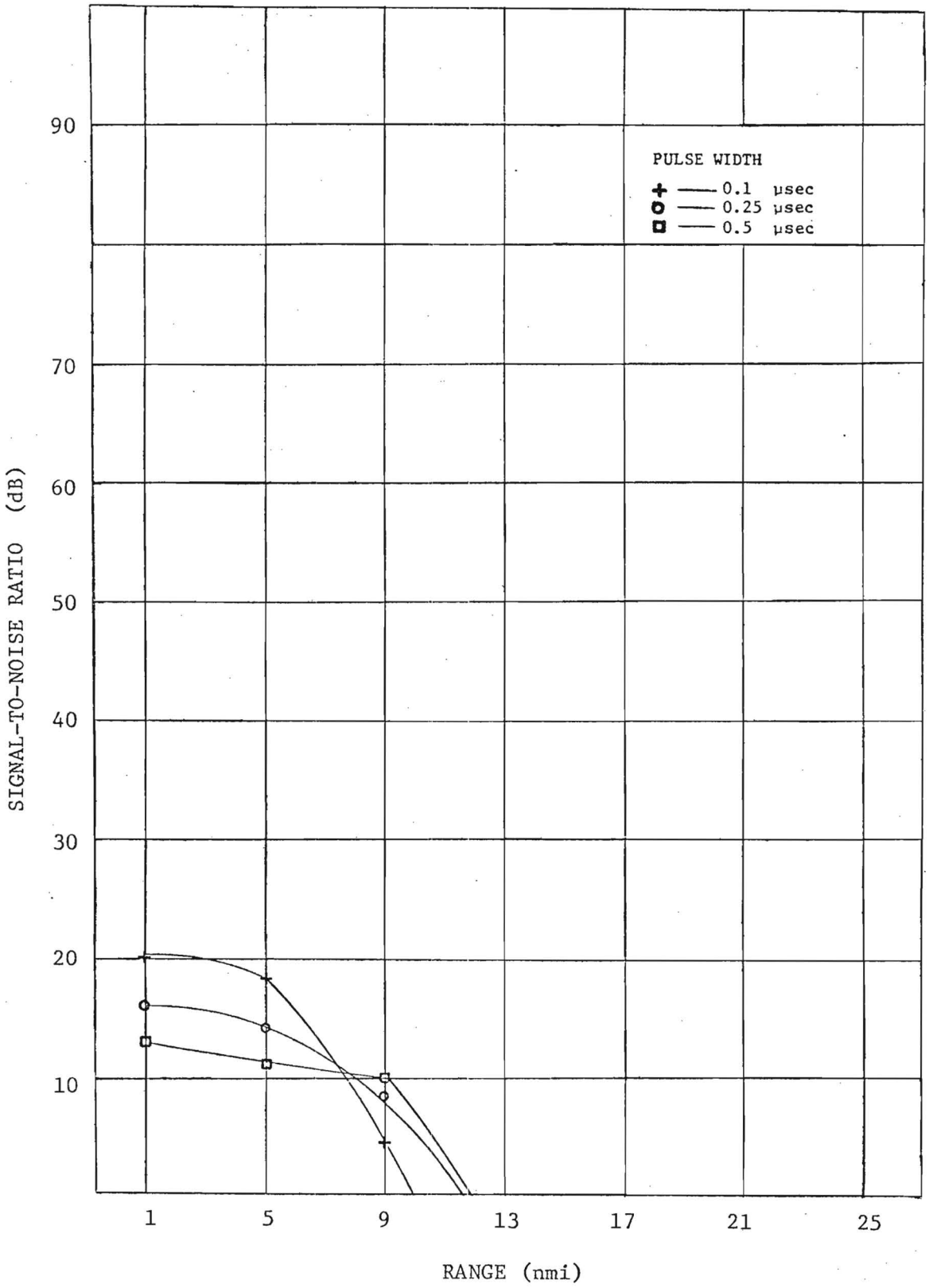

Figure 6. Comparison of Signal-to-Noise Ratios with Pulse Width as a Parameter for a G-Band Radar with an Antenna Height of 100 Feet, Sea State 3, Target III (Approximately 30 Foot Length - See Chapter III, Section B).

E. Transmitter Power

As has been seen earlier, the limiting factor on the detection of large targets for the situation described is antenna height. Thus, selection of peak transmitter power should be made with that constraint in mind. Additionally, for a van-portable system, there are advantages to maintaining the power level as low as possible. Among these factors are: size and complexity of the power supply and modulator, which increase with increasing peak power; waveguide breakdown and arcing considerations; and isolation between transmitter and receiver. Power handling capability of waveguide may be increased by pressurization. However, it would be well to avoid this design complication unless absolutely necessary. Under this consideration the allowable peak power would be in the range of 1.5 MW at F-Band, 500 kW at G-Band, 200 kW at I-Band, and 80 kW at J-Band [13]. Pressurization of the waveguide to 1 psig with Freon-12 can raise these values by as much as a factor of 5.

Figures 7 through 14 illustrate the effect of varying power from 5 to 500 kW on each of the postulated radars. As expected, increased power gives increased signal return. However, the benefits must be weighed against the additional equipment complications incurred. Also, for the larger targets, the rate at which signal strength falls off at long ranges makes the additional range of detection obtained negligible. Thus a power level of about 200 kW seems to be a practical choice for the system. This allows operation with an unpressurized system, reducing significantly the problems associated with erection of a mobile system at an arbitrary site. It provides for a radar much less complicated to build and maintain, factors offsetting the loss in performance. The comparisons given herein were made for a power level of 500 kW; however, the signal-to-noise ratios may be very simply scaled for other choices of transmitter power.

F. Degradation Due to Rain or Fog

Hawkins and La Plant [17] present figures showing the effect of fog and rain on radar operation. Values of attenuation due to fog and rain, and rain backscatter cross-section per unit volume of air (meters^2 per meter^3)

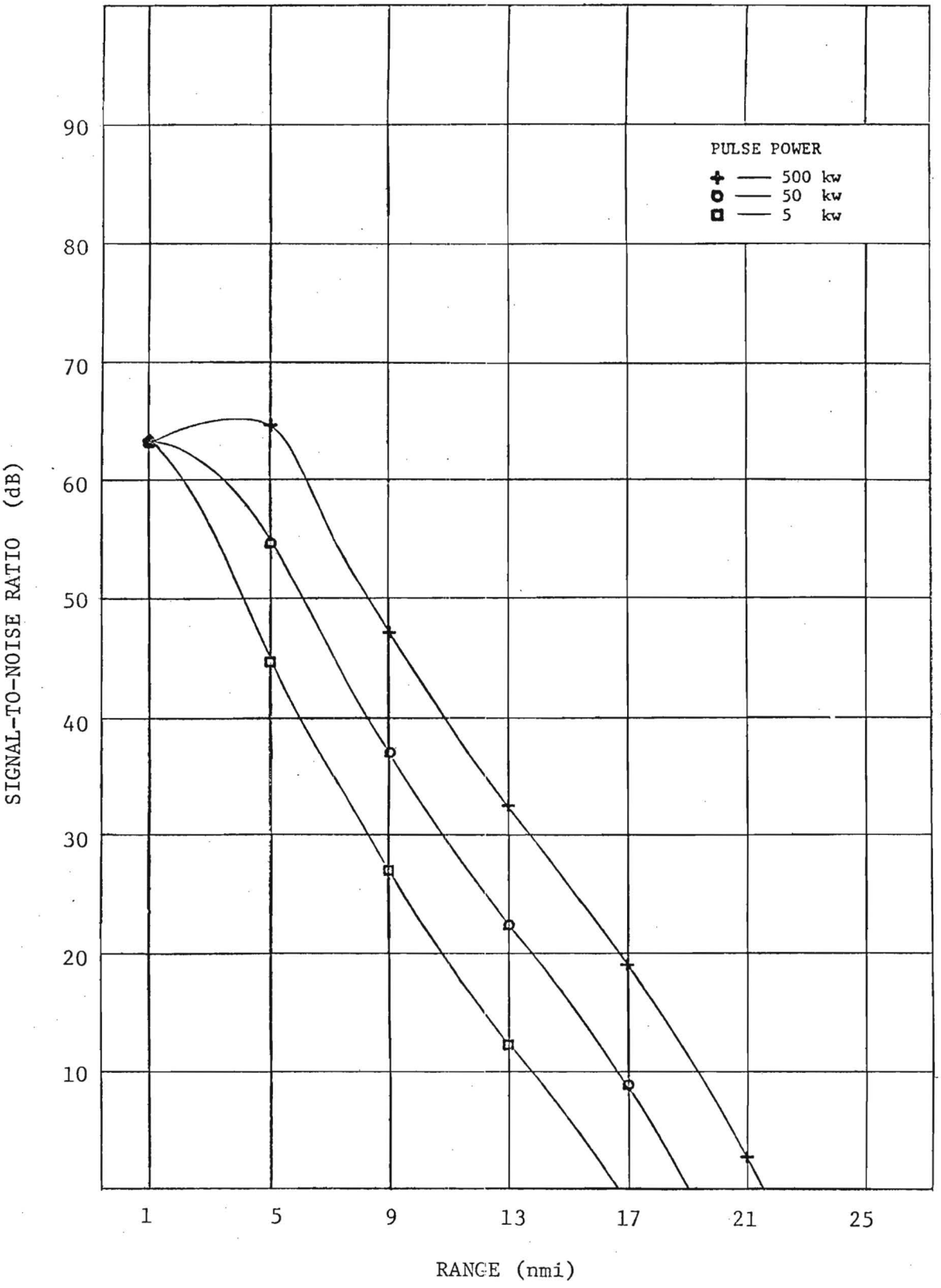

Figure 7. Comparison of Signal-to-Noise Ratios with Peak Power as a parameter for an F-Band Radar with an Antenna Height of 100 Feet, Sea State 1, Target II (Approximately 100 Foot Length - See Chapter III, Section B).

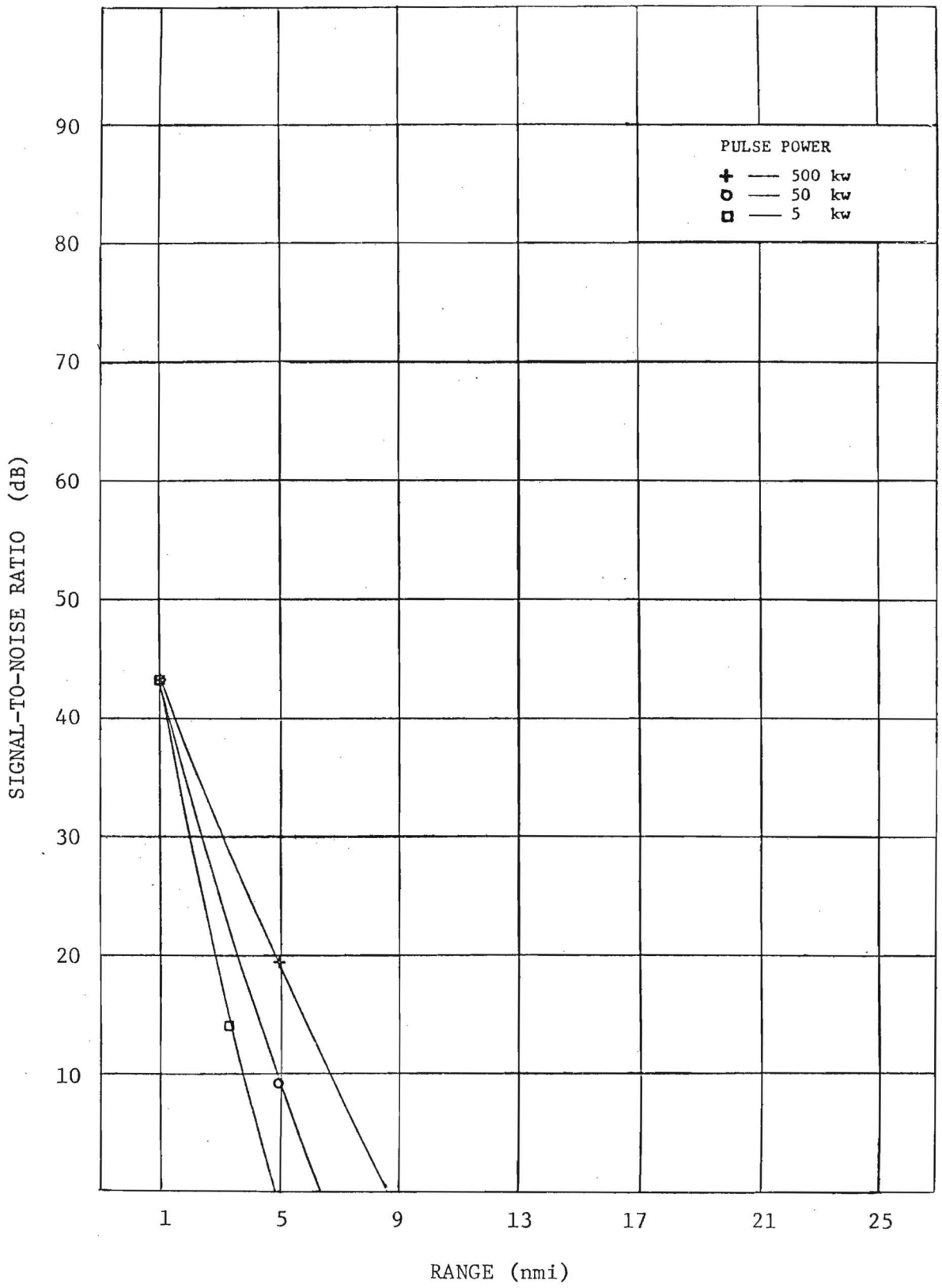

Figure 8. Comparison of Signal-to-Noise Ratios with Peak Power as a Parameter for an F-Band Radar with an Antenna Height of 100 Feet, Sea State 1, Target III (Approximately 30 Foot Length - See Chapter III, Section B).

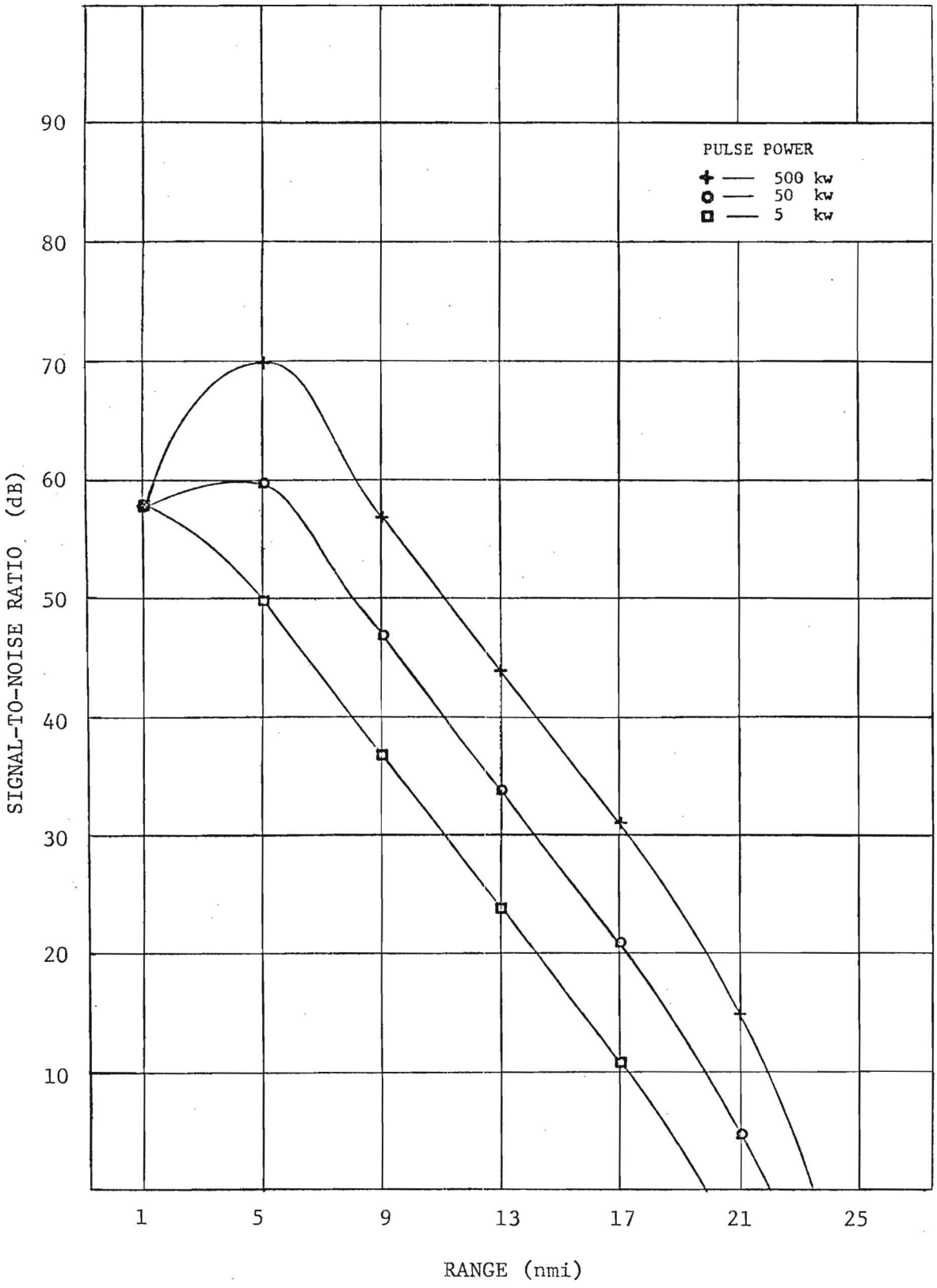

Figure 9. Comparison of Signal-to-Noise Ratios with Peak Power as a Parameter for a G-Band Radar with an Antenna Height of 100 Feet, Sea State 1, Target II (Approximately 100 Foot Length - See Chapter III, Section B).

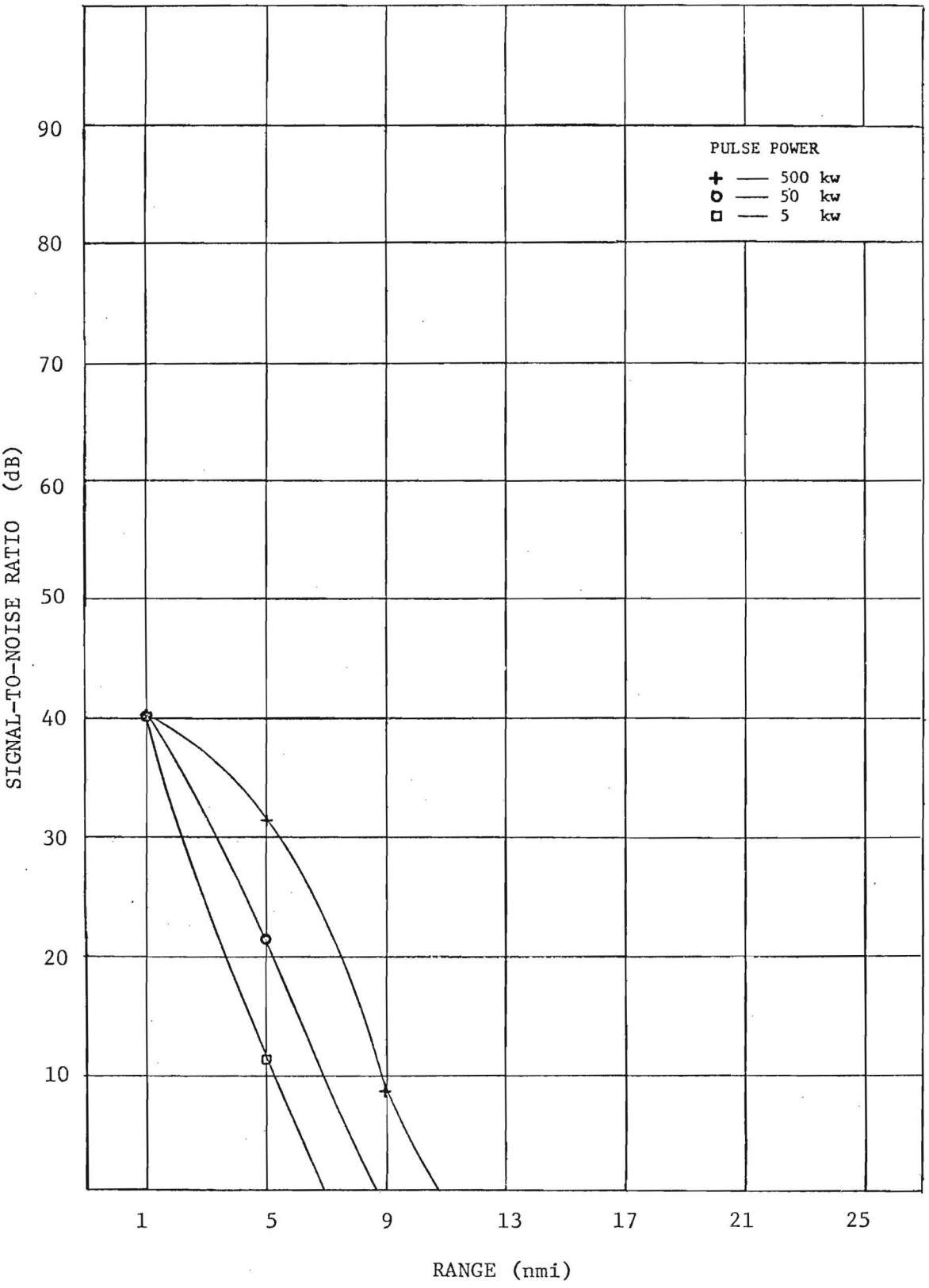

Figure 10. Comparison of Signal-to-Noise Ratios with Peak Power as a Parameter for a G-Band Radar with an Antenna Height of 100 Feet, Sea State 1, Target III (Approximately 30 Foot Length - See Chapter III, Section B).

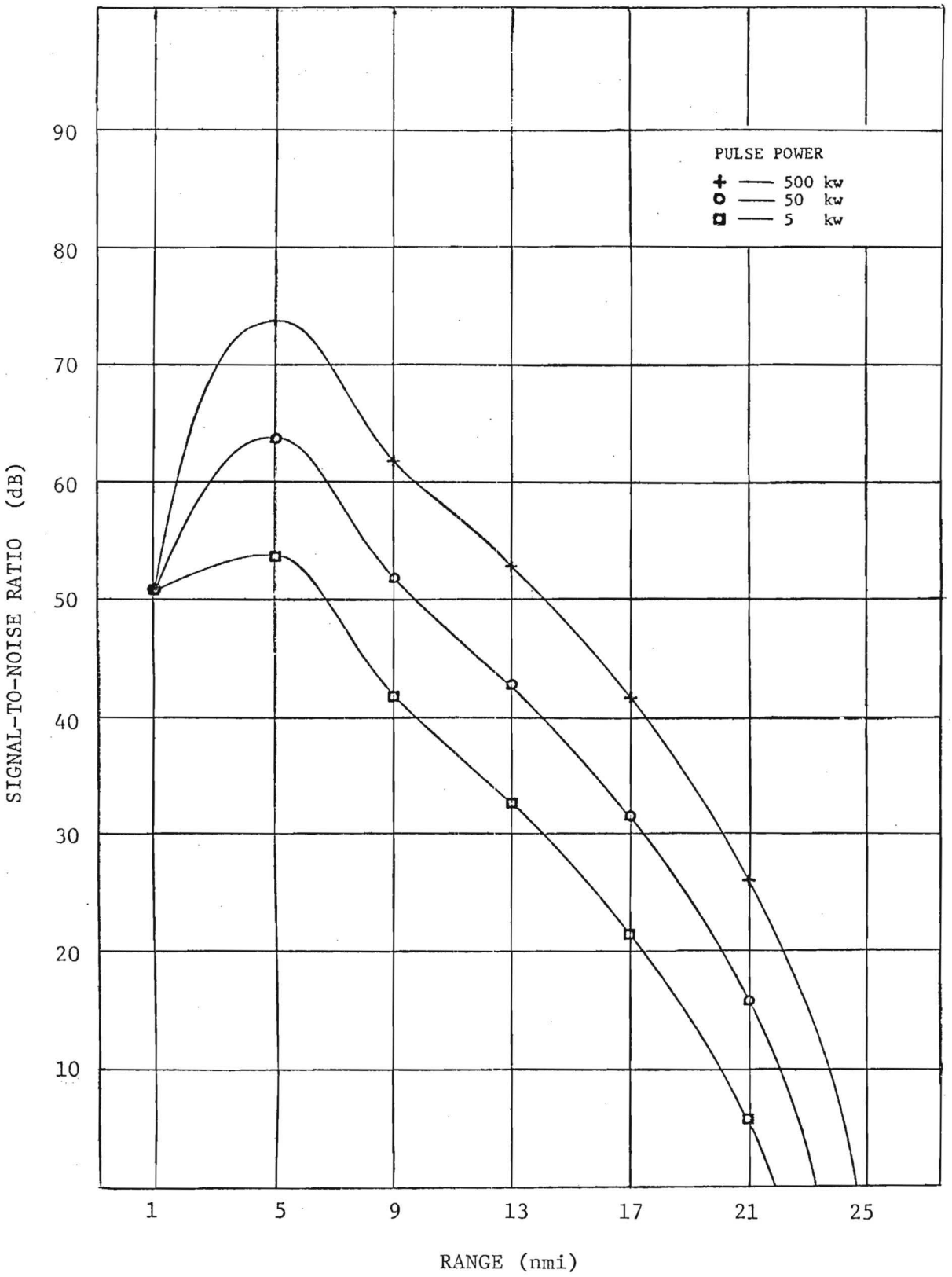

Figure 11. Comparison of Signal-to-Noise Ratios with Peak Power as a Parameter for an I-Band Radar with an Antenna Height of 100 Feet, Sea State 1, Target II (Approximately 100 Foot Length - See Chapter III, Section B).

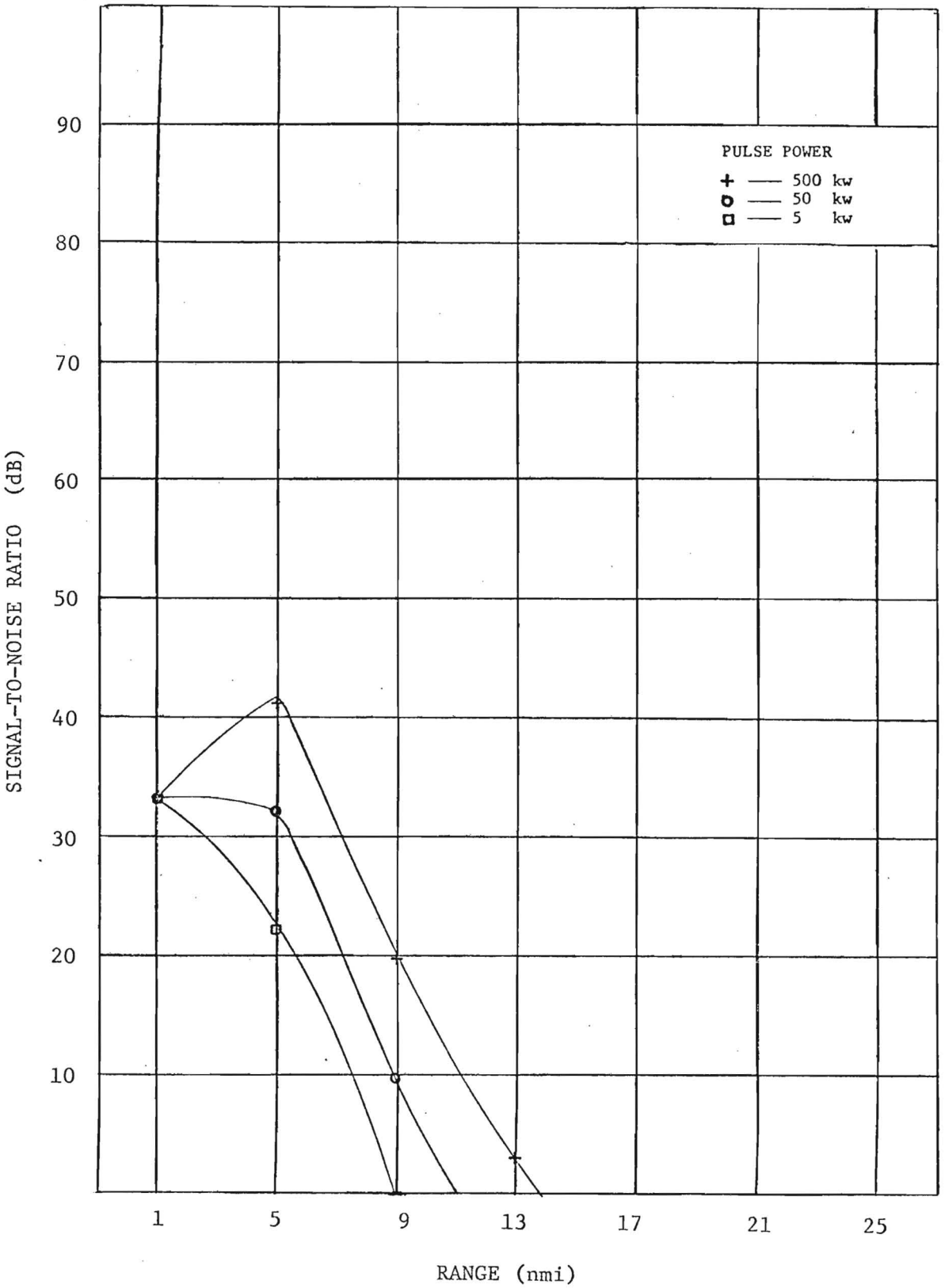

Figure 12. Comparison of Signal-to-Noise Ratios with Peak Power as a Parameter for an I-Band Radar with an Antenna Height of 100 Feet, Sea State 1, Target III (Approximately 30 Foot Length - See Chapter III, Section B).

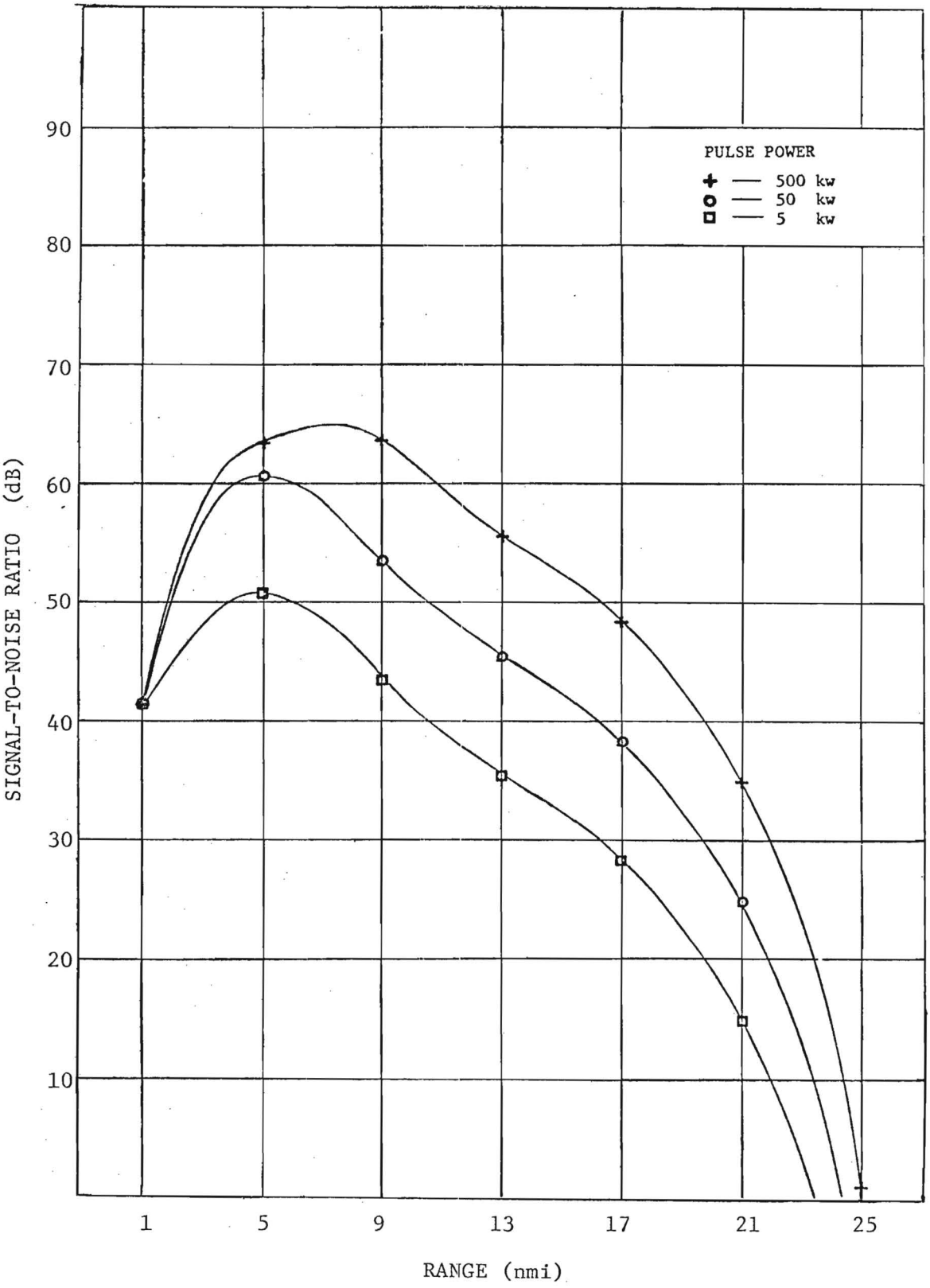

Figure 13. Comparison of Signal-to-Noise Ratios with Peak Power as a Parameter for a J-Band Radar with an Antenna Height of 100 Feet, Sea State 1, Target II (Approximately 100 Foot Length - See Chapter III, Section B).

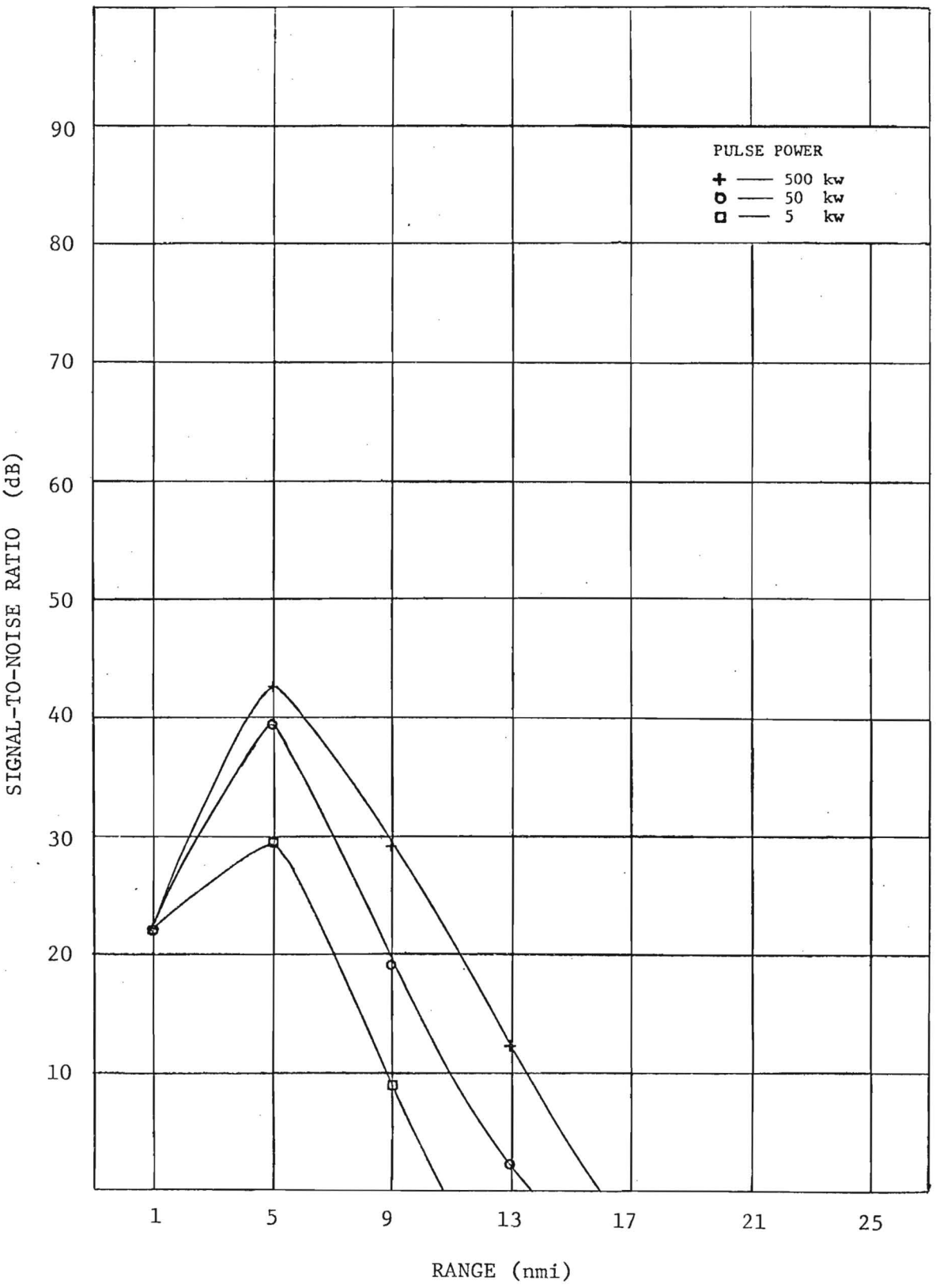

Figure 14. Comparison of Signal-to-Noise Ratios with Peak Power as a Parameter for a J-Band Radar with an Antenna Height of 100 Feet, Sea State 1, Target III (Approximately 30 Foot Length - See Chapter III, Section B).

are reproduced as a function of wavelength in Figures 15, 16, and 17.

These effects are examined in detail in Reference 18 for an example of an I-Band radar with a 100 nsec pulse length and beamwidths of 2.2^{o} in azimuth and 4^{o} in elevation. For a fog allowing a visibility of 100 feet, the two-way attenuation for a range of 10 nmi would be 8 dB at I-Band. For moderate rain and a range of 10 nmi, the attenuation would be 2.4 dB. At G-Band these values have dropped to 2 dB and 0.4 dB, respectively.

The cross-section per unit volume for moderate rain at a wavelength of 3 cm is given in Figure 17 as 1×10^{-6} sq. meter per cubic meter. The volume of a radar resolution cell is given by

$$V \simeq \frac{C\tau}{2} \cdot \frac{\pi R^2 \theta_a \theta_e}{4}$$

For the selected example, with the center of the beam at the surface of the water and for a range of 10 nmi, the volume of rain is 5×10^{6} cubic meters; therefore, the cross-section for moderate rain is

$$\sigma_{HH} = \sigma_{VV} = 5 \text{ m}^2 \text{ or } 7 \text{ dBsm.}$$

For an equivalent size cell at G-Band, the cross-section is

$$\sigma_{HH} = \sigma_{VV} = 0.5 \text{ m}^2 \text{ or } -3 \text{ dBsm.}$$

The improvement at G-Band will normally not be this dramatic, as the cell volume in the case we are considering will be almost twice what it is at I-Band, effectively adding 3 dBsm to the cross-section. However, it is recommended that consideration should be given to operation at the lower frequencies if optimum performance in rain or fog is critical.

G. Polarization and Receiver Considerations for Operation in Sea Clutter or Severe Weather Conditions

For incidence angles of less than 5^{o}, the characteristics of sea

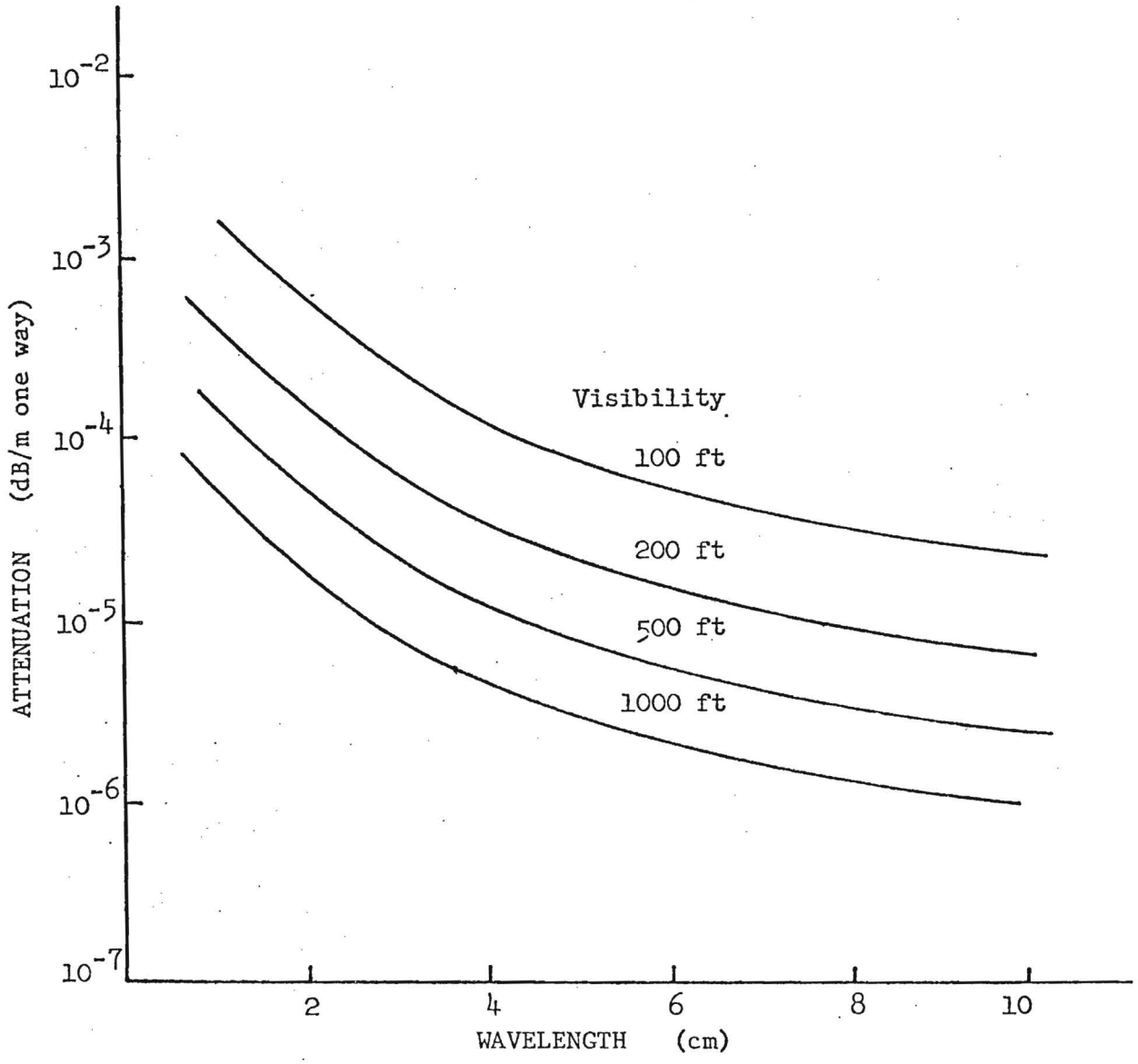

Figure 15. Fog Attenuation.

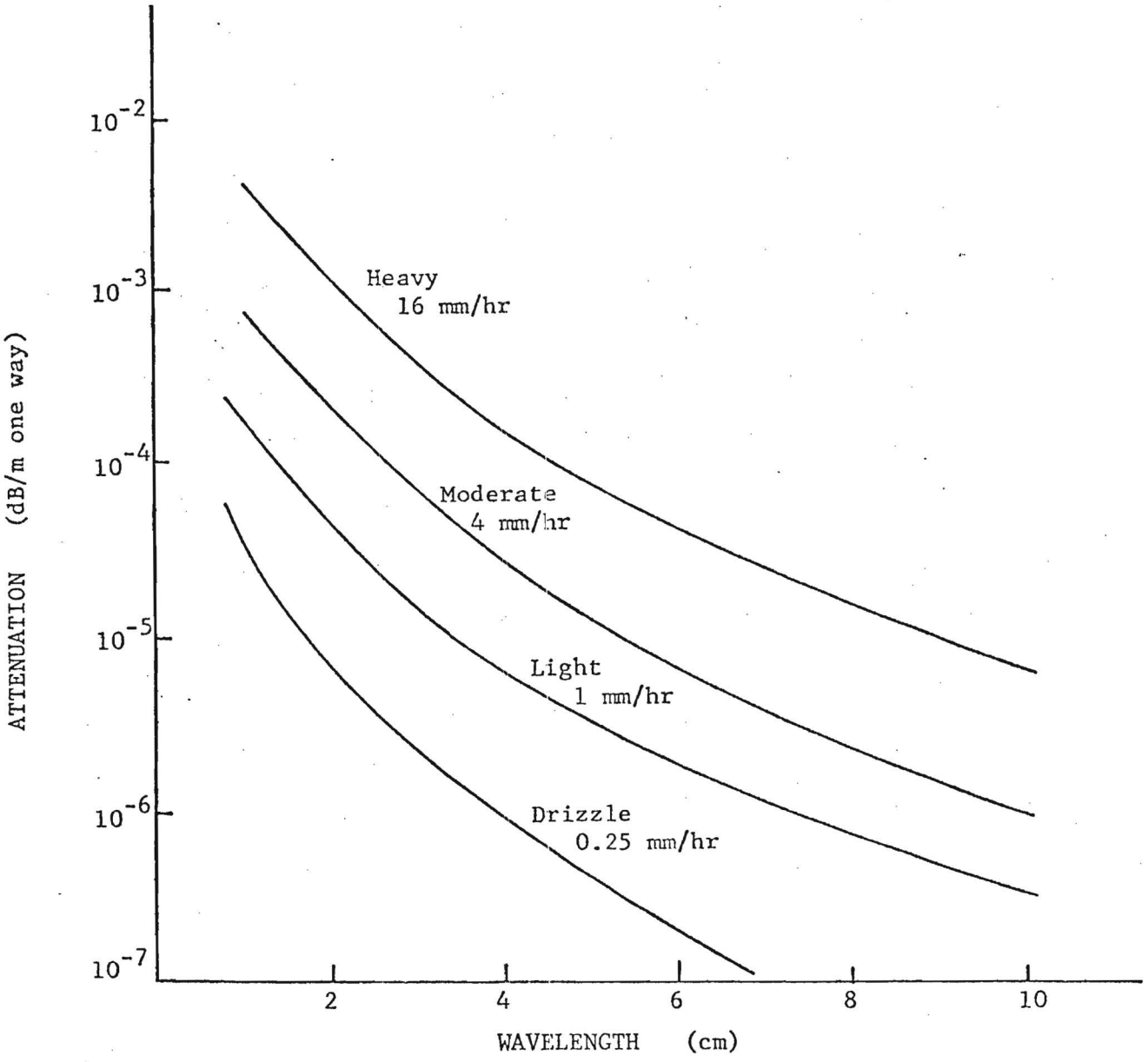

Figure 16. Rain Attenuation.

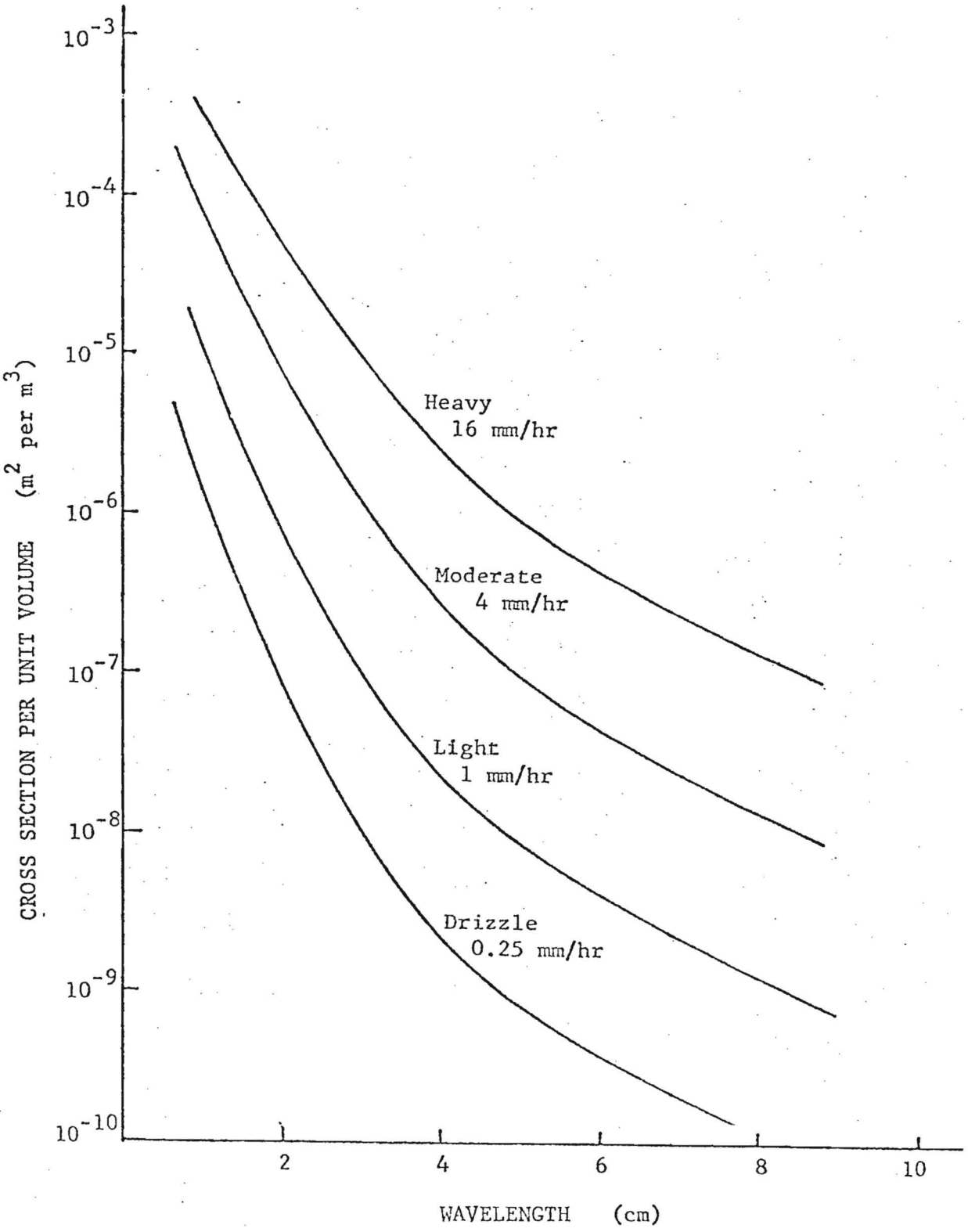

Figure 17. Rain Cross-Section per Unit Volume.

clutter for horizontal and vertical polarization can be summarized as follows [19]:

> Horizontal Polarization - The return for horizontal polarization is spikey in nature and appears to be zero for a considerable portion of the time if a linear receiver is used and gain settings are adjusted to eliminate saturation on spikes. The echo pulses are well defined and appear to have the same shape as that of the transmitted pulse. These pulse-type returns appear and disappear in somewhat periodic fashion; the period of these returns is on the order of seconds.
>
> Vertical Polarization - The return for vertical polarization resembles limited-bandwidth random noise. The fluctuations appear more uniform and very few large isolated spike-like echos can be identified. The dynamic range over which the fluctuations occur is less than that for horizontal polarization and few prolonged periods of very-low-amplitude return occur.

As explained above, the characteristics of sea clutter are vastly different for vertical and horizontal polarization. In addition, for radar return from seas up to Sea State 4, it may be expected that the average cross-section of sea clutter for horizontal polarization will be several dB less than for vertical for upwind and downwind directions, and only slightly greater for cross-wind directions. Based on average values alone, the choice of horizontal transmit-receive polarization seems reasonable. Dr. Croney [20] suggests that the spikey nature of sea return for horizontal polarization may indicate consideration of vertical polarization for a radar to detect targets on the ocean's surface. A major series of measurements by Georgia Tech tends to confirm this behavior for Sea State 2 or greater [21,22]. However, recent data collected by Georgia Tech [23] on small cross-section targets in connection with the Swimmer Defense program indicates consistently higher signal-to-background ratios for horizontal polarization, even after post-detection integration and processing for very low sea states.

Operation in fog or rain presents additional considerations in the choice of polarization. Available data indicate little choice between horizontal or vertical polarization with respect to the cross-section of rain or hail at G-Band over a wide range of precipitation rates [24].

However, reliable data have shown improvements of 10 to 30 dB rain cross-sections for radars using cross-polarized linear or same-sense circular returns [24,25]. For most targets of interest the reduction in cross-section for cross-linear polarization is greater than 10 dB, rendering it less attractive. With same-sense circular return, the loss on most ship targets (i.e., complex scatterers) is low or negligible; however, many marker buoys are odd-numbered reflection devices (i.e., trihedral reflectors). Typical improvements in signal-to-background of 15 dB on ships and boats in heavy rain might be expected.

Superheterodyne receivers are almost universally employed in modern microwave radar systems, usually with AFC (Automatic Frequency Control). Because of reliability considerations, crystal mixers are used and typical noise figures are about 9 dB at I-Band. This is by no means the best which may be accomplished. Commercial mixers using quad Schottky diodes are available which provide a 6 dB noise figure at 10 GHz. Use of a parametric amplifier as an RF stage can provide noise figures of 4 to 5 dB at 10 GHz. Use of a cryogenic maser can provide a noise figure of a few tenths of a dB; but, except for applications such as satellite communications, the cost and complexity are not warranted. Thus, in construction of an optimum radar, a noise figure of 6 dB seems reasonable to assume at I-Band.

Reduction of noise through use of an improved receiver obviously provides a better signal, whatever the clutter or weather conditions; however, other steps should be taken to enhance operation under sea clutter or rain conditions since under conditions where clutter is important, target-to-clutter ratio rather than target-to-noise ratio is the key factor. The use of a logarithmic receiver characteristic is an important step, as a large class of clutter-reduction schemes are based on its properties [26]. For example, if clutter echoes may be described as Rayleigh distributed, the function of a sensitivity time control circuit (STC) may be automatically provided by a logarithmic receiver followed by differentiation (FTC or fast time constant circuit). The resulting clutter output is theoretically independent of range. Even under actually observed clutter conditions, this approach provides a remarkably good STC function at low costs. In addition, a wide dynamic variation in signal strength may be

handled easily, as commercially available logarithmic IF sections can typically handle an 80 dB dynamic range.

Figures 18-21 present what might be expected from each of the postulated radars in detection of typical targets. Parameters are chosen as shown in Table XI with 500 kW as the output power and 0.25 μsec as the pulse width. Note that for both targets in a State 1 sea, the higher frequency systems provide a longer detection range. However, Figures 19 and 21 illustrate the degradation in signal experienced in the higher State 3 sea, particularly at J-Band. Experience has shown that this is the case in actual operating situations [23]. For this reason, coupled with parts availability, reliability, and operation in rain or fog, G- or I-Bands present a more logical selection for the system chosen.

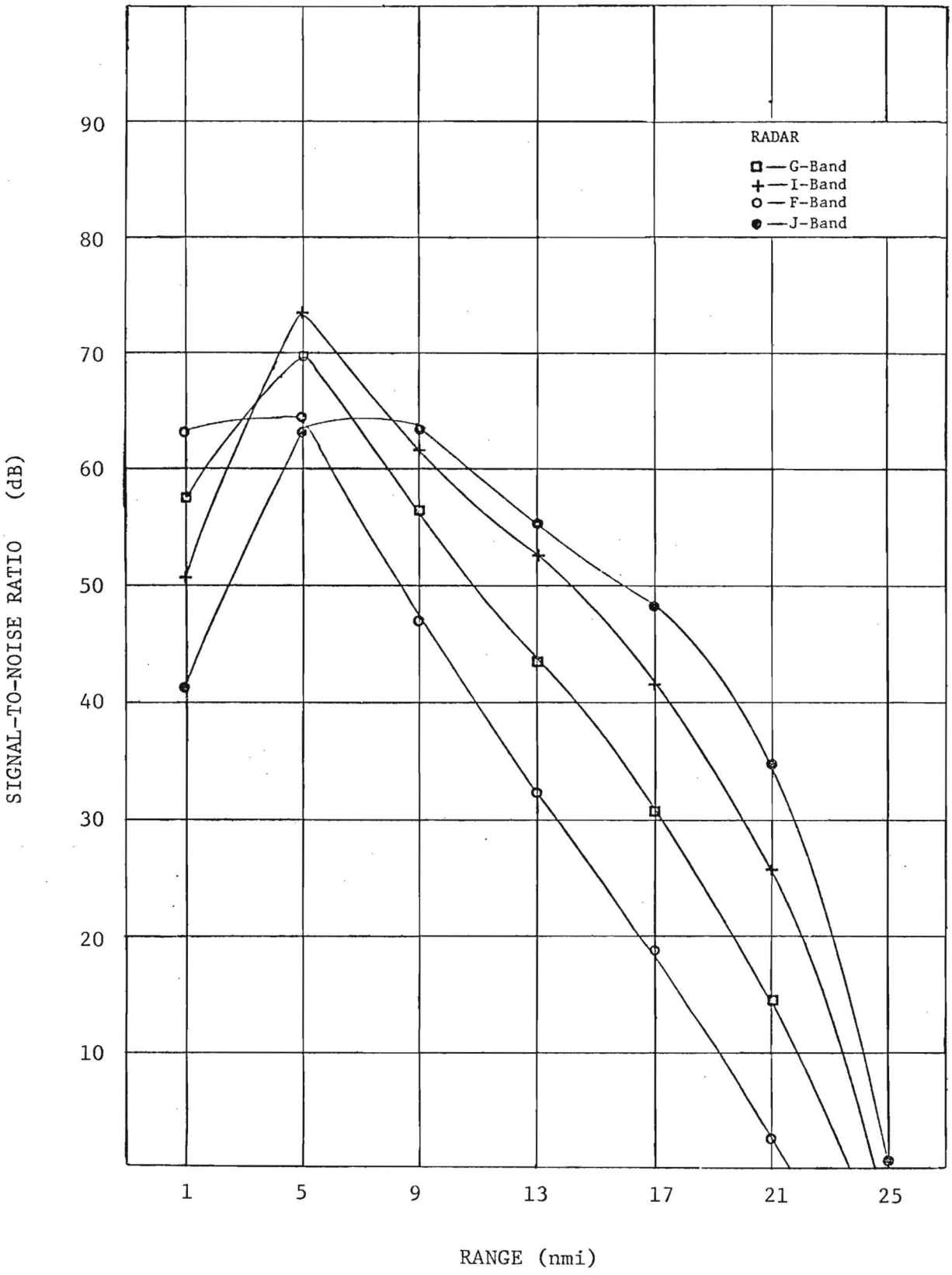

Figure 18. Comparison of Signal-to-Noise Ratios for Radars Listed in Table XI with an Antenna Height of 100 Feet, Sea State 1, Target II (Approximately 100 Foot Length - See Chapter III, Section B).

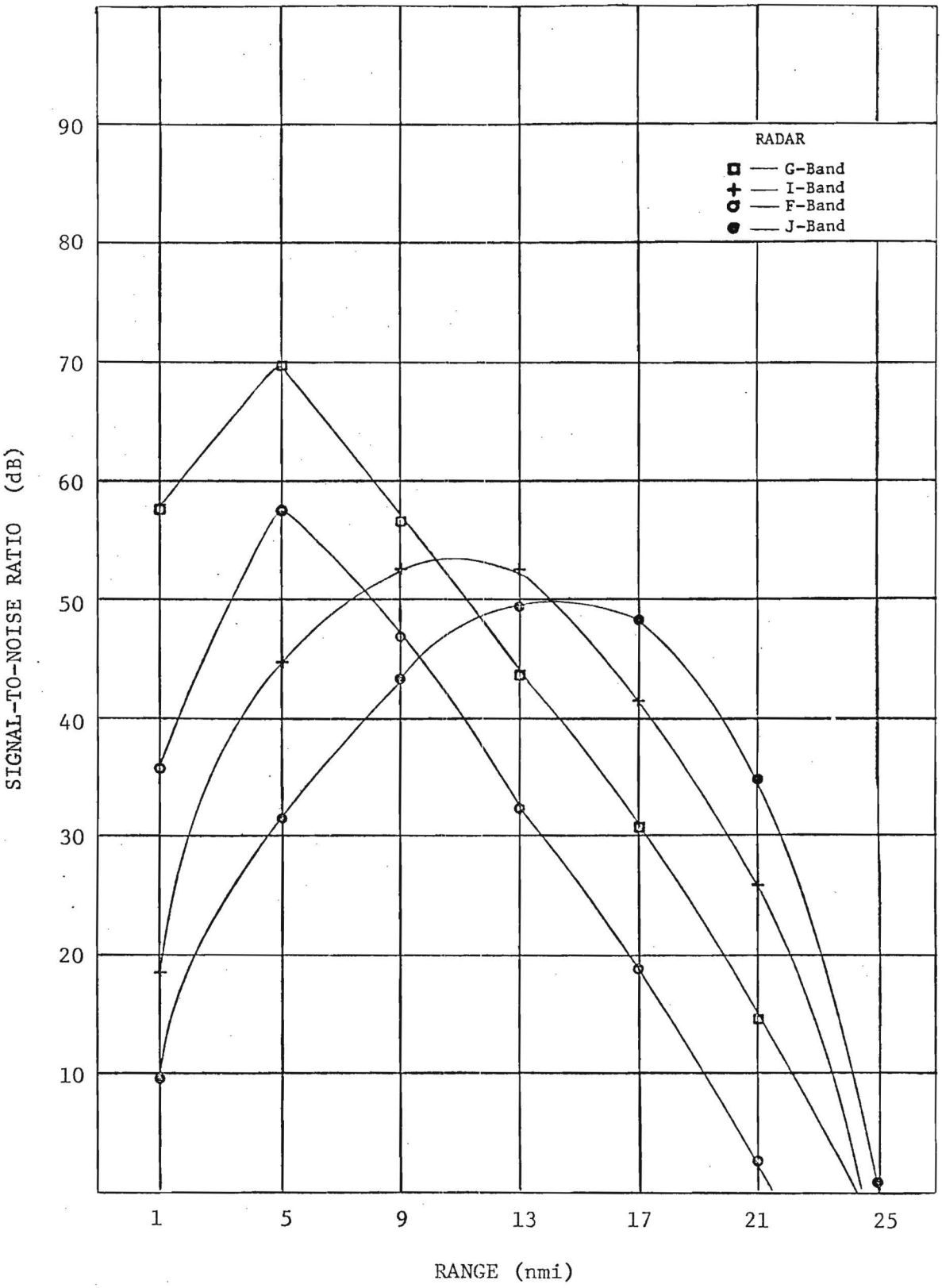

Figure 19. Comparison of Signal-to-Noise Ratios for Radars Listed in Table XI with an Antenna Height of 100 Feet, Sea State 3, Target II (Approximately 100 Foot Length - See Chapter III, Section B).

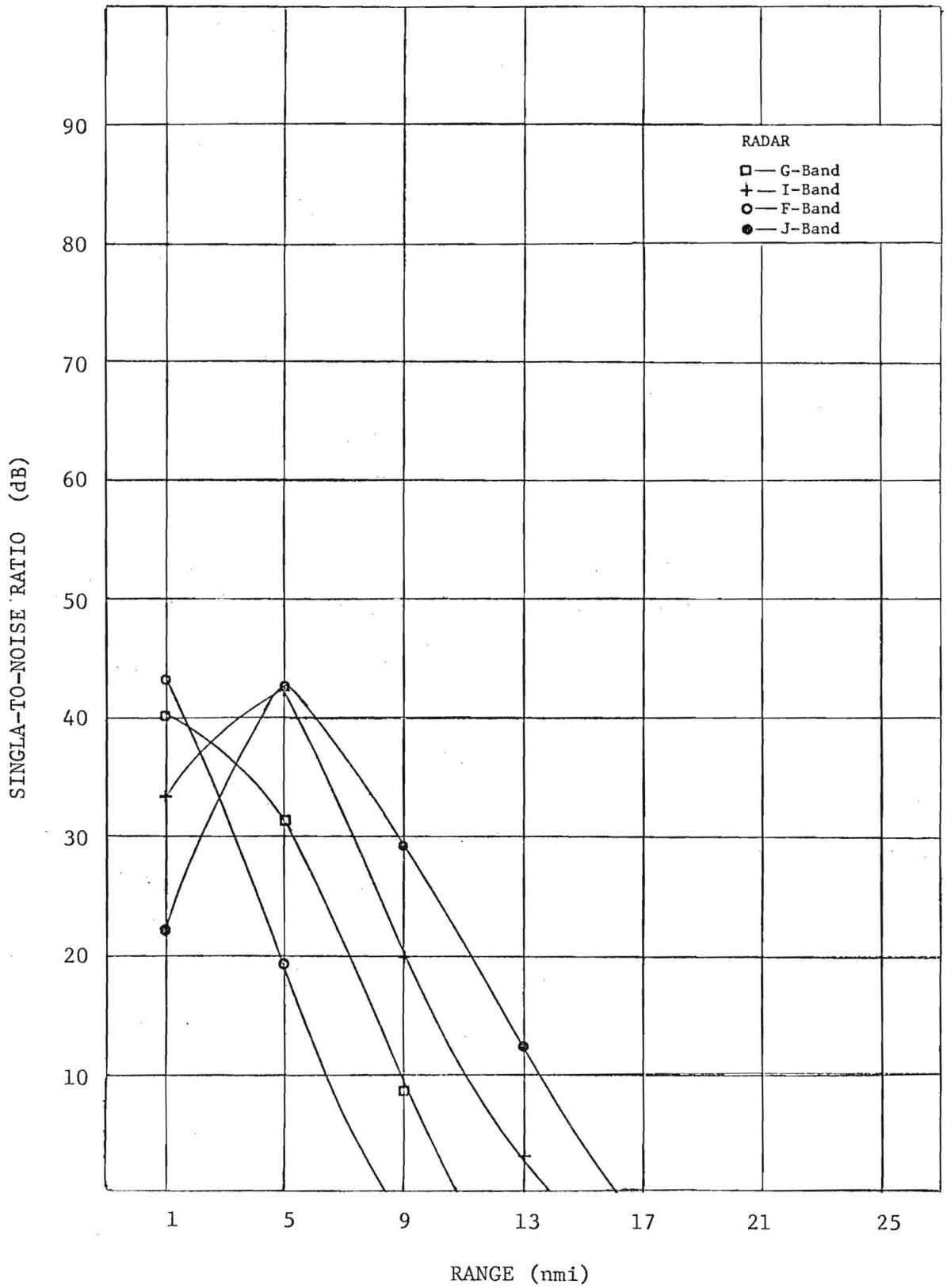

Figure 20. Comparison of Signal-to-Noise Ratios for Radars Listed in Table XI with an Antenna Height of 100 Feet, Sea State 1, Target III (Approximately 30 Foot Length - See Chapter III, Section B).

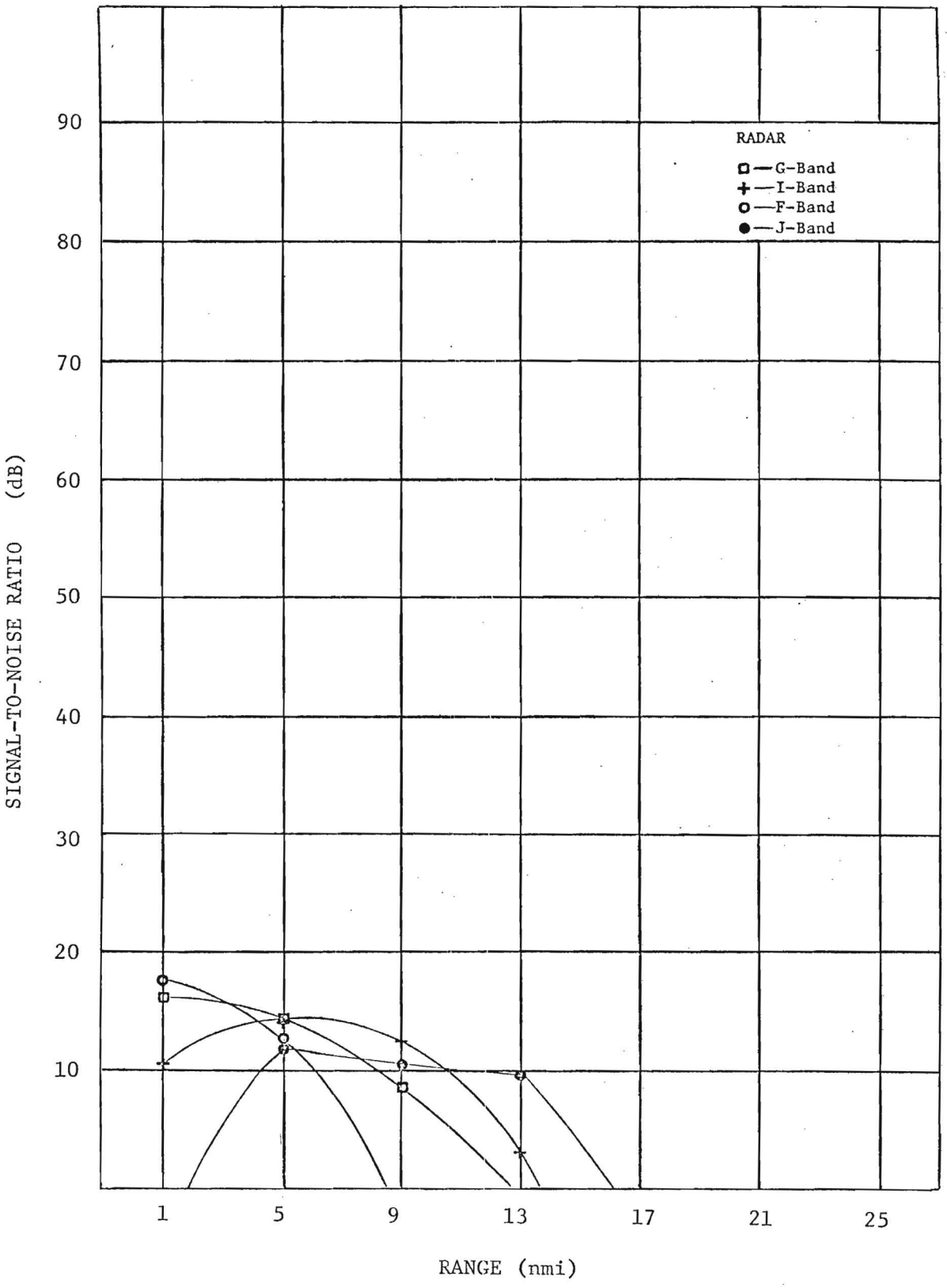

Figure 21. Comparison of Siganl-to-Noise Ratios for Radars Listed in Table XI with an Antenna Height of 100 Feet, Sea State 3, Target III (Approximately 30 Foot Length - See Chapter III, Section B).

III. Performance of Candidate Systems

A. Discussion of Systems Selected for Analysis

The necessity of providing a demonstration surveillance system by June 1974 constrains the system that can be chosen. There is insufficient time to develop a new radar, and thus the existing systems must be evaluated for their potential in monitoring harbor traffic. Table XII lists a number of commonly available shipboard surface-search radars. This list is not intended to include all potential radars that might be used. However, it is believed that the radars listed adequately represent the radars which are available. From this list, radars showing promise for the desired surveillance application are analyzed. Chosen from F-Band (3.0 GHz) is the Decca TMS-2400, from G-Band (5.6 GHz) the AN/SPS-10, and from I-Band (9.4 GHz) the AN/SPS-53 and LN-66 (High Power). In addition, to demonstrate performance at J-Band (16.5 GHz) the AN/ASQ-42 is considered. To set an upper bound on obtainable performance, the AN/APS-116, which is the present state-of-the-art in airborne surface-search radar, is also analyzed.

B. Explanation of Target Models for Analysis

Performance of each of the radars is, of course, closely tied to the antenna height and the type of target to be detected. For this study three targets are considered as typical the harbor traffic situation. Figure 18 indicates the model used in the computer program to simulate each of the targets. As noted in Chapter I, cylinder sizes are chosen to reproduce the effective cross-section of the target. Target Type I simulates ocean-going vessels of the destroyer class or larger. Target Type II is sized to resemble boats typically 100 to 150 feet in length such as large patrol craft or large fishing boats. Target Type III simulates much smaller boats such as a 20-30 foot pleasure craft or small fishing boat.

It is anticipated that these target classes are adequate for use in realistically assessing the detectability of craft encountered in monitoring harbor and coastal traffic. An additional case not considered explicitly herein is that of very small boats which are close to the water (e.g. rubber

TABLE XII

Marine Radar Specifications

Mfg.	Model	Freq GHz	Ant Gain dB	Az bw Deg	El bw Deg	Pol	Scan Rate rpm	PRF Hz	Peak Power kW	Pulse Length μs	N.F. dB	IF band MHz	Displ dia inch	Displ range nmi
U. S. Coast Guard	AN/SPS-57	9.4	(26.0)	1.9	23-30	HH	25	2K/1kHz	3	0.1/0.5	12.5	(10/2)	7	.5,1,2,4,8, 16 nmi
U. S. Navy	AN/SPS-10	5.6	31	1.5	12-16	HH	15	625	285	0.25/1.3	15	(5/1)	9	1,2,5,10 50 nmi
Sperry (3)	AN/SPS-53	9.4	(27.2)	1.6	20		15	1.5k/750	35	0.1/0.5	11	(12/4)		0.5 - 32
Kelvin Hughes (1)	17R	9.45	27	1.2	25	HH	24	2.2k/1.1k	3	.05/.2/.5	13	30 MHz	4 or 9	.3,.6,.9,1.2, 1.5,2.5,5,10
Kelvin Hughes (1)	14/9R2us	9.4	27 or 30	1.2 or 0.7	25	HH	24	1.1kHz	60	.05/.3	(12)	20 MHz	9	.25,5,1,1.5, 3,6,12,24,48
Kelvin Hughes (1)	19/9 or 12	9.45	31 or 32	1.0 or 0.75	18	HH	24	3.2/1.60.8k	25	.05/.25/.75	11	25/15/5MHz	12	.25,.5,.75, 1.5,3,6,12 24,48
Decca (3)	D-202	9.4	(25.2)	1.9	27		24	1k	3	0.1/0.5	12.5	(10/2)	7.5	0.5 - 24
Decca (3)	D-101	(9.4)	(25.2)	1.9	27		24	3k	3	.08/.25	(12)	(12.5/4)	7	0.5,1.5,5,15
Decca (2)	RM316	9.4		1.2				2k/1k	10	.05/.15/.5			9	0.5,.75,1.5,3 6;12,24,48
Decca (2)	RM326	9.4		1.2				2k/1k/500	25	.05/.15/.5/1.2			9	do
Decca (2)	TMS2400	3.4		2.0	(27)		24	1k	75	.1/.5	(11)	(10/2)	16.5	.75,1.5,3,6, 12,24,60
Raytheon (3)	1500	(9.4)	(26.6)	2.2	17		20	1.5k/750	7	0.2	(12)	(5)	10	0.5,1,2,4,8,16
Raytheon (2)	1640	9.4		.6				4k/1k	40	.05/.5			16.5	.5,1,2,4,8 20,50

TABLE XII (Cont.)

Mfg.	Model	Freq GHz	Ant Gain dB	Az bw Deg	El bw Deg	Pol	Scan Rate rpm	PRF Hz	Peak Power kW	Pulse Length μs	N.F. dB	IF Band MHz	Displ dia inch	Displ range nmi
Raytheon (2)	1650A	3.4		1.9				4k/1k	60	.05/.5			16.5	do
Raytheon (3)	1900	(9.4)	(23.2	3.0	27		20	2k	35	0.14	(12)	(7)	7	0.5,2,6,12
Raytheon (3)	2502	9.4	(26.6)	1.6	23		80	6k/2k/1k	20	.05/.5/1	12	8	10	0.5-48,24, 1.5,3,6,12
Bendix (3)	MR4	9.4	(23.4)	2.6	30		21	1.2 k	5	0.25	(12)	8	7	0.5 - 16
Bendix (3)	MR5	9.4	(23.4)	2.6	30		21	1.6k/625	7.5	.1/.4	(12)	(10/2.5)	7	0.5,2,4,8,16
RCA (3)	N3B3	9.4	(24.2)	3.2	20		25	2.3/1.1k	3	0.1/0.25	(12)	8		0.5 - 18
RCA (3)	N6A-10	(9.4)	(25.8)	1.8	25		20	800	1	.1/.6	(12)	10	7	0.5,1.5,4,12, 32
Phillips (3)	8GR260/00	9.4	(32.2)	0.6	17		40	2.5k	20	0.04	(12)	40		.3 - 2.5
Canadian Marconi (3)	LN-66	9.4	(31)	.93	24	HH	15	1.5k	75	.05/.1	12	20	10	0.5 - 16
USSR (2)	Lotsiya	9.4		1.5				1.6k/800	6	0.1/0.3			5	0.5,1,2,4,8,16
USSR (2)	Okean	9.4/3.4		0.75/2.3				2.55k/850	80	0.1/1.0			18	1,2,4,8,16,32, 64
Japan Radio (2)	JMA123	9.4		1.8				800	8	0.1/10.6			7	1,3,8,15,30
Japan Radio (2)	JMA131	9.4		1.0				2.5k/500	40	0.1/10.8			12	0.5,1,2,4,8,20, 60
Raytheon	AN/ASQ-42	16.5	33	1.3		HH		2050	100	.33	14	7	7	

NOTES: (1) Source; Manufacturer's Specifications
(2) P.J. Stahnke,"Small Boat Radar Evaluation,"Technical Memorandum Naval Electronics Laboratory Center, 18 Oct 1968
(3) K.N. Chernyayev and I.U. Lyubchenko, "Prospects for Developing Shipborne Radar," Sudostroyeniy, 229, (1968)

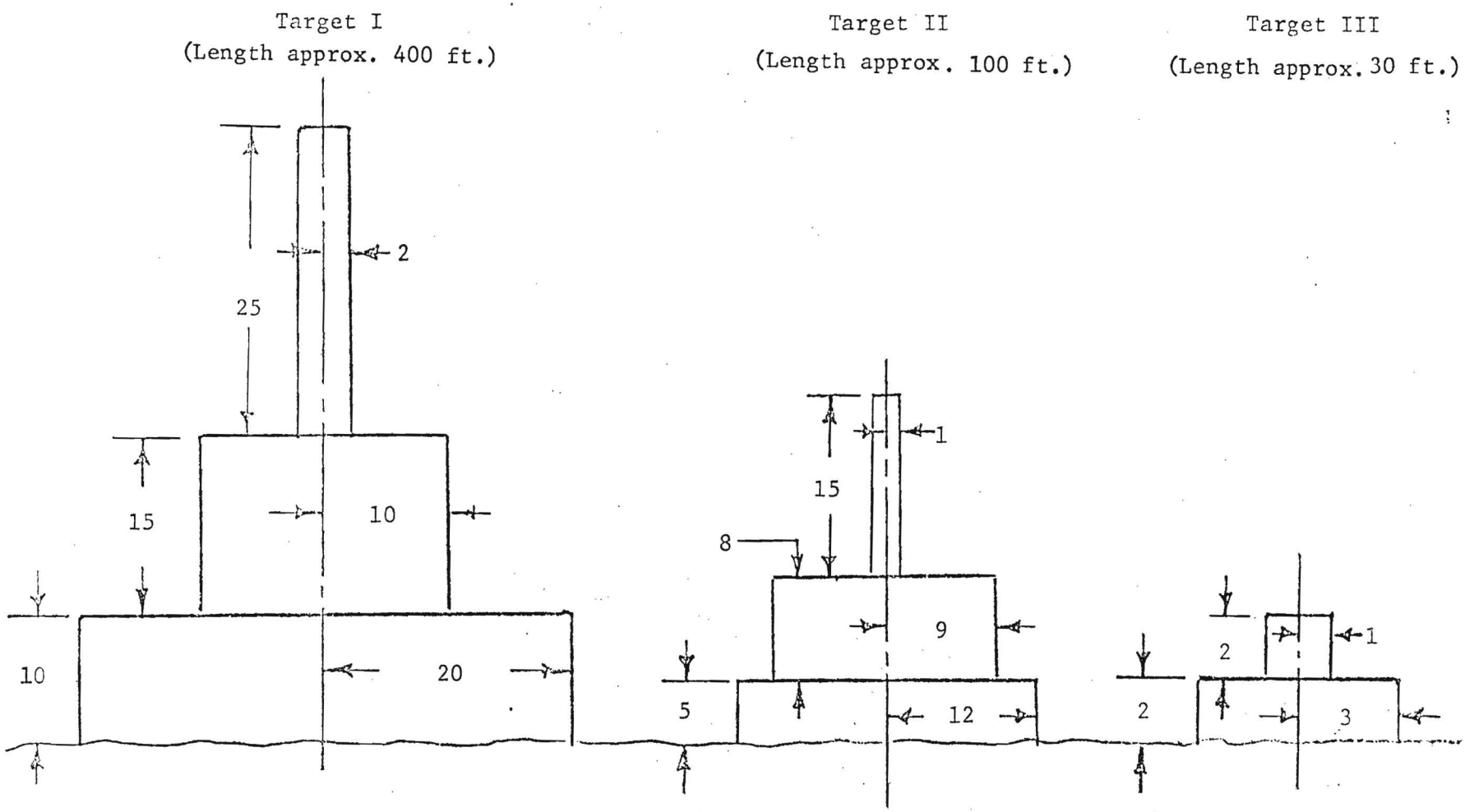

Figure 22. Stacked Cylinder Models of Various Ship Types as Entered into the Radar Prediction Computer Program.

rafts, row boats, etc.) The extremely small cross-section of such vessels makes their detection at ranges greater than a few miles virtually impossible, and at shorter ranges it is envisioned that they would become the province of the Swimmer Defense (S2705) System [4]. The system described in this study would have some capability for detecting small boats, but it is not considered optimum for such use.

C. Performance of the Selected Systems

In this section performance of each radar is evaluated against the three target models. Comparison is made between radars, and the limitations inherent in each situation are discussed. In addition, antenna heights of 30, 60, and 100 feet are considered to determine the resulting change in system effectiveness. For each target situation, the signal-to-noise ratio (S/N) required for a 50% probability-of-detection (P_D) is dependent on the probability of false alarm (P_{FA}) that can be tolerated [5]. Figure 19 is an illustration of the signal-to-noise ratio which must be achieved for a given probability-of-detection with probability of false alarm as a parameter in a log-normally distributed sea-clutter background. For the purpose of these comparisons, the probability of false alarm is defined as the probability per radar cell during one scan of falsely indicating the presence of a target when none exists. Both the target return and the clutter return are assumed to fluctuate with a log-normal distribution; however, the signal-to-noise required for a given P_{FA} and P_D is dependent on the actual statistics. Figure 19 is realistic for the smaller target in sea clutter and is useful as a bound in all cases considered here. The graph may be used with the figures which follow to convert signal-to-noise ratio into a single-scan probability-of-detection.

Figure 20 illustrates the signal-to-noise ratio versus range obtained with Target I for each of the six radars, all having an antenna height of 100 feet. From Figure 2, an antenna height of 100 feet corresponds to an optical horizon of 12.3 nmi, and past that point some portion of the target will be obscured. Thus, the limiting factor for a large target, such as Type I, is the horizon which depends upon antenna and target height rather than to radar power. Indeed, all radars investigated

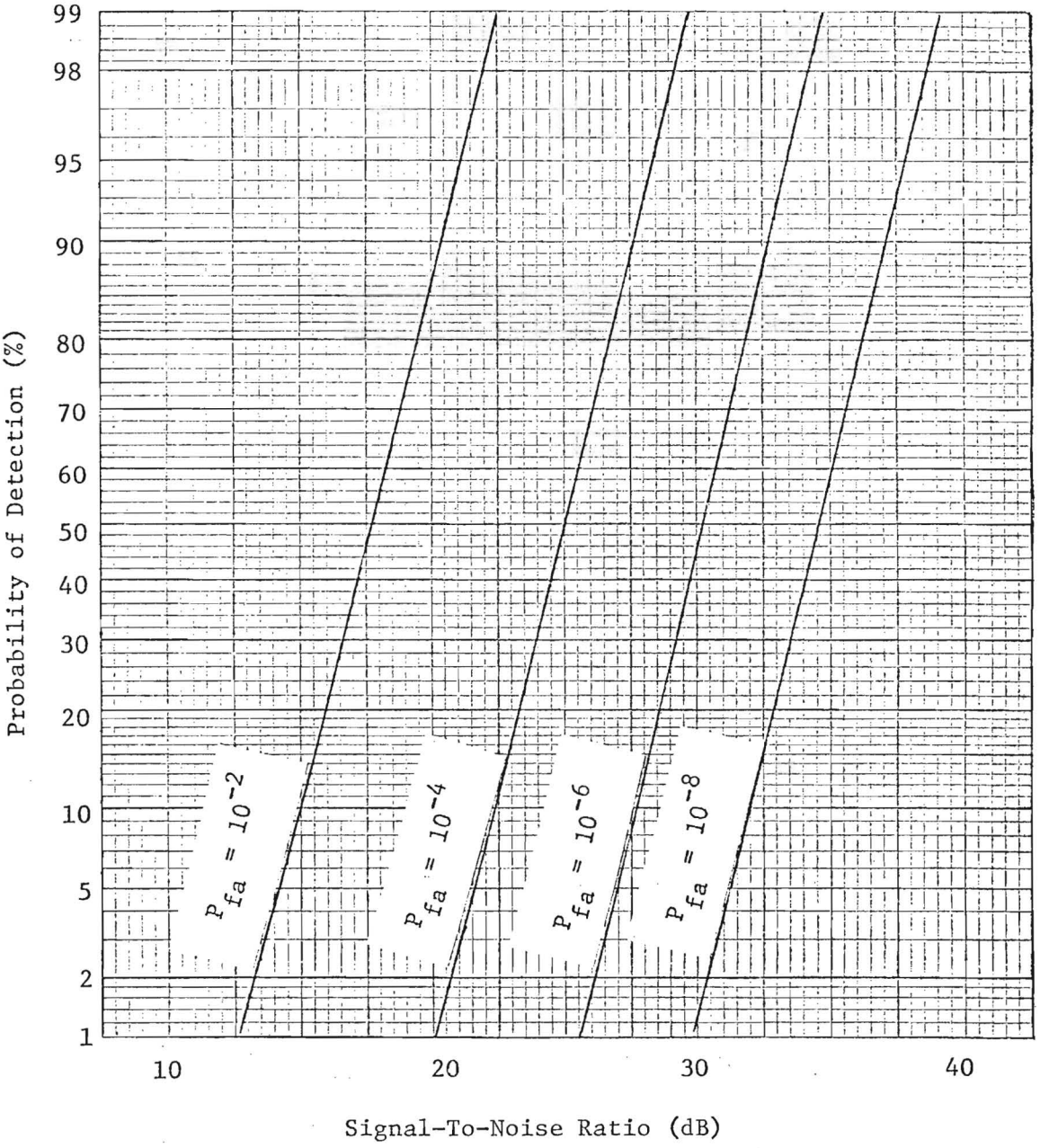

Figure 23. Receiver Operating Characteristic for Log-Normal Target and Clutter. Standard Deviations of 2 dB for the target and 5 dB for Clutter Were Used. Detection Based on a Single Received Pulse.

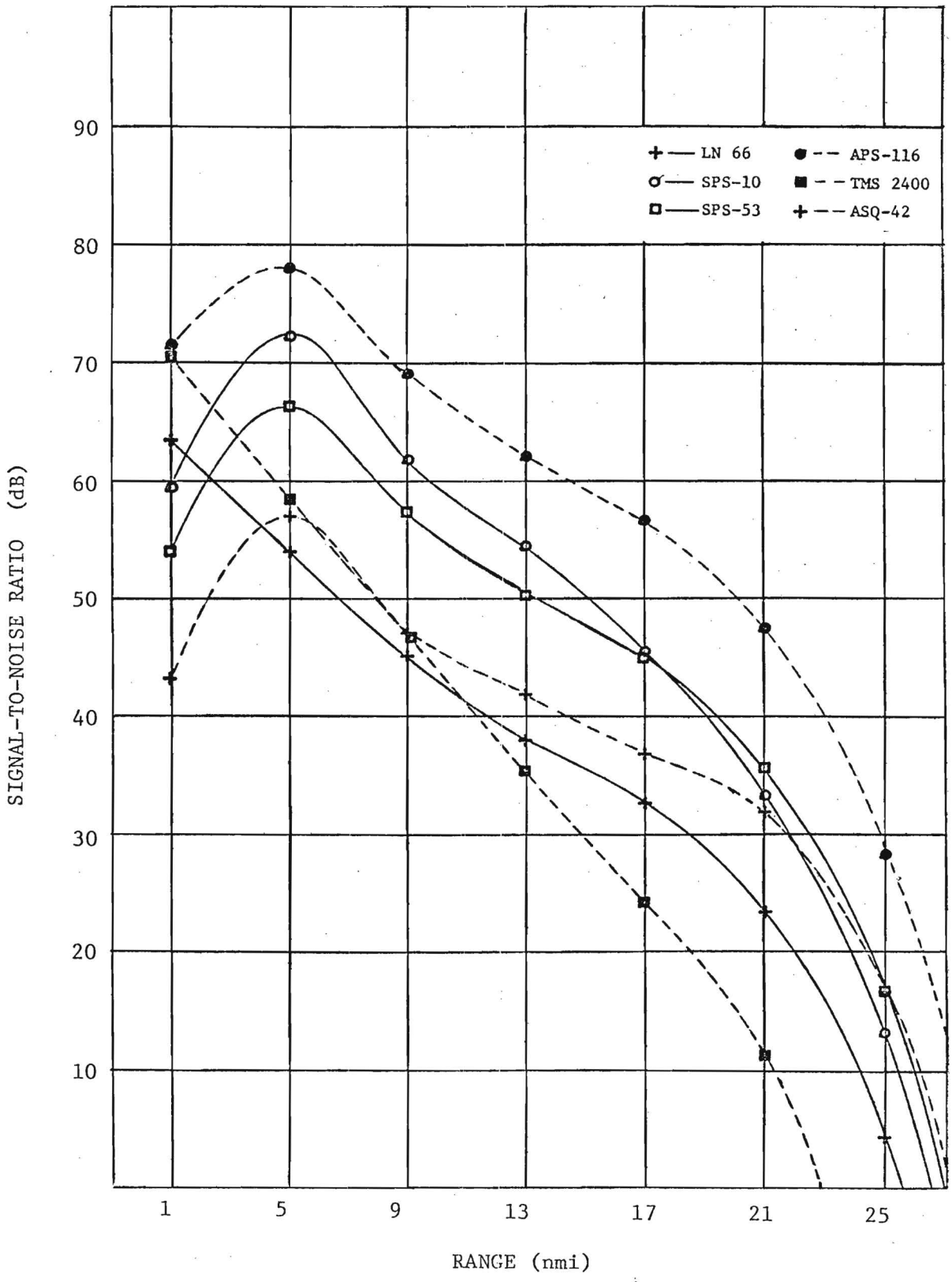

Figure 24. Comparison of Signal-to-Noise Ratios for Several Radars with Antenna Heights of 100 Feet, Sea State 1, Target I (Approximately 400 Foot Length - See Chapter III, Section B).

except the LN-66 and Decca TMS-2400 have reasonable signal levels out to 25 nmi but drop off rapidly after that. The importance of antenna height is further dramatized by Figures 25 and 26, which show predictions for the same target except for antenna heights of 60 and 30 feet, respectively. At 60 feet, maximum detection range for all but the high-performance AN/APS-116 has dropped to around 20 nmi, while for an antenna height of 30 feet, maximum detection ranges on the order of 17 nmi might be expected.

Figures 27, 28, and 29 illustrate the signal-to-noise ratios which might be expected for Target II using the same antenna heights previously discussed. Again, the cross-section of the target is sufficiently large so that the radars are basically horizon limited. Response curves of the radars relative to each other remain as in the earlier case, with the AN/APS-116 outperforming other candidates by at least 12 dB. The AN/SPS-10, AN/SPS-53, and AN/ASQ-42 are close in performance, particularly at longer range. The LN-66 and Decca systems again show shorter maximum detection ranges.

Target III is by far the most difficult for long-range detection, as would be expected from its small radar cross-section. Antenna height is still a factor in detection range; however, a change from 100 feet to 60 feet has much less effect than was the case for the larger targets. Figures 30, 31, and 32 are illustrations for the case of the Type III target. Note that none of the systems considered will necessarily provide single-scan detection (i.e., $P_D > 50\%$) out to the optical horizon, as even the AN/APS-116 would require integration processing to assure reliable detection. The reliable detection range for the LN-66 using an antenna height of 60 feet is predicted to be less than 5 nmi; observations made during field operations conducted at Boca Raton, Florida, in August substantially confirm these predictions.

It should be noted that at short ranges the signal-to-background ratio which may be obtained is drastically limited by the presence of sea clutter. The amount of the degradation for any given radar is a function of many parameters; however, generally the trend is for clutter return to increase with increasing frequency and to decrease as the resolution cell size is decreased. A comparison of Figure 33, with Figure 27 illus-

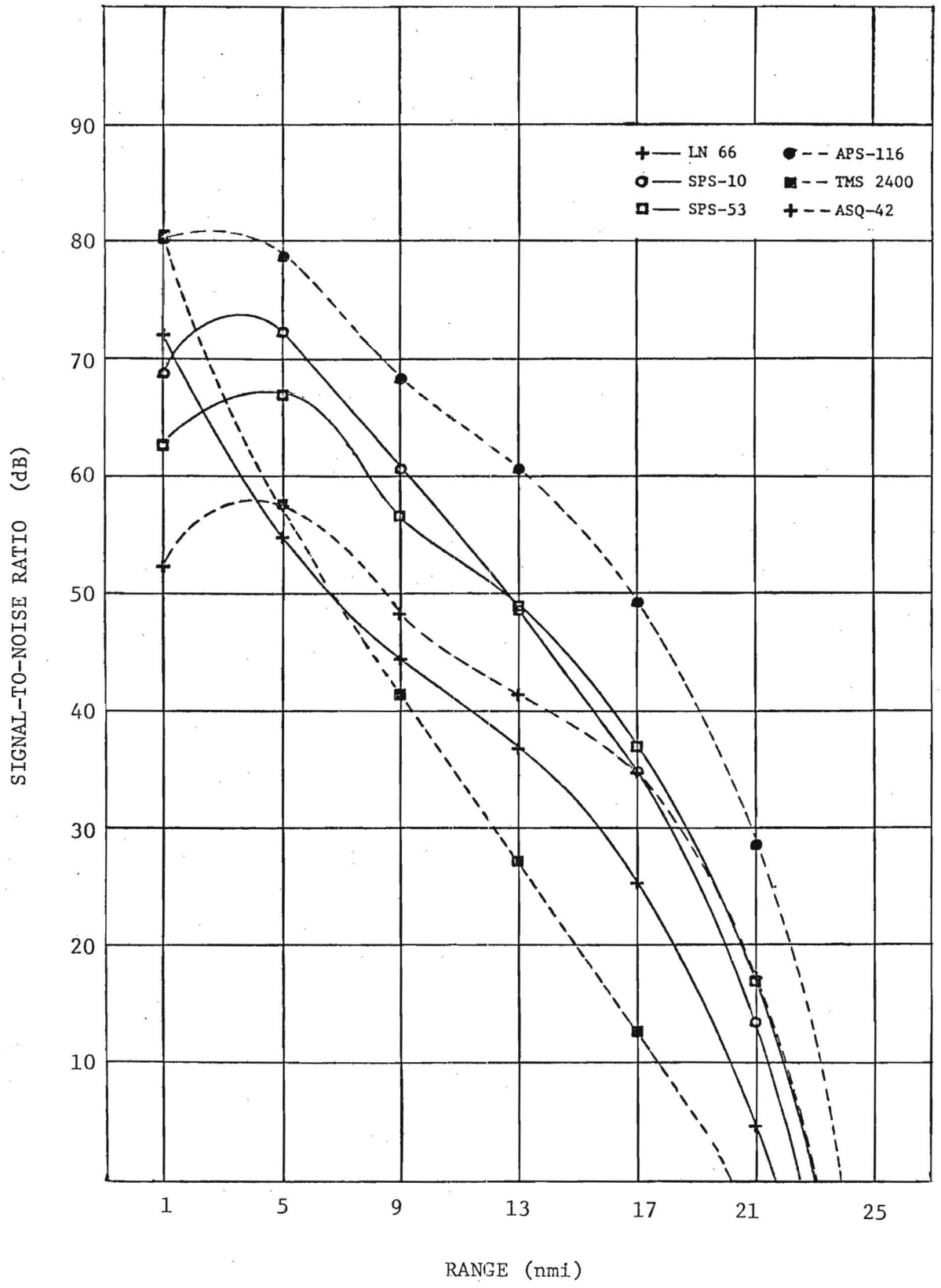

Figure 25. Comparison of Signal-to-Noise Ratios for Several Radars with Antenna Heights of 60 Feet, Sea State 1, Target I (Approximately 400 Foot Length - See Chapter III, Section B).

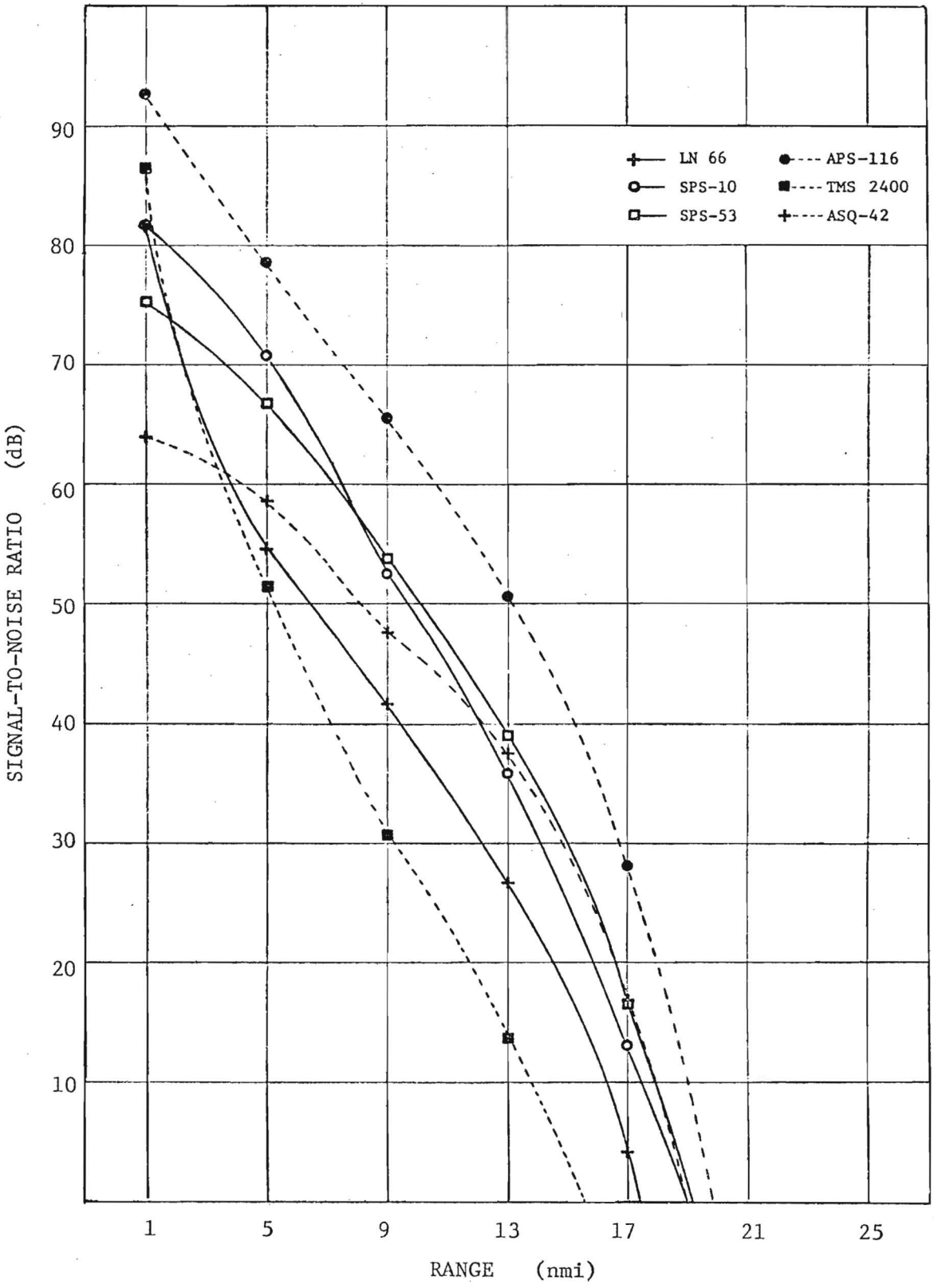

Figure 26. Comparison of Signal-to-Noise Ratios for Several Radars with Antenna Heights of 30 Feet, Sea State 1, Target I (Approximately 400 Foot Length - See Chapter III, Section B).

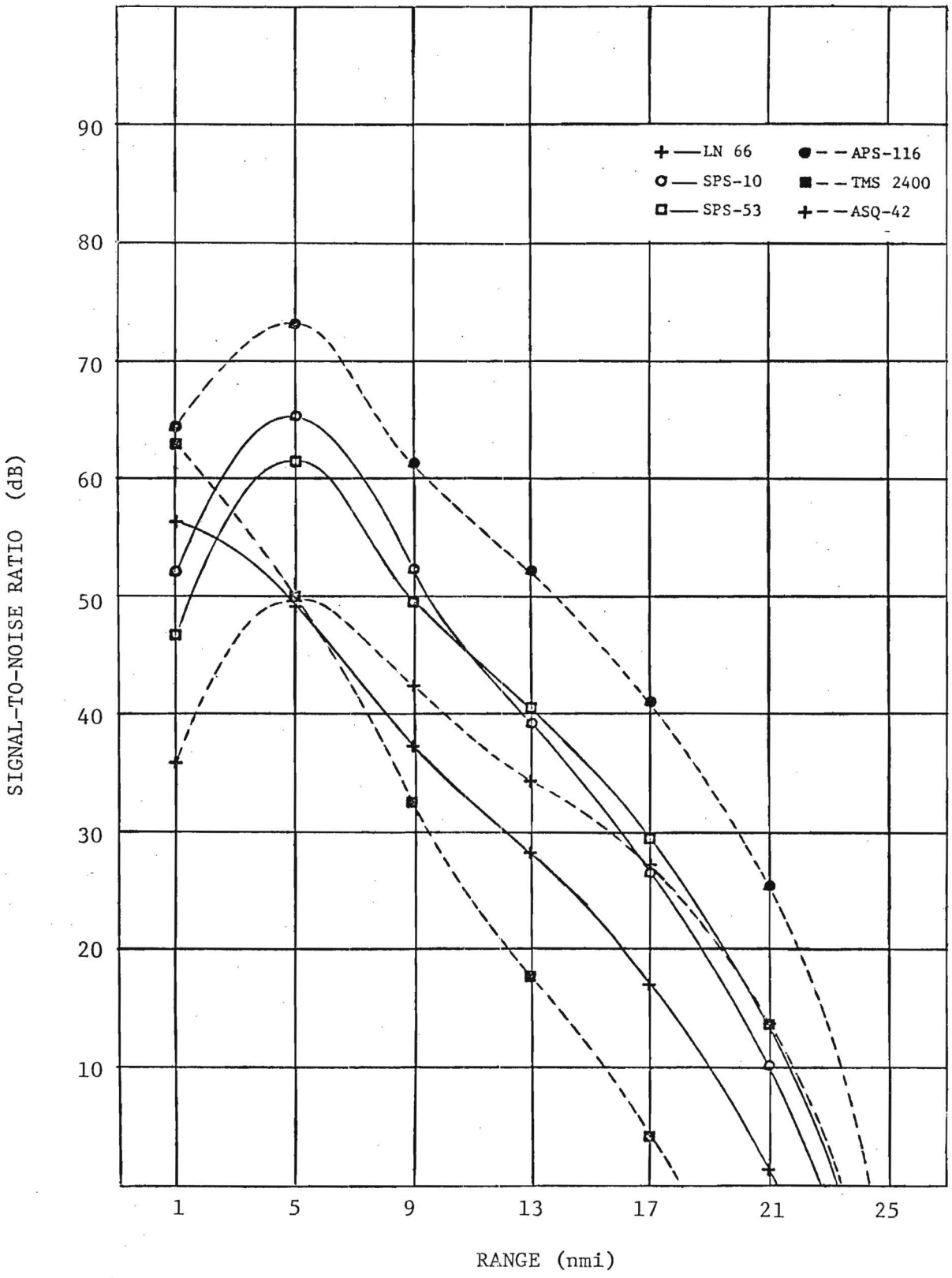

Figure 27. Comparison of Signal-to-Noise Ratios for Several Radars with Antenna Heights of 100 Feet, Sea State 1, Target II (Approximately 100 Foot Length - See Chapter III, Section B).

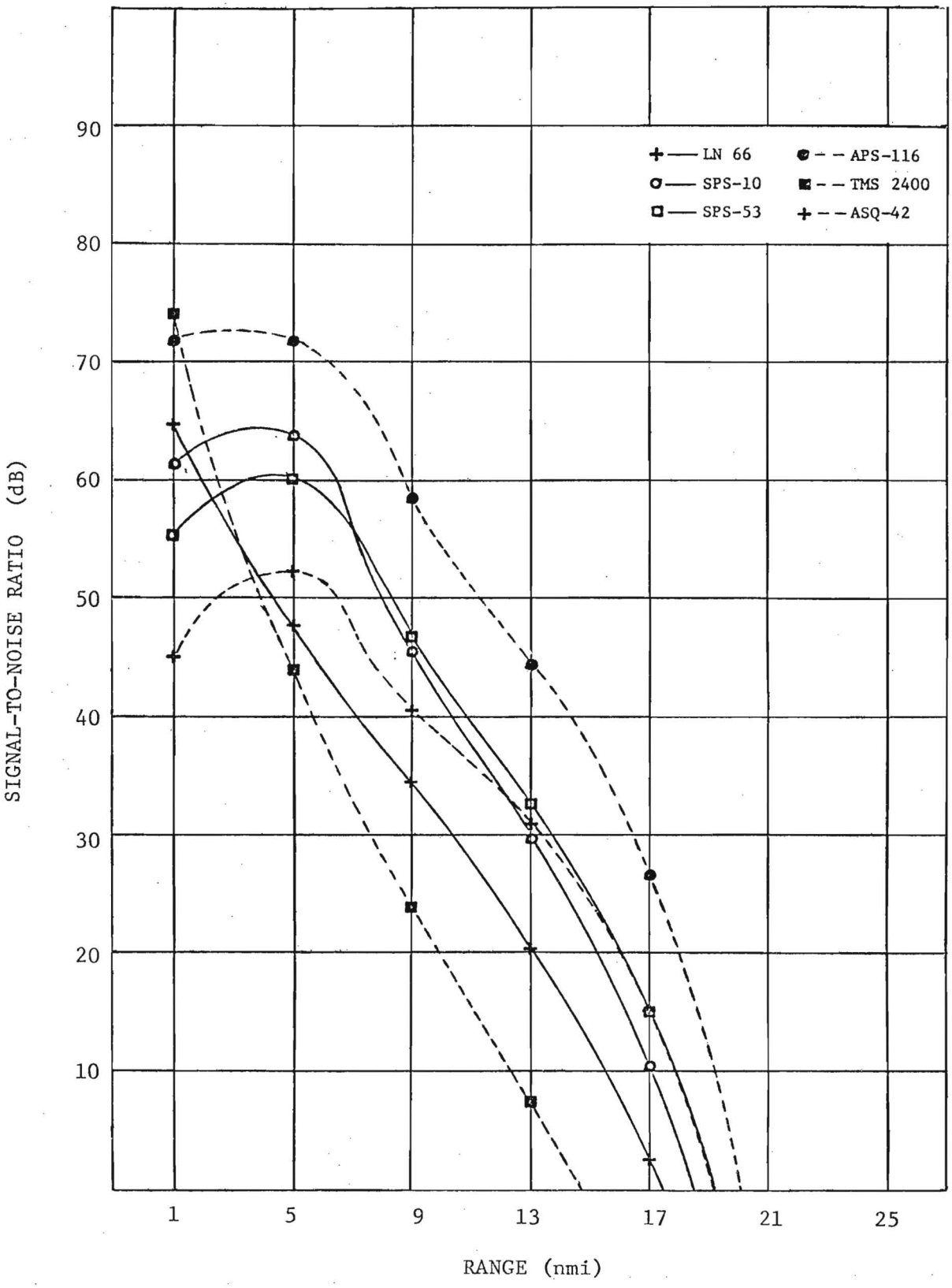

Figure 28. Comparison of Signal-to-Noise Ratios for Several Radars with Antenna Heights of 60 Feet, Sea State 1, Target II (Approximately 100 Foot Length - See Chapter III, Section B).

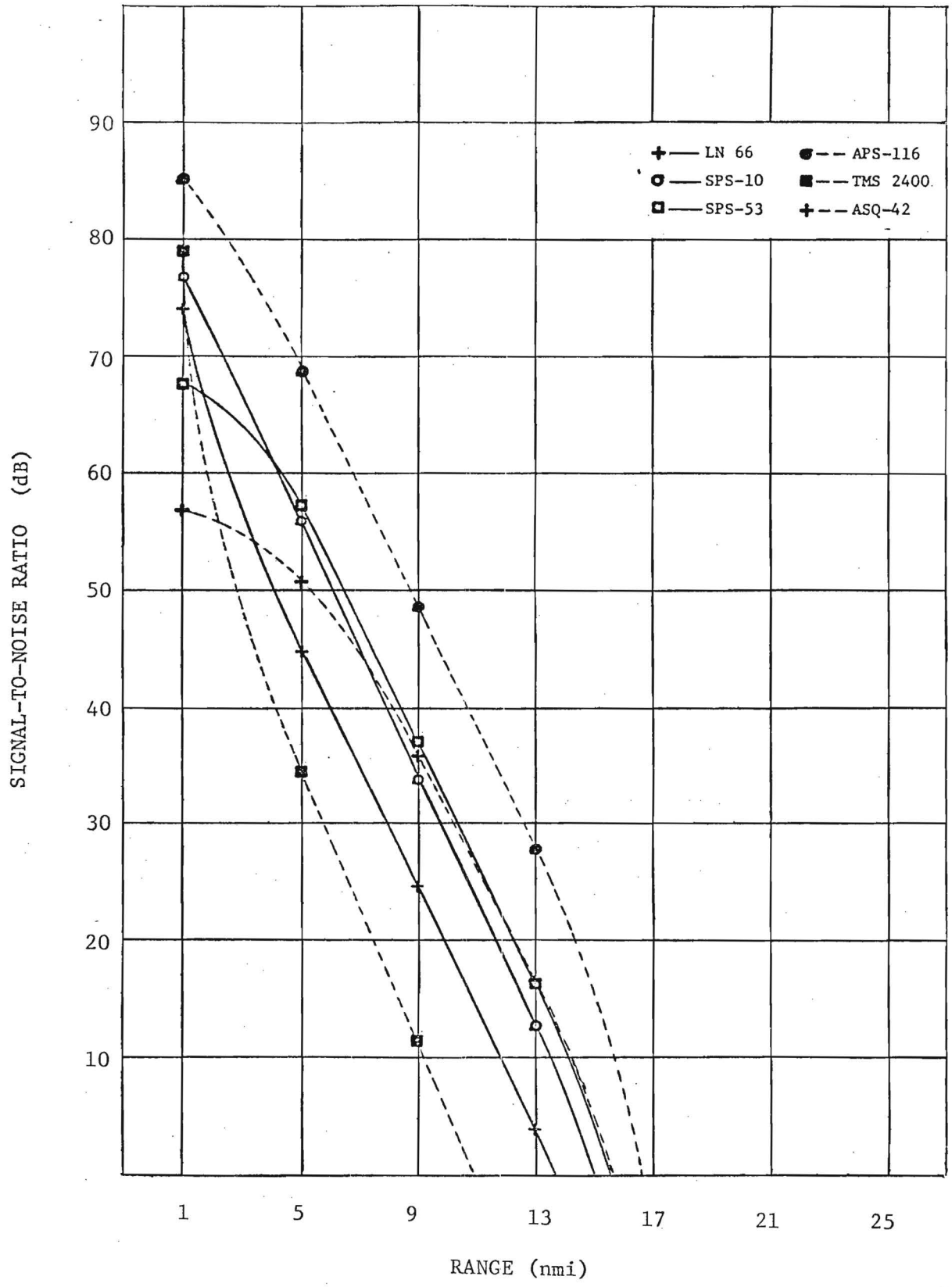

Figure 29. Comparison of Signal-to-Noise Ratios for Several Radars with Antenna Heights of 30 Feet, Sea State 1, Target II (Approximately 100 Foot Length - See Chapter III, Section B).

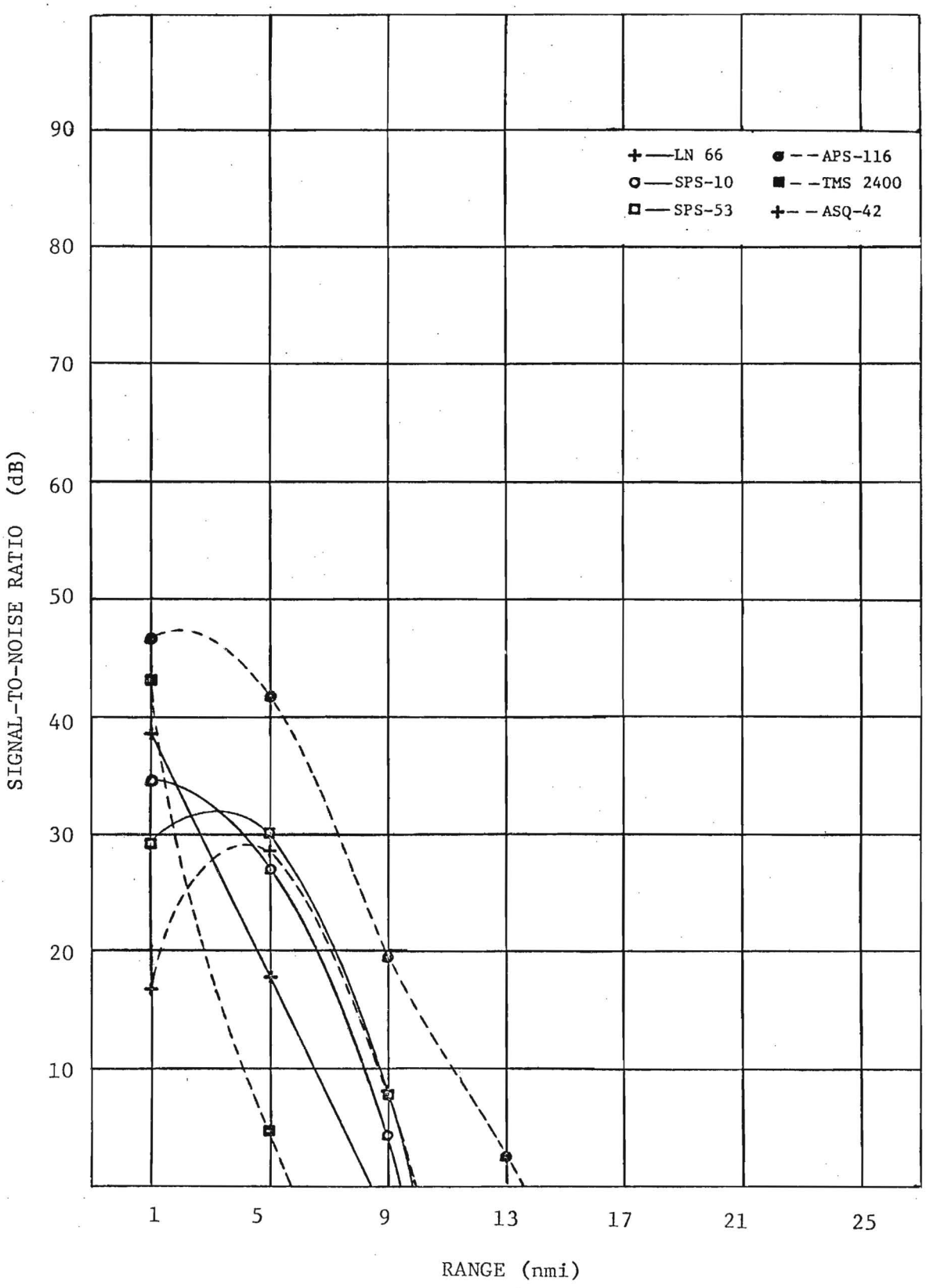

Figure 30. Comparison of Signal-to-Noise Ratios for Several Radars with Antenna Heights of 100 Feet, Sea State 1, Target III (Approximately 30 Foot Length - See Chapter III, Section B).

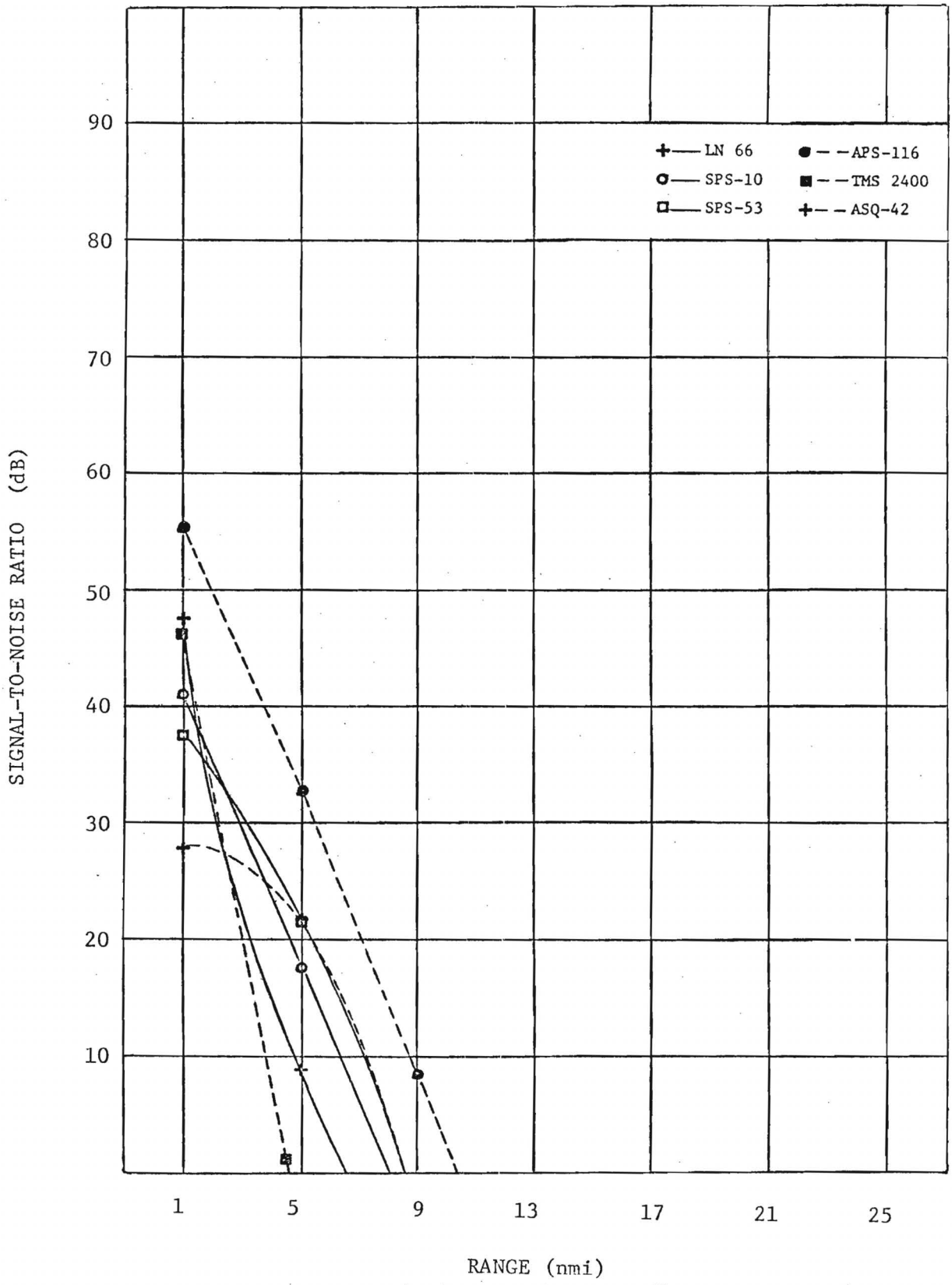

Figure 31. Comparison of Signal-to-Noise Ratios for Several Radars with Antenna Heights of 60 Feet, Sea State 1, Target III (Approximately 30 Foot Length - See Chapter III, Section B).

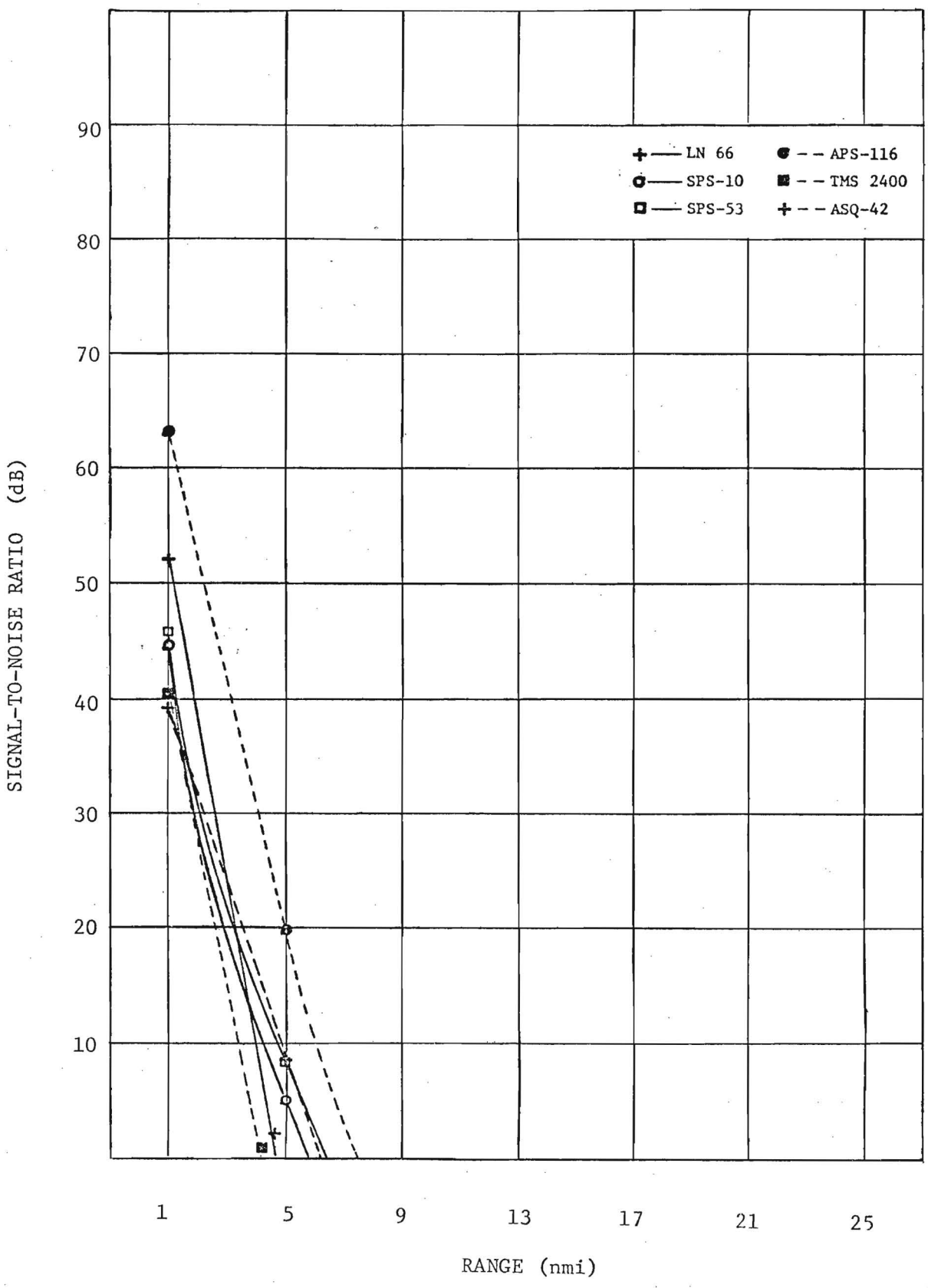

Figure 32. Comparison of Signal-to-Noise Ratios for Several Radars with Antenna Heights of 30 Feet, Sea State 1, Target III (Approximately 30 Foot Length - See Chapter III, Section B).

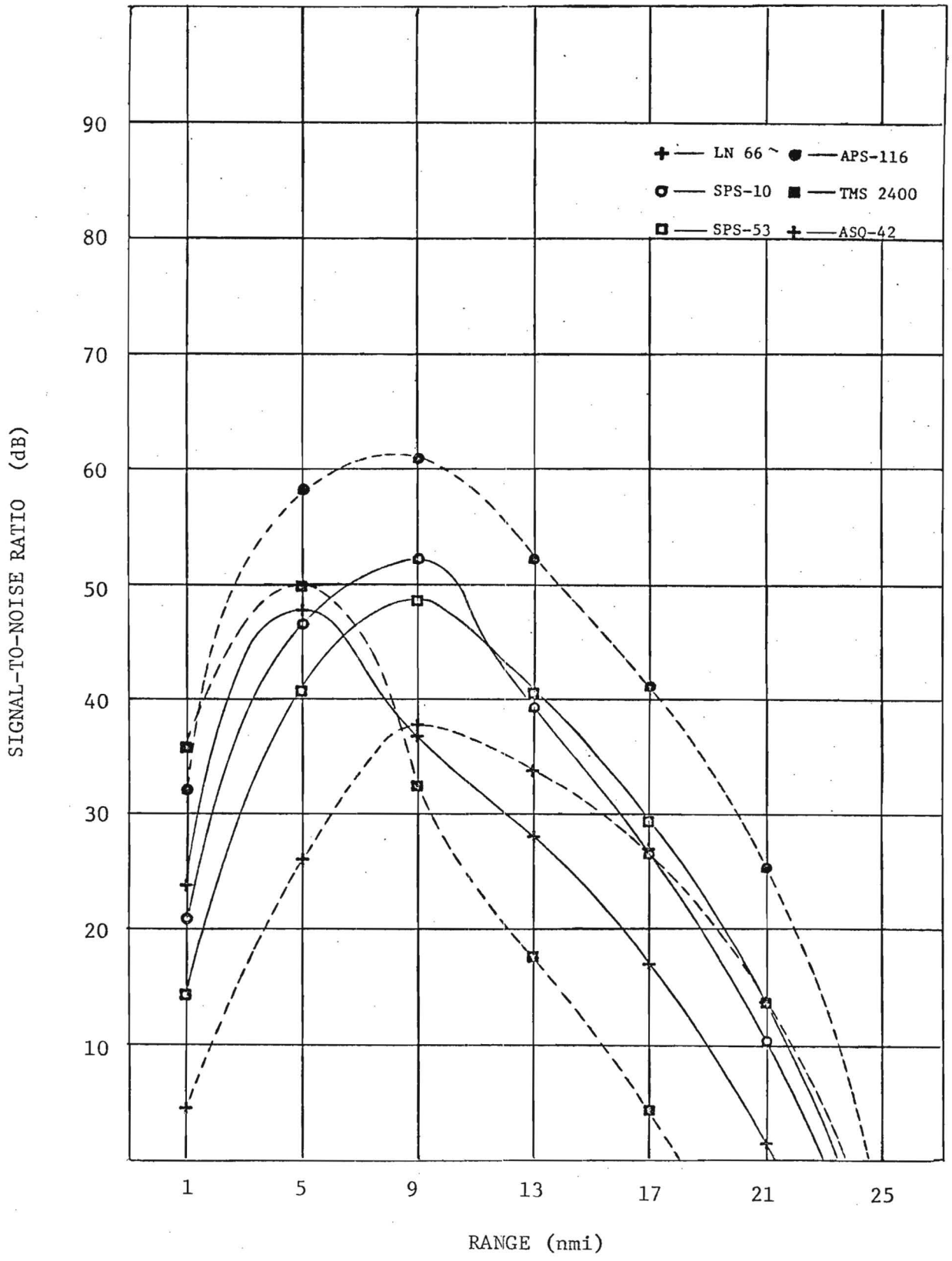

Figure 33. Comparison of Signal-to-Noise Ratios for Several Radars with Antenna Heights of 100 Feet, Sea State 3, Target II (Approximately 100 Foot Length - See Chapter III, Section B).

strates the reduction in signal-to-background produced at short range by a Sea State 3. Although all radars are affected by the higher sea state, the J-Band radar is clutter-limited out to a range of 3 to 4 nmi. Processing could be done on all of the radars to reduce the problem. Several methods, discussed in Chapter II, Section G, will relieve though not solve the problem of detection in a high-clutter environment. More extensive discussions of signal processing techniques and philosophy of clutter reduction can be found in several of the references (cf., References 4, 5, 22, 23, 26).

IV. Automated Displays

The modern surveillance radar system is required to give rapid and accurate assessments of target position in the face of a multiple target environment in which target cross-sections can vary from a few square meters to hundreds of square meters and target speeds range from near zero to several hundred knots. Often optimum performance is required in an environment which presents severe clutter or where interference signals produce many false target returns. Further, the radar sensor may be only one of a number of sources of data for a centralized control center. The volume of data available and the necessary speed and accuracy in handling suggest the importance of using digital computers and automated data handling and display. [28,29]

It is important that the data extraction system match the potential of the data sources to the capacity of the overall data handling system. In a high traffic, high stress environment, it is difficult for the human operator/radar display combination to fulfill the need. Unfortunately, automated systems can be both expensive and unsuccessful alternatives to the "conventional" man/display system. Limited assessments of potential computer/display systems were undertaken as a part of this study with the goal of defining the salient requirements for a system suitable for use in the Harbor Traffic Surveillance (HTS) environment. A limited field evaluation of one potential candidate, the Digiplot*, was also undertaken as a part of this program (see Chapter VI). [30,31]

A number of existing automated display systems were noted during the current investigations; however, none of the currently available systems are immediately applicable to the requirements of the Harbor Traffic Surveillance (HTS) system. Generally, current systems can be considered to fall into four classes: (1) air traffic control (FAA), (2) maritime traffic control (USCG), (3) marine collision avoidance (commercial), and (4) weapon systems control (Navy, Air Force). A few representative systems are listed in Table XIII [32,33,34]. It is anticipated that selected versions from any of these classes can be made to work successfully for HTS;

---

*Trademark of the Iotron Corporation, Bedford, Mass.

TABLE XIII

Classes of Automated Display Systems

Class	Description	Agency/Vendor
I	Air Traffic Control	
	Automated Radar Terminal System	
	ARTS-2	FAA/Lockheed
	ARTS-3	FAA/Univac
II	Harbor Vessel Traffic System	USCG/APL, AIL
III	Marine Collision Avoidance Systems	
	DIGIPLOT	/Iotron
	MAPS	/Sperry
	COMAN	/Marine Digital Systems
	PREDICTOR	/Marconi
	AUTOWATCH	/Automated Marine
	SCAN-100	/F&M Systems
	ACMRS	/Decca Marine
IV	Weapon Systems Surveillence and Control	
	AGEIS	Navy/APL, RCA
	A-NEW	Navy/Various
	Integrated Swimmer Defense System (S2705)	Navy/NAFI

however, this approach would in all probability require an extensive development program, even though other agencies have already undertaken major development efforts for their application.

The most nearly similar system currently existing is the prototype Vessel Traffic System (VTS) currently being evaluated by the U. S. Coast Guard at San Francisco [33]. This system is composed of two redundant radar sensors, several computers, several displays, and a semi-automated evaluation and communication system. Extensive additional testing is required for a realistic assessment of this system's performance. Chief among the difficulties of this system for use with the current HTS requirement are its size and cost. It is intended as a permanent facility, and to rework this system into a transportable system would not only result in an essentially all new hardware system, it would still be so costly and complex as to be suitable primarily for a limited number of installations. The software and interfacing of this system are currently designed for only a limited number of sensor inputs; unfortunately, this last limitation is true of all systems considered except certain versions of the ANEW system.

The various commercial marine collision avoidance systems represent a totally different approach to the concept of automated display and processing. First, these systems are very low cost and relatively simple. Moreover, they have the advantage of immediate availability, which may be an important consideration in the current stage of the HTS program. No currently available system will fulfill the need without extensive new development or rework. Thus, it is appropriate to consider use of a low-cost, but upward expandable, commercial system, which would serve a dual role as a tool for the Navy to use for investigation of the detailed requirements of the HTS application and as a breadboard for exploring specific hardware problems. It was on this basis that the field evaluations of the Iotron Digiplot were conducted. Table XIV summarizes some of the pertinent characteristics of the Digiplot [35].

The Digiplot is intended to provide ship's personnel with detailed navigation information, especially data on course, speed, CPA and Time-to-CPA, on a large number of targets within a 16 nmi radius of the ship. It also provides an audible alarm and other warning indications of poten-

TABLE XIV

Digiplot Characteristics

Power -	110 volts, 50-60 Hz, 750 watts
Display -	16-inch CRT
Range Scales -	3, 6, 12, and 24 nautical miles
Target Presentation -	Up to 40 automatically selected targets shown as circles with attached vector representing course and speed
Coastline Presentation -	Series of illuminated dots outlining the edge of the nearest extended land
Bearing Accuracy -	within 1^{o}
Range Accuracy -	$\pm$ 1 1/2% of the maximum of the range scale in use or $\pm$ 250 feet, whichever is the greater
Target Course and Speed Accuracy -	$\pm 3^{o}$ course and $\pm$ 10% speed or $\pm$ 10.5 knots, whichever is the greater
Digital Data Readout -	Target Position: Range indicated to $\pm$ 0.1 nmi, Bearing indicated to 1^{o}. Target Motion: Course indicated to 1^{o}, speed indicated to $\pm$ 0.1, all with accuracy indicated above
Automatic Target Acquisition -	Up to 40 targets including all targets within one mile of own ship and remainder are the most threatening others up to a maximum of 40 out of the closest 200 targets
Information Update -	Once each scan
Automatic Alarms -	At operator selected CPA distance and time to CPA, audio alarm and flashing light

tially dangerous situations. Because of the requirement that the Digiplot be capable of interfacing to a wide range of commercial radar sensors, it has a fair degree of flexibility in its video interface circuitry. Although a number of the capabilities of the software system, as currently implemented, are not applicable to the HTS requirement, the tests were generally encouraging.

A key feature of the field evaluations of automated display techniques was the validation of the potential of a modular surveillance system which uses low-cost radar sensors, simple video interfaces, and a relatively low-cost digital processing/display system. The tradeoffs between the requirements for low personnel need, large- and small-scale coverage, and moderate system cost have not been fully explored; however, the concept of a modular system which has as its basic units (1) a sensor, (2) a video preprocessor and automated display, and (3) a command and communications center would appear to provide the highest degree of flexibility. The use of standardized automated displays in both the radar sensor control hut and in the command center appears desirable, as does the use of an expandable network of small computers instead of one large central computer. The current state of knowledge of automated target acquisition, tracking, and identification is such that any near-term HTS system should clearly include manned displays and manual sensor control and monitoring as back up to the computerized systems.

One potential problem area which was identified is the degraded performance of the automated system in the presence of interference and/or high-alarm-rate situations. This problem has been a recurring one with computerized systems, and a great deal of attention has been directed to solutions with varying degrees of success [36,37]. It is important that the sensor and video interface be properly chosen to minimize the overloading of the computer. Although additional investigations are needed to define the specific requirements and specifications of suitable approaches, it is recommended that the modular concept be used. Such an approach allows for the possibility of replacing sensor, interface, computer, or display with an upgraded subsystem with a minimum of impact on other subsystems.

V. Radar Beacon Requirements

The harbor traffic surveillance problem is rendered more severe by the volume of targets that may have to be handled. Obviously, a method of uniquely identifying some number of the targets involved would simplify the analysis problem presented to the operator. One of the simplest ways to implement a unique identification is through the use of a radar beacon or transponder system [14]. The advantage of such a system lies in its ability to provide an enhanced target signal return, plus coding for a positive means of target identification.

The advantages of beacons can be realized only with cooperative targets who are willing to carry and use the necessary transponder. This type of system has been found to be quite useful for the control of civilian air traffic in the form of the Common Air Traffic Control System of the Federal Aviation Agency. However, beacons do have limitations, chief among which is limited traffic capacity. Also, under certain circumstances, emission control measures may not allow the use of beacons or transponders. These limitations, combined with the fact that not all targets will carry beacons, mean that a beacon system complements rather than replaces the primary radar system.

A typical beacon system consists of an interrogating transmitter, which may be part of the radar transmitter itself or a separate unit, and a transponder located on the target. Each pulse from the interrogating radar triggers a reply from the transponder, which may be a simple pulse, but is usually coded for purposes of identification. A video diode transponder receiver, one of the simplest types of receivers, requires a signal level of about -40 dBm to trigger it, a level easily provided at 30 miles by any of the radars considered. The reply returned by the transponder must be well above the minimum detectable signal for the interrogating radar. Typically a signal of -70 dBm at the radar receiver would give sufficient signal-to-noise ratio for good display in noise; however, proportionally more signal would be required in high sea clutter. Table XV lists the power output required of the transponder operating with a radar at each band considered. These levels assume free-space

TABLE XV

Transponder Pulse Power Required

for Operation With Various Radars to 30 nmi

Radar	Transponder Power Output (Watts)
TMS-2400	6
AN/SPS-10	7
AN/SPS-53	44
AN/ASQ-42	37

propagation and a 3dB antenna gain for the transponder antenna. As can be seen, required power outputs are all under 100 watts, levels which might be cheaply obtained using a magnetron output fed by a solid state modulator.

The discussion above has considered a radar beacon system which operates at the frequency of the search radar. There are advantages however, in use of a transponder operating on a completely separate frequency from the primary search radar. First, if the system is triggered by the search frequency, but replies at a much lower frequency (for instance, D-Band, as in the Common Air Traffic Control System or in current military IFF systems), higher power outputs may be obtained using all-solid-state technology [27]. Next, the transponder signal does not compete with clutter return. Attenuation in severe weather conditions is reduced, allowing track on targets which might be obscured by rain clutter or attenuation at the higher frequencies. Finally, significant work has been done on implementing these systems for aircraft, reducing the development necessary to adapt such a system for shipboard use. This approach also allows more flexibility when an automated display is considered, since the beacon signal can be handled separately from the radar return signal. This approach might eventually allow for a system where each contact which carried a transponder would be tagged with an alpha-numeric code for identification. Unfortunately, two-frequency operation does have several disadvantages. For example, it requires a separate receiving antenna for the coded reply, mounted with the search radar antenna, and separate receiver and decoder circuits must be implemented to provide the necessary output signals to either a PPI video presentation or an automated display.

Advances in technology over recent years have rendered the implementation of an all-solid-state beacon system more feasible. Relatively high power devices for use in a pulse mode have been developed for use at frequencies through I-Band. For example, powers greater than 600 watts pulsed have been achieved with an I-Band L.S.A. diode. About a decade below this in power are CW IMPATT diode oscillators and varactor harmonic generators. At frequencies around D-Band, where the Air Traffic Control System operates, transistors using planar epitaxial structure can achieve significant power levels. All of these devices have the advantages of requiring low supply

voltages, of being small and rugged, and of being easily environmentally proofed. To complement these devices, integrated digital logic circuitry presents an easy method of providing coding and decoding functions to the system.

The transponders most highly developed and readily available at this time are those for Air Traffic Control. They range from all-solid-state devices with pulse power outputs of 100 watts to devices using planar triode and cavity outputs producing 1 kW. They also enjoy the advantage of already having incorporated relatively sophisticated coding circuitry which might be used for identification purposes. Commercially available G-Band and I-Band all-solid-state transponders are presently limited to several watts output, at best. However, units having solid state modulators and magnetron outputs can easily be ordered and provide power outputs in the region of 500 watts pulsed. Although most of these are constructed to provide single pulse replies, some do exist which have incorporated limited coding ability.

VI. Field Operations

During the period 20 August through 24 August 1973, field operations were conducted at the Georgia Tech Field Site, Boca Raton, Florida, in an effort to obtain preliminary information on the feasibility of a harbor surveillance system using an automated display. Figure 34 details a block diagram of the experimental set-up. The radar employed was an LN-66 (HP) owned by the Naval Coastal Systems Laboratory, which was provided in conjunction with the S2705 Swimmer Defense field operations. Automated display was provided through use of the Digiplot described more fully in Chapter IV. Quantitative and qualitative data were taken under varying conditions of sea clutter and weather [38].

A. Equipment Configuration

The LN-66 (HP) radar used in the field tests is a typical commercial shipboard radar. It employs a magnetron output operating around 9375 MHz and providing 75 kW peak power. The receiver is a single-crystal mixer, superheterodyne receiver employing a linear IF section. The receiver also has incorporated an adjustable Fast Time Constant (FTC) circuit to reduce the effects of sea clutter and rain. The video output, which is normally connected only to the PPI display, was connected to the Digiplot interface, and also, for this test, to an A-scope display. As the Digiplot signal tap is taken before the FTC, the Digiplot provides its own threshold and anticlutter circuits. A calibrated I-Band signal generator was used to provide a test signal to the receiver so that signal-to-background ratios could be measured. Measurements were performed by searchlighting the antenna on the target of interest and matching signal generator output to target signal level on the A-scope. This procedure, combined with a measure of Minimum Detectable Signal for the radar, gave a signal-to-background ratio for the target. However, as the receiver employed a linear IF section, care had to be taken to ensure that the receiver did not saturate, giving false data. Also, since there is no automatic searchlight feature for the radar, care had to be taken that the target remained in the main beam during the measurement. For this experiment, the antenna height was 50 feet, so that measured results should lie close to those for an antenna height of 60 feet presented in Chapter III.

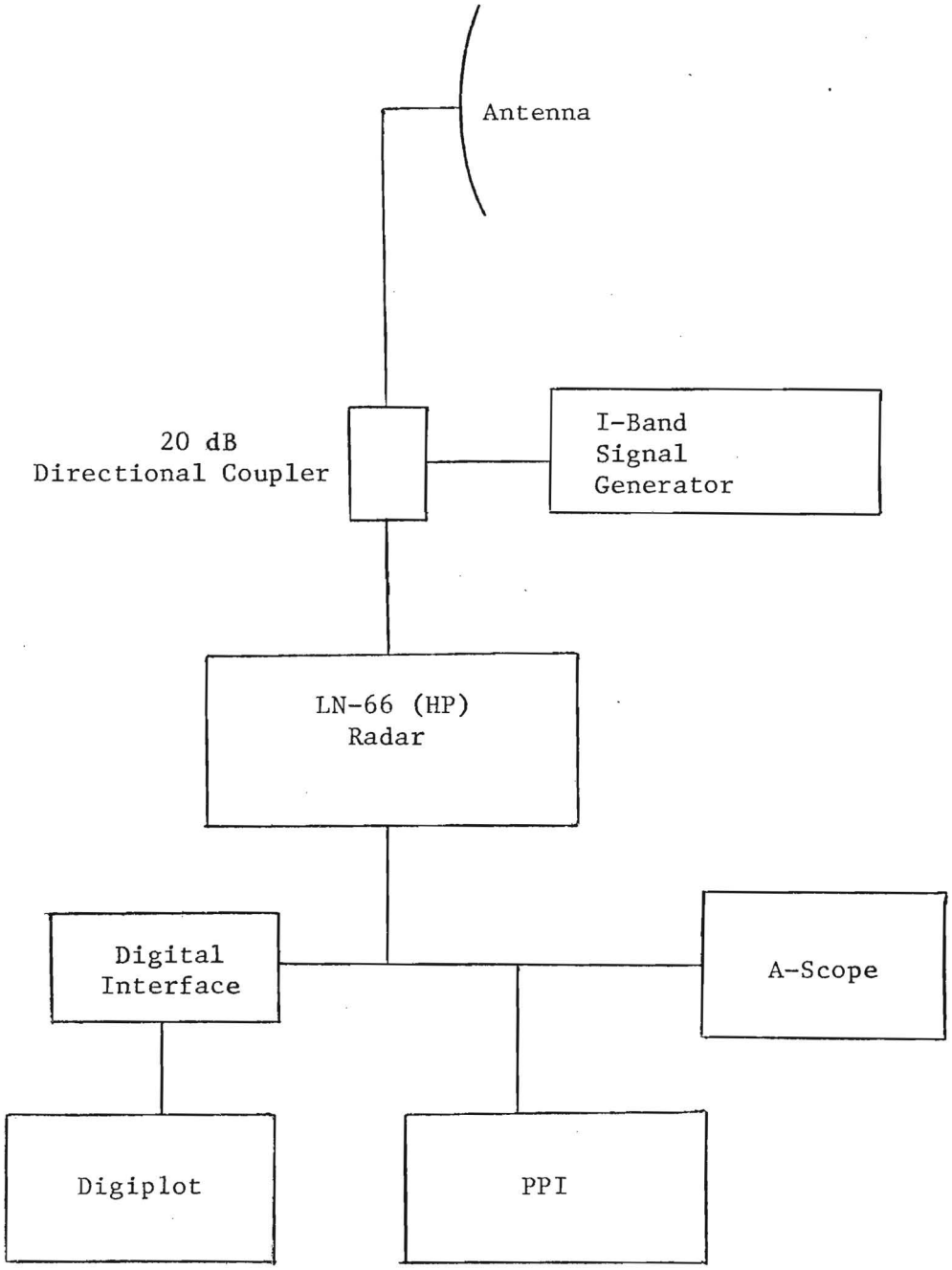

Figure 34. Experimental Equipment Set-Up for Data Collection During Field Tests at Boca Raton, Florida.

In addition to evaluation of the LN-66/Digiplot combination, a limited test was done to evaluate the feasibility of a transponder system operating with the radar system. To provide this capability, two simple transponders were constructed. The first used a Gunn diode oscillator to produce a CW signal at I-Band. The incoming radar signal triggered a PIN modulator to provide a return pulse to the radar. The second transponder used an I-Band signal generator as a power source. A crystal detector was used to trigger this signal generator, providing a return signal to the LN-66 radar. Neither transponder had any means of coding the return signal, and so returned a simple marking pulse.

B. Results of the Field Tests

Table XVI presents data taken on targets of opportunity during the field operation described. Data appear for a large tanker (estimated to be about 500 feet long), small freighter (about 250 feet long) and a fishing boat (about 35 feet long). As can be seen, the signal-to-background ratio of the large tanker matches predictions very well. The actual ratio is several dB above that predicted for a bow aspect, due to the fact that the tanker had approximately a beam aspect when the measurement was taken. The data point taken on the small freighter at 8.0 nmi seems very reasonable. However, the value of signal-to-background ratio measured at the shorter range indicates that for the 5.9 nmi data point, the video gain was sufficient to put the IF in saturation, invalidating the measurement. The fishing boat measured had a flying bridge and was therefore larger in cross-section than the model used in the predictions for Target III. Thus it does not seem unreasonable that its return was about 10 dB over predicted.

Additional qualitative data were taken on targets of opportunity. There are two shipping lanes which run close to the shore at Boca Raton. The closer, generally containing southbound traffic, has a CPA of about 2 to 3 miles. The farther lane generally contains ships northbound whose CPA's are on the order of 15 miles. During the field operation ships were tracked in both lanes. In the closer lane the radar exhibited normal characteristics throughout, giving a very large return as would be expected at those short ranges. The Digiplot acted normally from the time the ships came into view (about 8 nmi due to shielding from large buildings

TABLE XVI

Signal-to-Background Ratios for Targets of Opportunity

Target	Range (nmi)	Signal-to-Background (dB)
Large Tanker	15.5	35
Smaller Freighter	8.0	31
	5.9	32
Fishing Boat	5.0	21

on the beach) until the range was approximately 3 to 4 miles. At that time the Digiplot began plotting the ship return as a land mass. This phenomenon is most probably due to high return in the sidelobes of the radar. When the target length as seen by the Digiplot reached 2500 feet it would be considered land and plotted as such. Adequate monitoring of longer range targets was hampered by the 16 nmi maximum display range for the LN-66 PPI display. However, several large ship targets were tracked by the Digiplot at ranges just in excess of 20 nmi, even though not visible on the PPI. In this case the LN-66 performed somewhat better than might be predicted, probably due to some amount of surface trapping which gave enhanced propagation.

Operation of the various features of the Digiplot was examined for their usefulness in the harbor surveillance situation. The display, which produced velocity vectors for each target indicated, gave the operator a much better feeling for the dynamic situation than did the conventional PPI. The ability to pick one target and have its course, speed, CPA, and time-to-CPA displayed also gave valuable information. However, the amount of time required to get accurate information from the computer, even for targets making greater than 18 knots, was on the order of 3 minutes after target detection. One persistent problem of the Digiplot was a tendency to identify clutter at ranges less than 2 nmi as targets. If no minimum acquisition range was set in, all 40 displayed targets would consist of clutter return which was normally bunched within the 2 nmi radius. This problem could be alleviated by setting a 2 nmi minimum acquisition range, at the expense of the loss of ability to track actual targets inside that range.

On the 24th of August, performance of the LN-66/Digiplot combination was observed during a heavy rain. Figure 35 indicates the LN-66 PPI and Digiplot displays for that situation. Note that rain backscatter obscured all targets on the PPI to a range greater than 5 nmi. The rain return on the PPI could be reduced through use of the FTC feature of the radar but with a corresponding excessive loss of sensitivity. The Digiplot recognized the rain as a land target and gave the characteristic dot display. Operation of the anti-clutter thresholding seemed to make little difference

(a)

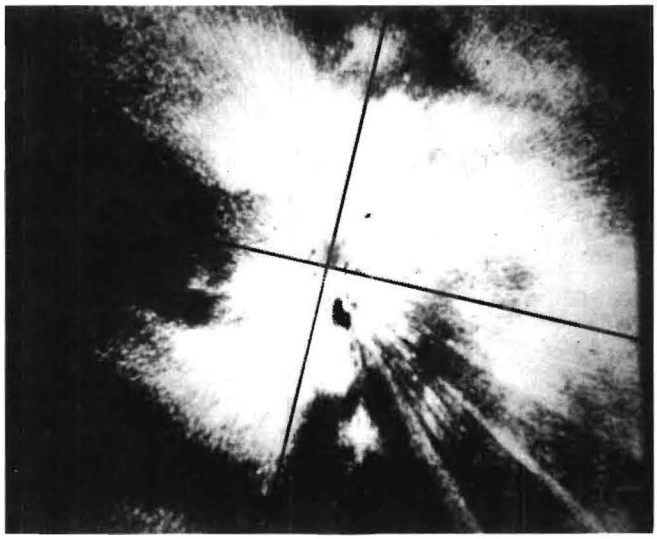

(b)

Figure 35. Photographs of Radar Displays During Heavy Rainstorm: (a) LN-66 (HP) PPI (b) Digiplot.

in the observed Digiplot display. At another time, with patchy rain clouds obscuring a 10^{o} sector at about 8 nmi, the FTC feature of the LN-66 was easily able to provide a clean display while the Digiplot again presented the rain cloud as land.

The radar transponder was used to provide two types of information. The first was an indication of system calibration. Assuming free-space propagation, MDS for the LN-66 receiver was calculated to be -91 dBm through use of the beacon equation [27]. Second, various pulse widths and beacon powers were examined for their effect on the LN-66 display and Digiplot. Initially the transponder was set up with minimum internal delay and an 8 μsec pulse width. This should correspond to a return 3/4 of a mile long on the bearing of the target. Indeed, the transponder when switched on did give a sharp 3/4-mile-long radial pulse return, separated about 1/4 mile in range from the target, which effectively pinpointed the target of interest. The display on the Digiplot, however, was not nearly as graphic. Since targets over 2500 feet in length are assumed to be land and are indicated by dots, it was expected that the transponder return would be displayed as a series of dots stretching radially behind the target circle. This was not necessarily the case, as the display of dots was intermittent, even with a pulse width greater than 10 μsec. This indicated that for use with an automated display, a coded return which might be handled by additional software implementation, and might be displayed as some sort of alpha-numeric flag next to the appropriate target, would be worth investigation.

VII. Conclusions and Recommendations

A. Conclusions

The goal of this study has been to examine the harbor surveillance problem and determine what hypothesized radar would best perform the desired function under the constraints imposed by portability, power requirements, size, and antenna limitations. In addition, the use of automated displays and radar transponder systems has been considered to determine if they might improve system performance. These points were considered in light of the results of field operations conducted by Georgia Tech at the Boca Raton Field Site in August 1973.

To provide reasonable limits for the computer modeling performed, a number of assumptions are inherent in this analysis. First, because the radar must be van-portable and use an erectable tower, a maximum antenna height of 100 feet is considered. This assumption would not necessarily hold for areas where there is a sharp rise in elevation close to the shoreline. For example, areas such as San Francisco might provide effective antenna heights of greater than 300 feet with no tower. However, for predicting maximum detection range, 100 feet is a reasonable estimate of the maximum height that might be expected for a portable system at shoreside. A 30 nmi radius of operation must be considered a practical limit based on the assumption on antenna height. Operation beyond this range would require a significantly higher antenna and so, for a single radar sensor, this is a realistic constraint on range of operation for the system. Tied to the choice of maximum range are the choices of scan speed and PRF, which are picked to provide as high a data rate as possible. Finally, antenna patterns are selected to provide the narrowest azimuth beamwidth consistent with an antenna which might reasonably be mounted on an erectable tower. Radar band selection is determined on the basis of maximum detection ranges, but is tempered with considerations for size, cost, availability and reliability of components, and operation in rain or fog.

The following conclusions can be drawn from the study:

(1) Under the constraints discussed previously, an optimum set of parameters may be chosen for a radar designed to provide

a harbor surveillance function. These guidelines are based on performance (i.e. maximum detection range), but are tempered with considerations for reliability, ease of maintenance, and cost. For instance, a power output of about 250 kW represents a break point for magnetrons. Above this limit, special power supplies, mounting, considerations for arcing and (at I-Band) pressurized waveguide are required. Since doubling power to 500 kW adds only 3 dB and to 1 MW only 6 dB to signal level, it seems hardly worth the additional complexity incurred.

(2) The choice between bands presents trade-offs which must be considered. I-Band provides longer maximum ranges, better resolution, and smaller components and installation size, but suffers more from operation in bad weather or heavy sea clutter environments. G-Band gives up some range and resolution capability for more reliable operation in bad weather and heavy sea clutter. The provision for a circular polarization mode of operation provides increased performance in rain or fog at either band. PRF and antenna scan speed have been chosen to maximize the data rate obtainable, a goal consistent with the desire to use a computer-controlled automated display. Table XVII lists the parameters chosen for the optimum radar.

(3) For larger targets (i.e., ship targets of greater than 100 foot length), the hypothetical radar is essentially horizon limited. This problem may be somewhat alleviated at times by surface ducting effects as discussed in Chapter I, Section D. However, during conditions of normal propagation, maximum detection ranges to be expected should vary from about 15 to in excess of 25 nmi for the larger targets, with variations due to masthead height of the target, its aspect, and weather conditions. For reasonable range performance, an antenna height of at least 50 feet is required.

(4) For small boats (i.e., 20 to 30 foot fishing boats and smaller) performance is much less satisfactory. In this case, the small radar cross-section of the target must compete on almost equal terms with background due to sea clutter and thermal noise. For this size target, maximum reliable detection ranges on the order of 10 nmi might be expected. Somewhat longer ranges can be obtained on targets this size by going to a higher frequency radar with higher resolution. This increase, however must be paid for with poorer operation in bad weather and increased susceptibility to sea clutter effects.

(5) As demonstrated in the field operations and as stated in Chapter V, a radar transponder system has the potential of adding significant capability to the system. Particularly if operated at the lower frequencies (D-Band, for example), present technology allows the use of low power consumption, all-solid-state devices. Coding can be accomplished so that targets may be distinguished in heavy traffic conditions. At G- or I-Band

TABLE XVII

Recommended Parameters for

Harbor Traffic Surveillance Radar

Band*	I-Band or G-Band
Peak power (kW)	200
Receiver bandwidth (MHz)	4
PRF (Hz)	2500
Scan speed (RPM)	30
Pulse length (μsec)	0.25
Receiver noise figure (dB)	6
Antenna height (1 ft)	50-100
Elevation beamwidth (degrees)	10
Polarization	Vertical and Circular
Receiver law	Logarithmic
Special processing	Log FTC, Interface to Automated Display

*Tradeoffs discussed in Chapter VII, Sections A and B.

the power levels required would make the use of all-solid-state devices prohibitively expensive. However, small, light, reliable transponder systems could be constructed at the higher radar frequencies using a solid state modulator with a magnetron output.

(6) To derive maximum benefit from a surveillance system, some type of automated display should be considered. Particularly in concert with a transponder system, the display would allow better determination of the status of all targets, reduce the total number of operators required, and could provide an alarm function. Nevertheless, computer controlled displays should not be considered a cure-all. As discussed in Chapters IV and VI, state-of-the-art automated displays, both commercial and military, have limitations on sensitivity, clutter control, threshold, and cost, and generally are much more complicated to maintain than the conventional PPI display. Civilian automated display systems do have the advantage at the present time of availability, as most military systems are still in development or are in a limited procurement status.

B. Recommendations

The analysis undertaken here indicates that it is practical to assemble a radar sensor which is suitable for use with a portable Harbor Surveillance System under the constraints imposed. The recommended approach to the radar would result in a relatively low-cost development having a high probability of achieving the desired performance. Many critical questions relating to the feasibility of a portable Harbor Surveillance System have not been directly addressed in this study, although the considerations given here, especially in Chapters IV and V, are pertinent. Although a portable system appears feasible, it is important to consider the next steps of investigation very carefully. In particular, a good understanding of the capabilities and limitations of the portable Harbor Surveillance System must be developed, and the potential traps due to equipment limitations studied. To this end, the modular approach described in Chapter IV is important because it would allow conceptual investigations and equipment development to proceed along essentially parallel paths. The following recommendations are designed to provide the Navy with guidance in formulating a program to explore the feasibility of the portable Harbor Surveillance System concept and to provide specification for the major subsystems.

(1) Using the guidelines of this report, further studies should be instigated in preparation for design of a radar, processing,

and display system specifically tailored to the problem of Harbor Traffic Surveillance. The radar parameters stated here should be examined with regard to expected changes in the priority and characteristics of targets of maximum interest. Specific, detailed analysis for design of the accompanying interface, display, and transponder systems should be performed concurrently with the design of the radar sensor. Use of present technology embodied in the air traffic control system and marine collision avoidance systems should be seriously considered, again with a modular system in mind.

(2) In lieu of constructing a new radar system, and for the purpose of providing a readily constructed demonstration system, existing radars have been considered. In the authors' opinion, the one which most nearly matches the optimum system is the AN/SPS-55. This radar, whose exact parameters are presently classified, is an I-Band surface search system designed for the U. S. Navy. It uses a solid-state modulator, would be easily van-mounted, and could be adapted with a minimum effort for the harbor surveillance situation. The AN/SPS-55, however, is not in general fleet service at this time and might be difficult to obtain.

(3) A choice which involves more modification of an existing system, but which might be more easily accomplished, is the AN/SPS-10. This G-Band radar is readily available, and, with certain modifications, would perform very creditably. In addition, its lower frequency of operation poses less problems for good performance in severe weather. The most important modification would be replacement of the receiver and IF sections with a low-noise receiver and logarithmic IF. Addition of a circular-polarization mode, increase of the PRF to 2 kHz, and provisions for interface to an automated display system would also be necessary.

(4) Less desirable is use of the AN/SPS-53 as the radar sensor. It, however, with the addition of a low-noise receiver, logarithmic IF, and circular-polarization mode would provide an adequate demonstration system.

(5) Of the available commercial systems, the LN-66 (HP) is probably an adequate choice, but is less desirable than the above systems. Modifications required would include replacing the present power converter by a more reliable unit, upgrading the receiver section as in (3) and (4) above, adding a circular-polarization mode, and extending the range of operation to 30 nmi.

(6) For the purposes of a demonstration system, use should be made of the Digiplot already in hand at NCSL. Any radar chosen, however, should have additional preprocessing for the input to the Digiplot. This processing should be aimed at

increasing reliability in sea clutter and severe weather. Additional software investigation for the automated display should be done to provide compatibility with the transponder system chosen.

(7) Investigation of available transponder systems should continue. Feasibility for integration into the chosen demonstration system should be carefully considered. At this time, a system similar to the currently used air traffic control beacon system seems promising.

VIII. REFERENCES

1. W. K. Rivers, S. P. Zehner, and F. B. Dyer, "Modeling for Radar Detection (U)," Final Report on Contract N00024-69-C-5430, Georgia Institute of Technology, 31 December 1969, Secret, Excluded from GDS (formerly Group 3), AD 507 375L.

2. F. B. Dyer and W. K. Rivers, "Radar Detectability Study (U)," Final Report on Contract N00024-70-C-1219, Georgia Institute of Technology, 30 July 1971, Secret, Excluded from GDS (formerly Group 3), AD 518 599.

3. W. K. Rivers, "Models for Radar Displays," Technical Report No. 1 on Contract N00024-70-C-1219, Georgia Institute of Technology, 17 July 1971, AD 729 684

4. G. W. Ewell and F. B. Dyer, "Swimmer Detection Radar Studies (U)," Final Technical Report on Contract N00024-72-C-5517, Georgia Institute of Technology, February 1973, Confidential, GDS.

5. J. V. DiFranco and W. L. Rubin, Radar Detection, Prentice-Hall, 1968.

6. W. K. Rivers, "Aids-to-Navigation Radar Requirements," Technical Report No. 1 on Contract DOT-CG-10657-A, Georgia Institute of Technology, 31 January 1971.

7. D. R. Burrows and S. S. Atwood, Radio Wave Propagation, National Defense Research Committee on Propagation, Academic Press, 1949.

8. R. L. Smith-Rose and A. C. Strickland, "An Experimental Study of the Effect of Meteorological Conditions Upon the Propagation of Centimetric Radio Waves," Meteorological Factors in Radio Wave Propagation, The Physical Society (London), Volume 18, 1946.

9. P. J. Rubenstein, et al., "Microwave Transmission Over Water and Land under Various Meteorological Conditions," Report 547, Radiation Laboratory, MIT, 13 July 1944.

10. R. F. Jones, "Low Level Atmospheric Ducts," Nature 163 1949.

11. V. W. Pidgeon, "Frequency Dependence of Radar Ducting," Technical Memorandum, Applied Physics Laboratory, JHU, 9 June 1969.

12. G. D. Smith, "Preliminary Report on Results Obtained from the Radar Ducting Experiment at Wallops Island, Va.," Technical Memorandum, Applied Physics Laboratory, JHU, 6 April 1970.

VIII. REFERENCES (Cont'd)

13. V. W. Pidgeon, "X-band Height-Gain Profiles with an Oceanic Duct," Technical Memorandum, Applied Physics Laboratory, JHU, 24 July 1970.

14. M. I. Skolnik, Introduction to Radar Systems, McGraw-Hill, 1962.

15. H. A. Ecker, Editor, "Principles of Modern Radar," Radar Short Course Notes, Georgia Institute of Technology, October 1972.

16. D. K. Barton, Radar System Analysis, Prentice-Hall, 1964.

17. H. E. Hawkins and O. LaPlant, "Radar Performance Degradation in Fog and Rain," IRE Transactions ANE-6, Volume 26, March 1959.

18. W. K. Rivers, G. W. Ewell, E. L. Tomberlin, and S. P. Zehner, "Airborne Search Radar Design Study," Final Report on Contract DOT-CG-83 141A , Georgia Institute of Technology, 20 February 1969, AD 685 911.

19. J. G. Boring, et al., "Sea Return Study, "Final Report on Contract NObsr-49063, Georgia Institute of Technology, 1 Aug 1957, AD 246 180.

20. M. I. Skolnik, Editor, Radar Handbook, McGraw-Hill, 1970, Chapter 31.

21. F. B. Dyer, et al., "Clutter Reduction Radar: Target and Clutter Characteristics, Part II (U)," Technical Report No. 4 on Contract N00024-68-C-1125, Georgia Institute of Technology, March 1969, Confidential, GDS (formerly Group 4), AD 518 349L.

22. F. B. Dyer, "Clutter Reduction Radar (U)," Final Report on Contract N00024-68-C-1125, Georgia Institute of Technology, 31 July 1973, Secret, Excluded from GDS (formerly Group 3), AD 527 269L.

23. G. W. Ewell, "Testing of Radars to Determine Characteristics for Swimmer Defense Program," Final Recommendations on Contract N00024-73-C-5414, Georgia Institute of Technology, October 1973, Confidential.

24. L. J. Battan, Radar Meteorology, University of Chicago Press, 1959.

25. M. W. Long and S. P. Zehner, "Effects of the Sea on Radar Echo from Rain," IEEE Trans. on Aerospace and Electronic Systems AES-6, 821 - 824, 1970.

26. N. C. Currie and F. B. Dyer, "Methods for Comparison of Clutter Processing Techniques," Technical Report No. 5 on Contract N00024-68-C-1125, Georgia Institute of Technology, February 1971, AD 883 474L.

27. M. I. Skolnik, Editor, Radar Handbook, McGraw-Hill, 1970, Chapter 38.

28. R. G. Swallow and D. Deacon, "In Control of Ship-Borne Radar," Paper No. 3/1, Ship Operation, Proceedings of SHIPS' GEAR Symposium on "The Future Technical Pattern of Control Engineering Experiment and Ship Operation," J. Anthony Hind (Editor), FISHING NEWS (Books) LTD., London, 1966.

29. C. J. Collingwood, "Progress in Marine Radar," Paper No. 2/3, The Bridge, Proceedings of SHIPS' GEAR Symposium on "The Future Technical Pattern of Control Engineering, Equipment and Ship Operation," J. Anthony Hind (Editor), FISHING NEWS (Books) LTD., London, 1966.

30. F. J. Wylie, "The Case for Fully Automatic Plotting Radar," The Journal of Navigation, Vol 25, No. 1, London, January 1972.

31. J. C. Herther and J. S. Coolbaugh, "A Fully Automatic Marine Radar Data Plotter," The Journal of Navigation, Vol 24, No. 1, London, January 1971.

32. G. Lain, "Ship Collisions, What's Being Done to Prevent Them Ocean Industry, 19-37, December 1971.

33. W. K. Rivers, et al., "San Francisco Vessel Traffic System Test and Evaluation Plan," Final Report on Task 002 of Contract DOT-CG-04132-A, Georgia Institute of Technology, 30 June 1972, Unclassified.

34. F. B. Dyer, "Surface Effect Ship Navigation and Collision Avoidance System Radar Test and Evaluation Plan," Technical Report No. 1 on Texas Instruments P. O. W-660425 (under Contract N00024-73-C-0901), Georgia Institute of Technology, 22 December 1972.

35. _____, Digiplot Operation and Maintenance Manual, Iotron Corporation, Bedford, Massachusetts, December 1972.

36. J. C. Plowman, "Automatic Radar Data Extraction by Storage Tube and Delay Line Techniques," The Radio and Electronic Engineer (J. Brit. IRE) 26, No. 4, 317-326, October 1963.

37. J. V. Hubbard, "Digital Automatic Radar Data Extraction Equipment," The Radio and Electronic Engineer (J. Brit. IRE) 26, No. 5, 397 405, November 1963.

38. G. W. Ewell, "Test Plan for S2705 Radar Tests," Final Report on Contract N61331-73-C-0046, Georgia Institute of Technology, May 1973

UNCLASSIFIED
Security Classification

DOCUMENT CONTROL DATA - R & D

Security classification of title, body of abstract and indexing annotation must be entered when the overall report is classified)

1 ORIGINATING ACTIVITY (Corporate author)	2a. REPORT SECURITY CLASSIFICATION
Engineering Experiment Station Georgia Institute of Technology Atlanta, Georgia 30332	Unclassified
	2b. GROUP N/A

3 REPORT TITLE

HARBOR TRAFFIC CONTROL STUDY

4 DESCRIPTIVE NOTES (Type of report and inclusive dates)

Final Technical Report

5 AUTHOR(S) (First name, middle initial, last name)

Michael T. Tuley and Frederick B. Dyer

6 REPORT DATE	7a. TOTAL NO. OF PAGES	7b. NO. OF REFS
6 October 1973	98 + xii	38

8a. CONTRACT OR GRANT NO.	9a. ORIGINATOR'S REPORT NUMBER(S)
N61331-73-C-0087 b. PROJECT NO.	EES/GIT Project A-1548
c. d.	9b. OTHER REPORT NO(S) (Any other numbers that may be assigned this report)

10. DISTRIBUTION STATEMENT

11. SUPPLEMENTARY NOTES	12. SPONSORING MILITARY ACTIVITY
	Naval Coastal Systems Laboratory Panama City, Florida 32401

13. ABSTRACT

A significant problem during operation in harbor and coastal areas is that of detecting and identifying marine traffic. In this report a study using computer modeling techniques is performed to specify what parameters should be chosen for a van-portable radar system that is capable of performing the harbor surveillance function. The composite model used contains: (1) an algorithm for characterizing sea and target return as functions of target elements, geometry, and weather and sea conditions; (2) a semi-empirical model for computing single-scan probability-of-detection; and (3) a computer program that combines (1) and (2) into a functional framework.

In addition, several readily available radars are chosen and their performances versus the optimum radar and each other are compared. Also investigated is the potential for use of automated displays and radar beacon or transponder systems to aid in identifying targets, and to provide additional information on their movements. Results of a field operation evaluating one such automated display are presented.

DD FORM 1 NOV 65 1473 (PAGE 1)

S/N 0101-807-6801

UNCLASSIFIED
Security Classification

4-3

14. KEY WORDS	LINK A		LINK B		LINK C	
	ROLE	WT	ROLE	WT	ROLE	WT
Radar						
Computer						
Microwave						
Search						
Computer						
Display						
Sea Clutter						